Apoptosis- and Bcl-2- Induced Alterations of the Nucleocytoplasmic Barrier

Dissertation

Zur Erlangung des akademischen Grades des

Doktors der Naturwissenschaften

an der Universität Konstanz

Fachbereich Biologie

vorgelegt von

Christine Strasser

Tag der mündlichen Prüfung: 30.07.2010

Referentin: Frau apl. Prof. Dr. Elisa Ferrando-May

Referent: Herr Prof. Dr. Alexander Bürkle

List of Publications

Major parts of this thesis are to be submitted for publication.

C. Strasser, P.Grote, K. Schäuble and E. Ferrando-May: *Ca2+ regulates nuclear envelope permeability independently of cell fate.* To be submitted

Further contributions to publications, not integrated into this thesis:

S. Kreissl, C. Strasser, CG. Galizia: *Allatostatin immunoreactivity in the honeybee brain.* J Comp Neurol. 2010 May 1;518(9):1391-417.

F. Kappes, J. Fahrer, M. S. Khodadoust, A. Tabbert, C. Strasser, N. Mor-Vaknin, M. Moreno-Villanueva, A. Bürkle, D. M. Markovitz, and E. Ferrando-May: *DEK is a poly(ADP-ribose) acceptor in apoptosis and mediates resistance to genotoxic stress.* Mol.Cell.Biol. 2008, **28**: 3245–3257

TABLE OF CONTENTS

TABLE OF CONTENTS

TABLE OF CONTENTS

TABLE OF CONTENTS

TABLE OF CONTENTS

TABLE OF CONTENTS

I. ZUSAMMENFASSUNG

Die strikte Regulation des aktiven und passiven Molekülaustausches über die Kernmembran ist eine Grundvoraussetzung für das Überleben der Zelle. In bestimmten physiologischen Situationen kann die Kernmembran verändert werden so z.B in der Mitose, der Apoptose und während der Entwicklung. Pathopyhsiologische Veränderungen der Kern-Zytoplasma-Barriere werden mit Krankheiten wie Krebs, Autoimmunerkrankungen und Virusinfektionen in Verbindung gebracht.

Ziel der Arbeit war es, vertiefte Kenntnisse über die Zelltod-abhängige Regulation der Permeabilitätsbarriere der Kernmembran für passive Diffusion zu erzielen. Um dies zu erreichen, wurden zwei, von ihren Auswrikungen her gegensätzliche zelluläre Modelle betrachtet; die Apoptose-Induktion mittels TRAIL und Staurosporin (STS) und die Apoptose-Inhibition durch Überexpression des anti-apoptotischen Proteins Bcl-2. In beiden Modellen wurde der, die Permeabilität verändernde Mechanismus im Detail charakterisiert.

Apoptose-induzierte Veränderung der Kern-Zytoplama Barriere

Um die Apoptose-vermittelten Veränderungen der Kernpermeabilität zu detektieren wurden Lebendzellmikroskopie-Experimente mit Hilfe eines in unserer Gruppe etablierten Reportersystems durchgeführt. Der Verlauf der Apoptose- und die damit verbundene Veränderung der Kernpermeabilität wurden mit Hilfe fluoreszenter Marker-Proteine detektiert. Da Chromatinkondensation als Hauptmerkmal der Apoptose gilt, wurde diese als Zeitpunkt der Apoptoseexekution definiert. Die Ergebnisse zeigen, dass in beiden verwendeten Apoptosemodellen, STS und TRAIL, die Caspase-vermittelte Spaltung der Kernpore und der damit verbunde Verlust der Kernpermeabilitätsbarriere zum Zeitpunkt der Chromatinkondensation stattfinden. Allerdings unterscheiden sich die beiden Apoptoseauslöser im Verlauf der Permeabilisierung der Kernhülle vor diesen finalen Veränderungen. Während die Permeabilität der Kernhülle nach TRAIL-Zugabe unverändert bis zur Caspasenaktivierung bleibt, tritt früh nach

ZUSAMMENFASSUNG

Zugabe von STS eine Caspase-unabhängige Zunahme der Kernpermeabilität auf. Um die zugrunde liegenden Mechanismen zu identifizieren, wurde zunächst der Einfluss von zwei verschiedenen Typen von Proteasen untersucht. Die erste waren Serin-Proteasen, welche mit STS vermittelter Apoptose in Verbindung gebracht werden. Weiterhin deuten frühere Ergebnisse aus unserer Gruppe auf einen Einfluss von Serin-Proteasen auf die Kernpermeabilität hin. In dieser Arbeit konnte keine Veränderung der frühen STS vermittelten Zunahme der Kernpermeabilität durch Serinproteaseinhibition festgestellt werden. Die zweite untersuchte Gruppe von Proteasen waren Ca^{2+}-abhängige Proteasen, Calpaine. Es wurde kürzlich gezeigt, dass diese für die exzitotoxischen Veränderungen der Kernpermeabilität in neuronalen Zellen verantwortlich sind. Interessanterweise führte die Inhibierung von Calpainen nicht zu einer Verringerung der frühen Kernpermeabilisierung sondern verstärkte diese zusätzlich.

Viele Arbeiten haben einen Einfluss des Ca^{2+}-Gehalts des endoplasmatischen Retikulums (ER) auf die Kernpore gezeigt. Um die Rolle von Ca^{2+} in der STS vermittelten Apoptose zu untersuchen wurden Lebendzellmikroskopie-Experimente in Gegenwart des Ca^{2+}-Chelators BAPTA-AM durchgeführt. Dies resultierte in der vollständigen Unterbindung der frühen STS-induzierten Permeabilitätszunahme. Die dadurch implizierte entscheidende Funktion von Ca^{2+} wurde durch Messung des Ca^{2+}-Gehalts im ER weiter untermauert. Hierbei konnte gezeigt werden, dass Stimulation mit STS aber nicht mit TRAIL zu einer Reduzierung des ER Ca^{2+}-Spiegels führt. Desweiteren wurde die Abhängigkeit des aktiven Transports von der Kernpermeabilität untersucht. Die Ergebnisse zeigen, dass aktiver und passiver Transport unabhängig voneinander reguliert werden. So bleibt der aktive Transport in beiden verwendeten Apoptose-Modellen bis kurz vor Chromatinkondensation und Caspaseaktivierung funktional, trotz der im STS-Modell beobachteten frühen Veränderung der Permeabilität.

ZUSAMMENFASSUNG

Bcl-2-vermittelte Veränderung der Kern-Zytoplasma Barriere

Da Bcl-2 ein anti-apoptotisches Protein sowie ein Protoonkogen ist, wurde vermutet, dass es die STS-vermittelte Erhöhung der Kernmembran verhindern könnte. Erste Versuche mit Bcl-2 überexprimierenden HeLa Zellen, zeigten jedoch überaschenderweise, dass Überexpression von Bcl-2 zu einer konstitutiven Zunahme der Kernpermeabiliät führt. Es wurde von anderen Gruppen berichtet, dass die funktionellen Eigenschaften der Kernmembran über den veränderten Ca^{2+} Spiegel im ER reguliert werden, ein Parameter der wiederum durch Bcl-2 beeinflusst wird. Die Bestimmung des ER Ca^{2+} Spiegels zeigte, dass Bcl-2 überexprimierende Zellen tatsächlich einen geringeren Ca^{2+}-Gehalt im ER, sowie eine reduzierte kapazitive Ca^{2+} Aufnahme aufweisen. Die erhöhte Kernpermeabilität nach Bcl-2 Überexpression konnte durch Adaption der Zellen an niedrige Ca^{2+} Mengen im Medium nachgestellt werden. Weiterhin konnte durch Überexpression der Ca^{2+} ATPase SERCA der Ca^{2+} Spiegel im ER regeneriert werden und gleichzeitig die Bcl-2 vermittelte Zunahme der Kernpermeabilität reduziert werden. Diese Ergebnisse deuten darauf hin, dass ein verringerter Ca^{2+} Gehalt im ER für die Bcl-2 vermittelte Zunahme der Kernpermeabilität verantwortlich ist.

Ein unerwartetes und bemerkenswertes Ergebnis dieser Arbeit ist die Feststellung, dass in zwei gegensätzlichen zellulären Paradigmen wie Apoptose-Auslösung und Apoptose-Inhibtion, die Kernpermeabilität über denselben Mechanismus gleich reguliert, nämlich erhöht, wird. Im Falle der STS-vermittelten Apoptose entspricht die verstärkte Durchlässigkeit der Kernmembran den Erwartungen, da bereits in anderen Arbeiten postuliert wurde, dass die Erhöhung der Kernpermeabilität den vermehrten Austausch von pro-apoptotischen Faktoren erleichtern könnte. In Anbetracht dessen scheint es überraschend, dass unter antiapoptotischen Bedingungen die Barriere für die passive Diffusion ebenfalls erniedrigt ist. Mögliche Hypothesen, die diesen Effekt erklären könnten werden in der vorliegenden Arbeit diskutiert.

II. SUMMARY

Precise regulation of active and passive nucleo-cytoplasmic exchange of molecules is a prerequisite for cell viability. Physiological alterations of these processes have been reported in many situations like in mitosis, during development and in apoptosis. Pathophysiological alterations of active and passive nuclear transport have been associated with varying diseases like cancer, autoimmune diseases and viral infection.

This work was aimed at elaborating a detailed knowledge on the regulation of the nuclear envelope permeability barrier in cell death. Therefore, the effects of opposing pathways, apoptosis-induction via TRAIL and staurosporine (STS) and apoptosis-inhibition mediated by overexpression of the anti-apoptotic protein Bcl-2, on nuclear envelope permeability were investigated. In both models the underlying mechanisms mediating the influence on nuclear envelope permeability were characterized in detail.

Apoptosis-induced alterations of the nucleocytoplasmic permeability barrier

To elucidate the alterations of nuclear envelope permeability, live cell imaging experiments were performed in a confocal setup using a reporter system established in our group. Kinetics of apoptosis and alterations of nuclear envelope permeability were assessed by fluorescently labeled marker proteins. As chromatin condensation is a hallmark of apoptosis, it was defined as time point of apoptosis execution. Our results reveal that caspase-mediated disruption of nuclear envelope permeability barrier and chromatin condensation occurs simultaneously in both models of apoptosis. However, the two employed apoptotic models differ in permeability barrier function prior to caspase activation. While in TRAIL induced apoptosis nuclear permeability is unaltered prior to caspase activation and chromatin condensation, in STS-induced cell death an early, caspase-independent nuclear leakage can be detected. To elucidate the mechanisms responsible for this latter effect, the involvement of two different types of proteases was investigated. The first one was serine proteases, which have been proposed to play a role in STS-

induced, caspase-independent apoptosis. In addition, preliminary data of our group indicated a role for serine proteases in influencing the nuclear permeability barrier. However, inhibition of serine proteases had no effect on STS-induced early nuclear leakage, excluding a possible role of serine proteases in mediating nuclear permeabilization. The second investigated proteases were calpains, Ca^{2+}-dependent proteases. These have recently been reported to be responsible for nuclear envelope permeabilization in a neuronal model of excitotoxiicity. Interestingly, calpain inhibition did not decrease early STS-induced nuclear leakage but even enhanced it.

Endoplasmic reticulum (ER) Ca^{2+}-level have been shown to influence the nuclear pore and nuclear envelope permeability. To investigate the role of Ca^{2+} in STS-induced apoptosis, confocal live cell imaging experiments in the presence of the Ca^{2+}-chelator BAPTA-AM were performed. This treatment resulted in the complete inhibition of early STS-induced nuclear leakage, indicating a pivotal role of Ca^{2+} in this system. This hypothesis was further strengthened by the finding that treatment with STS but not with TRAIL reduces ER Ca^{2+} content.

Furthermore, the dependence of active transport on nuclear envelope permeability alterations was investigated. The data show that active nuclear uptake and passive permeability are largely uncoupled as active transport is functional in both apoptotic models until chromatin condensation, despite the STS-induced early increase in nuclear envelope permeability.

Bcl-2-induced alterations of the nucleocytoplasmic permeability barrier

As Bcl-2 is an anti-apoptotic protein and a proto-oncogene, it was expected to counteract STS-induced alterations of nuclear envelope permeability. Surprisingly, preliminary data of our group indicated that Bcl-2 overexpression results in a constitutively increased nuclear permeability. It has been shown, that (ER) Ca^{2+}-level, which can be altered by Bcl-2, influence the nuclear envelope permeability barrier. Determination of the Ca^{2+}-level in the ER revealed that Bcl-2 overexpressing cells indeed show reduced ER Ca^{2+}-content and diminished capacitive Ca^{2+} uptake. The Bcl-2 induced effect on increased nuclear envelope permeability could be

mimicked by adapting cells to a medium with reduced Ca^{2+} content. Furthermore, replenishment of ER Ca^{2+}-content by overexpression of the sarcoplasmic/endoplasmic reticulum Ca^{2+}-ATPase SERCA reversed the Bcl-2 mediated increase of nuclear envelope permeability.

An unexpected and remarkable result of this work is the finding that in two opposing cellular contexts, apoptosis-induction and apoptosis-inhibition, the same mechanism to increase nuclear envelope permeability is engaged. For STS-induced apoptosis, an early increase in nuclear permeability is very plausible, sinces it has been proposed that increased nuclear permeability might be important for enhanced transport of pro-apoptotic factors. In light of this, it seems surprising that the anti-apoptotic protein Bcl-2 also increases nuclear envelope permeability. Possible interpretations of this unexpected result are presented in the discussion section of this thesis.

III. INTRODUCTION

III.1. Cell death: definition and general mechanisms

A cell is defined as dead, when one of the three following morphological or molecular criteria is met:

(1) the plasma membrane of the cell has broken down.

(2) the cell, including the nucleus, is completely fragmented into apoptotic bodies

(3) the cells, or fragments of it, have been engulfed by adjacent cells

III.1.1. Apoptosis

The term apoptosis was defined in 1972 by J.F. Kerr, A.H. Wyllie and A.R. Currie, (Kerr et al., 1972) to discriminate between uncontrolled, accidental cell death, necrosis and the programmed death of a cell. The word apoptosis was adapted from the greek expression for leaves falling from a tree: Apoptosis (apo= from, ptosis= falling). It is based on the morphological characteristics of the dying cell which include rounding-up of the cell, retraction of pseudopodia, reduction of cellular and nuclear volume (pyknosis), nuclear fragmentation (karyorrhexis), minor modification of cytoplasmic organelles, plasma membrane blebbing and engulfment by resident phagocytes *in vivo* (Kerr et al., 1972; Kroemer et al., 2009). The main characteristic of this form of programmed cell death (PCD) is the avoidance of inflammation. This is ensured by packing fragments of chromatin, cytosol and organelles into small, membrane enclosed particles, the so called apoptotic bodies. On the surface of the apoptotic bodies phosphatidylserine (PS) is exposed to attract macrophages, which then engulf the vesicles. Despite this precautions, in some cases an activation of the immune system by apoptotic cells has been reported (Zitvogel et al., 2008).

Apoptosis is associated with biochemical features like loss of mitochondrial membrane potential, outer mitochondrial membrane permeabilisation

(MOMP), activation of pro-apoptotic Bcl2-family members, and activation of caspases and chromatin fragmentation. For many years, only cell death which was accompanied by caspase activation, was considered apoptotic. A recent publication of the Nomenclature Committee on Cell Death (NCCD) in 2009 states that apoptosis also occurs in the absence of active caspases. Further, the appearance of more than one feature of apoptosis is necessary to determine the apoptotic mechanism of cell death.

The term apoptosis further indicates that this process is an essential part of the development of an organism and is conserved among plants and animals (Tittel et al., 2000). Apoptosis is a prerequisite for brain development as half of the initially created neurons die by apoptosis during the development from the embryonic to the adult brain. Furthermore, 100,000 cells are produced every second in the organism and therefore the same amount of cells has to die by apoptosis to maintain homeostasis.

Beside apoptosis, two other main mechanisms of cell death exist: autophagy and necrosis. The main function of autophagy is to ensure the survival of the cell by degradation of proteins and organelles by lysosomal proteases. In recent years a role of autophagy in cell death has been indicated. For example infection with human immunodeficiency virus HIV1 can lead to activation of autophagic cell death in uninfected CD4+ T-cells (Espert et al., 2006). Furthermore, autophagy mediated cell death can substitute for apoptotic cell death in BAX-/-Bak-/- cells in response to genotoxic or endoplasmatic reticulum (ER) stress (Shimizu et al., 2004).

Necrosis is characterized by swelling of the cytoplasm (oncosis), swelling of cytoplasmic organelles, rupture of the plasma membrane, and moderate chromatin condensation (Majno et al., 1995, Kroemer et al., 2009). Over many years, necrosis was considered to be an uncontrolled, accidental form of cell death, leading to inflammation. In the last years however, evidence has accumulated that necrosis might be a regulated death pathway (Golstein et al., 2007). For instance, death-domain receptors like Fas/CD95 and TRAIL-R and toll-like receptors like TLR-3 and TLR-4 can induce necrosis, especially in the presence of caspase inhibitors. This pathway seems to

require the RIP-kinase as effector molecule (Holler et al., 2000). Due to these findings regulated necrosis is also called necroptosis.

Other terms for cell death are being used in literature like PARP-induced cell death, mitotic cell death, excitotoxicity. All theses terms describe pathways that fulfill the criteria of either necrosis, apoptosis or autophagy are therefore no different pathways.

III.2. Apoptotic signaling

Apoptosis is executed via two different pathways, the death receptor mediated pathway and the intrinsic pathway.

III.2.1. Caspases

Both apoptotic pathways converge at the level of specific proteases - the caspases. Caspases are cysteine-dependent aspartate-specific proteases which contain a cysteine in their catalytic region and cleave their substrates after an aspartatic acid residue. Caspase activation is one of the main features of apoptosis (Kroemer et al., 2009; Feinstein-Rotkopf and Arama, 2009). So far, 14 members of the caspase-family have been described in mammals, whereas capase-11 and caspase-12 can only be found in the mouse (Denault and Salvesen, 2002; Degterev et al., 2003. The regulation of caspase activity is a prerequisite for keeping the balance between life and death. While overexpression of caspases in cell culture induces cell death, the genetically and pharmacologically inhibition of caspases suppresses apoptotic cell death (Kuida et., 1996; MacFarlane et al., 1997). Furthermore, mice embryos in which caspase-3 and -9 genes are knocked out die before birth as a result of severe defects in brain development (Kuida et al., 1996; Kuida et al., 1998).

In addition to their apoptotic function, caspases play an essential role in non-apoptotic or apoptosis-like processes, like erythrocyte differentiation, spermatid terminal differentiation, stem cell differentiation, cytokine maturation, and even in learning and memory (Feinstein-Rotkopf and Arama, 2009, Grütter et al., 2000).

INTRODUCTION

Caspases are synthesized as inactive zymogens and carry at their N-terminus a prodomain which is followed by a large (~20kDa) and a small (~10kDa) subunit. The two subunits can be separated by a linker. The prodomain mediates dimerization and promotes auto-processing of the procaspases. Furthermore, it can also contain a nuclear localization signal (Baliga et al., 2003; Colussi et al., 1998). Caspases can be grouped in three categories:

1) the initiator caspases that contain either a death-effector domain (DED) or a caspase recruitment domain (CARD) and are characterized by a long prodomain (> 90amino acids).

2) the effector or executioner caspases, containing a short prodomain and

3) the remaining group of caspases, whose major function is the maturation of cytokines (Grütter et al., 2000).

The mechanism of caspase activation is different for initiator and executioner caspases. Initiator caspases (caspase-2,-8,-9 and -10) are activated by dimerization at large multiprotein complexes (see below) and cleavage of the pro-caspase is not necessary but may stabilize the complex (Boatright and Salvesen, 2003).

Executioner caspases (caspase-3,-6 and -7) however, exist as zymogen dimers. Upon activation the two subunits are separated and the prodomain is cleaved off by caspases. Active caspases are heterotetramers consisting of two small and two large subunits. The active site is formed by the interaction of 1Arg, 1His, 1Cys of the large subunit and 1 Arg of the small subunit (Grütter et al, 2000). Executioner caspases cleave apoptotic substrates like inhibitor of caspase-activated DNase (ICAD) or poly(ADP-ribose)polymerase (PARP), nuclear pore proteins, actin, lamin and many more. These cleavage events lead to the typical morphology of apoptotic cells.

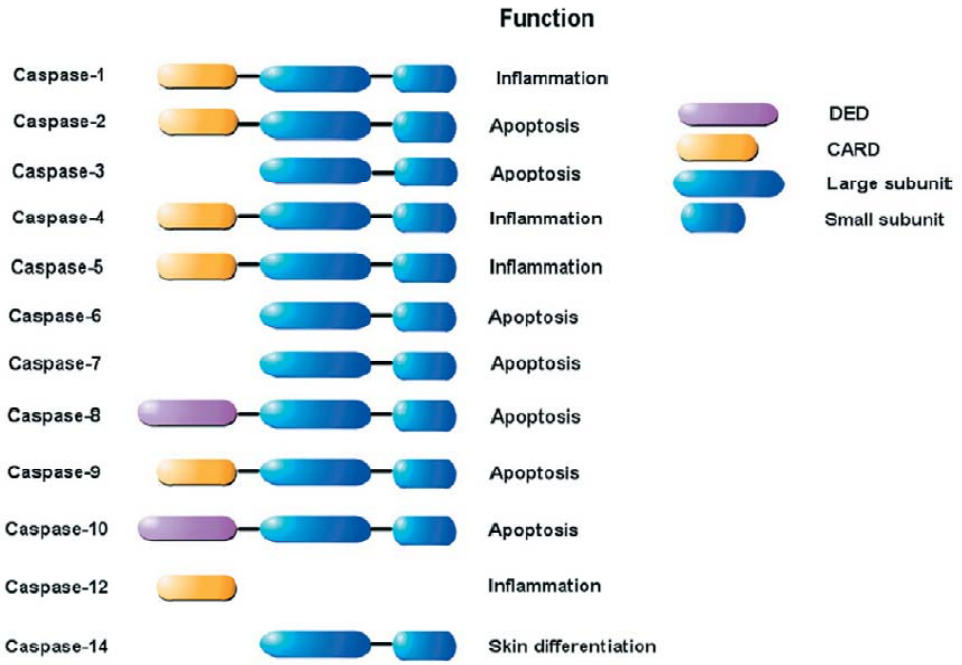

Figure 1: Schematic representation of the human caspases depicting their structure and proposed function (from Logue and Martin, 2008)

III.2.2. Extrinsic cell death

Extrinsic cell death or receptor mediated apoptosis is induced via the activation of death receptors and depends largely on caspases (Fig. 1). The death receptors, like Fas, tumor-necrosis factor receptor (TNF-R) and TNF-related-apoptosis-inducing-factor-receptor (TRAIL-R) -DR4 and -DR5 are located in the plasma membrane and induce apoptosis after binding of the appropriate ligand (Schulze-Osthoff et al., 1998). All these death receptors belong to the TNF-R family and contain cysteine-rich ligand binding domains and a cytosolic death domain (DD). Binding of the ligand to the receptor leads to its trimerisation and concomitant activation (Naismith, 1998).

Adaptor molecules like FADD or TRADD bind with their death- domain (DD) to the cytosolic death-domain of the activated receptor and build the so-called death-inducing-signaling–complex (DISC) (Kischkel et al., 1995; Muzio et al., 1996). In addition to their DD, the adaptor molecules also contain a death-effector domain (DED), which sequesters procaspase-8 or-10 to the DISC via DED-DED homeotypic interaction. Other initiator caspases (caspase-1, -2, -4, -5, -9,-11 and -12) bind to the adaptor molecule`s DD with their caspase activation and recruitment domain (CARD) The presence of

numerous procaspase-8 (or procaspase-10) molecules leads to their autocatalytic activation. FLIP-C, a dominant negative form of procaspase-8 inhibits binding of procaspase-8, therefore inhibiting apoptosis.

Active inducer caspases activate executioner caspases like caspase-3,-6, -7 by cleavage which then in turn specifically cleave many substrates, like nuclear pore proteins (Nups) (Ferrando-May et al., 2001) resulting in the death of the cell (Nicholson and Thornberry, 1997). Cells in which these caspase dependent mechanisms are sufficient to induce apoptosis are defined as Type I cells (Scaffidi et al., 1998).

In type II cells an amplification loop via the Bcl-2 family member Bid is needed. There, active caspase-8 cleaves Bid into the active form t-Bid which then activates pro-apoptotic Bcl-2 family members that trigger the intrinsic, mitochondrial pathway. At this point, the extrinsic and intrinsic pathway overlap, as mitochondria are an essential element in intrinsic cell death.

III.2.3. Intrinsic cell death

Intrinsic cell death can be induced by various agents and events like, DNA damage e.g. by irradiation, or chemical agents like etoposide (topoisomerase II inhibitor), oxidative damage, and chemical reagents like staurosporine, ceramide, *N*-methyl-*N*'-nitro-*N*nitrosoguanidine (MNNG) and many others.

A main role in mediating intrinsic cell death is fulfilled by the mitochondria (Fig. 2). How the stress signals are transmitted to the mitochondria is still unclear but Bcl-2 family members seem to play an important role. A critical point in intrinsic cell death is the perforation of the outer mitochondrial membrane (mitochondrial outer membrane permeabilization, MOMP) which is followed by the disruption of transmembrane potential (Δψ). This leads to the release of many apoptotic factors into the cytosol (Loeffler and Kroemer, 2000; Kroemer et al., 2007). Two mechanisms as to how the MOMP could be induced are currently discussed.

The first one involves two mitochondrial membrane components, the voltage dependent anion channel (VDAC also called porin) in the outer mitochondrial membrane, and the adenine nucleotide translocator (ANT) in the inner

mitochondrial membrane (Zamzami and Kroemer, 2001). VDAC is the most abundant protein in the outer mitochondrial membrane and forms non-selective pores. The ANT is responsible for the antiport of ADP and ATP and is the most abundant protein of the inner mitochondrial membrane. Overexpression of ANT-1, but not ANT-2 has been shown to induce apoptosis, indicating a specific function of ANT-1 in apoptotic mitochondrial events (Bauer, 1999). In the presence of Ca^{2+}, ANT and VDAC fuse at so-called `contact sites` and form a permeability transition pore (PTP) through which the apoptotic factors can be released (reviewed in Grimm and Brdiczka, 2007).

The second proposed MOMP mechanism involves the Bcl-2 family members Bax and Bak. Multimerization of Bax/Bak could lead to formation of the mitochondrial apoptosis-induced channel (MAC) in the mitochondrial membrane (Dewson and Kluck, 2009; Korsmeyer et al, 2000).

MOMP leads to the release of cytochrome c, which is needed to activate the caspase cascade by forming the apoptosome together with seven Apaf-1 molecules, seven ATP and seven pro-caspase-9 molecules. Over many years, the release of cytochrome c from the mitochondria was thought to be dependent on MOMP, in recent years, however, the MOMP-independent release of cytochrome c was shown (Ly et al., 2003).

Among other factors that are released from the mitochondria is the apoptosis inducing factor, AIF (Susin et al, 1999), which elicits caspase independent chromatin fragmentation (Andrabi et al., 2006). Poly(ADP-ribose) (PAR) was identified as the signal for AIF release in neuronal excitotoxicity (Andrabi et al., 2006). Furhermore, the endonuclease, endoG (Li et al., 2001), the IAP inhibitor Smac/Diablo (Verhagen et al., 2000), and the serine protease HtrA2/Omi (Verhagen et al. 2002) are released.

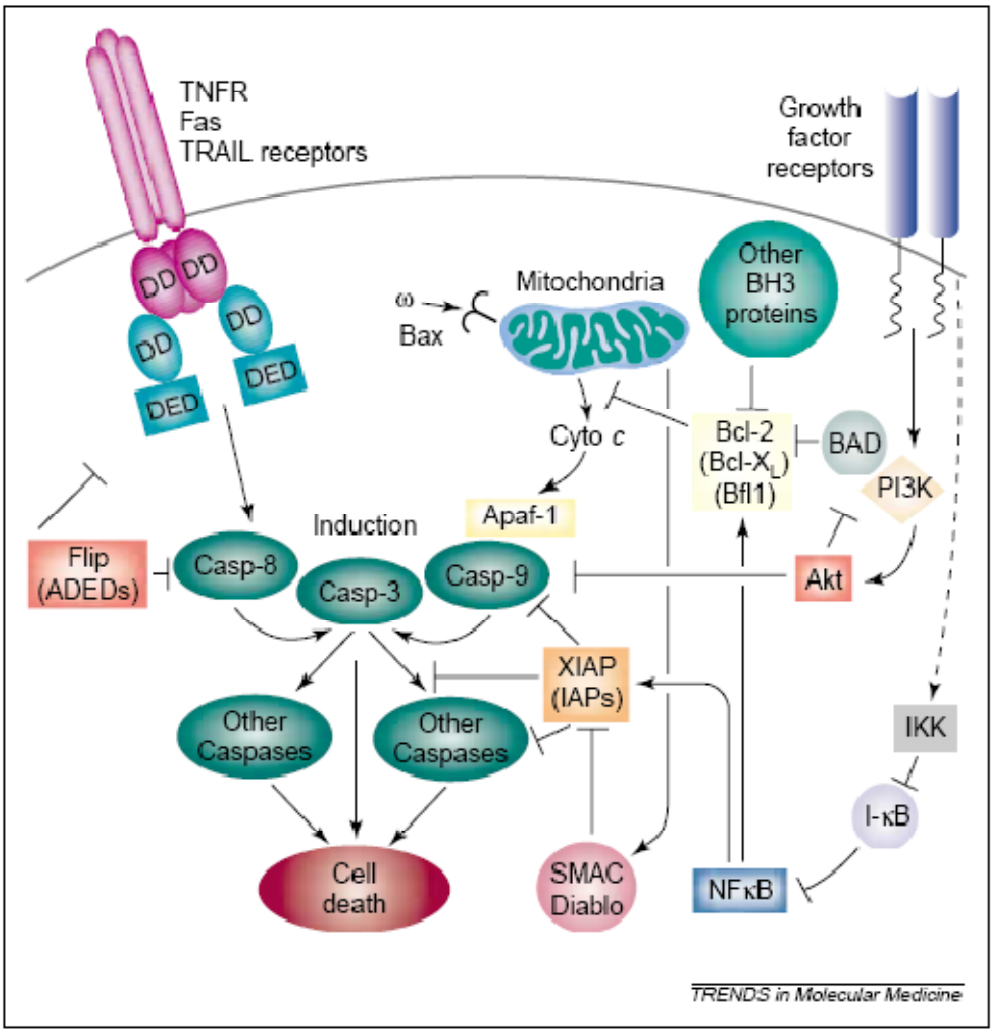

Figure 2: Apoptosis induction and regulation. Two major apoptotic pathways are presented. The extrinsic pathway (left side) and the intrinsic pathway (right side). The extrinsic pathway is triggered by members of the TNF-family of cytokine receptors such as TRAIL, Fas and TNFR1 receptors. These proteins recruit adaptor proteins including TRADD or FADD to their cytosolic Death Domains (DD), resulting in the death-inducing signaling complex (DISC) which leads to the activation of executioner caspase-3 via caspase-8 activity. The intrinsic pathway is triggered by release of cytochrome c from the mitochondria in response to various stimuli. Cytochrome c binds and activates Apaf1 enabling it to bind caspase-9 and subsequently leads to activation of executioner caspase-3.. This pathway is suppressed by anti-apoptotic Bcl-2-family members like Bcl-2 and Bcl-X_L that inhibit cytochrome c release. The anti-apoptotic family members, in turn, are suppressed by BH3-only proteins such as Bad, that heterodimerize with the anti-apoptotic Bcl-2 family proteins. Both pathways produce active caspase-3 which then cleaves other executioner caspases like caspase-6 and-7. Active caspases, such as caspase-3,-7 and -9 can be directly inhibited by inhibitors of apoptosis proteins, IAPs. IAPs, turn, are suppressed by Smac/Diablo, which is released from mitochondria. NF-κB induces expression of apoptosis suppressors such as certain IAP-family genes and some anti-apoptotic Bcl-2 family genes. The kinase Akt can phosphorylate and inactivate BAD, as well as caspase-9. The schematic is an oversimplification of the events that occur *in vivo*. From Reed, 2001.

III.2.4. Versatility of Ca^{2+} signals

The importance of Ca^{2+} in cell death was first described by Kaiser and Edelmann in 1977 who indicated that Ca^{2+} mediates the death of immature lymphocytes in response to glucocorticosteroid hormones. Since then, Ca^{2+}-signaling has been found to play a role in cell death, induced by various stimuli like staurosporine (STS) (Kruman et al., 1998; Seo et al., 2009), growth factor withdrawal (Baffy et al., 1993), hydrogen peroxide (H_2O_2) (Distelhorst et al., 1996; Rimpler et al., 1999), ceramide (Pinton et al., 2001), the Ca^{2+}-ATPase inhibitor thapsigargin (TG), FAS (Wozniak et al., 2006), tumor necrosis factor (Kim et al., 2002) and genotoxic stress (Mathai et al., 2005). The endoplasmic reticulum (ER) is the main Ca^{2+} store in the cell (Rong und Distelhorst, 2008). The cellular response to Ca^{2+} is largely dependent on the amount, the frequency and the duration of Ca^{2+} release. Under physiological conditions, Ca^{2+} released from the ER is taken up by the mitochondria, resulting in increased ATP production (Duchen et al., 2000). The versatility of Ca^{2+} signals can be shown by the response of immature T-cells in the thymus to T-cell receptor activation: a strong activation leads to a sustained Ca^{2+} elevation and cell death whereas a weak activation induces Ca^{2+} oscillations, expression of pro-survival IL-2 and cell survival (Lewis et al., 2001, Winslow, 2003, Zhong 2006).

Ca^{2+} release from the ER occurs mainly through the inositol-triphosphate receptor (IP_3R) which has three isoforms (Taylor et al., 1999) and is posttranslationally modified (Bezprozvanny et al., 2005; Mackrill et al., 1999). The expression levels of IP_3Rs differ in different tissues, rendering them differently susceptible to cell death. In tissues which have high rates of apoptosis, like developing postnatal cerebellar granule cells, dorsal root ganglia or intestinal villi, elevated levels of IIP_3R mRNA and protein are detected. Knock down of IP_3R abolishes T-cell receptor-induced apoptosis in T-cells and reduced expression of IP_3Rs inhibits glucocorticosteroid induced apoptosis in Lymphocytes (Jayaraman et al., 1997, Khan et al, 1996). IP_3R activity is enhanced by binding of Cytochrome c (Boehning et al. 2003). Cleavage by caspase-3 leads to a truncated form of IIP_3R which exhibits an increased leakiness (Assefa et al. 2004).

III.3. Regulators of apoptosis

Apoptotic signaling is strictly regulated, ensuring a balance between repair and destruction, cell life and death. Many factors are involved in this process. The most important ones will be shortly introduced in the following part.

III.3.1. IAPs

Eight human inhibitors of apoptosis proteins (IAPs) proteins have been identified which share homology to the originally identified baculovirus IAPS. The main function of IAPs is the inhibition of activated caspases (Fig.1) through direct interaction of the baculovirus IAP repeat (BIR) domain within the IAPs to active caspases (Takahashi et al., 1998; Salvesen, 2002a;). Different BIR domain can bind to different caspases. In case of XIAP, the BIR3 domain binds directly to the small subunit of caspase-9, whereas the BIR2 domain binds to caspase-3 and -7 (Huang et al., 2001; Srinivasula et al., 2001). IAP function is controlled by SMAC/Diablo. SMAC/Diablo contains a tetrapeptide motif with which it binds to IAPs and frees bound caspases (Srinivasula et al., 2001; Verhagen et al., 2000).

III.3.2. Bcl-2 family members

B cell lymphoma-2, the founding member of the Bcl-2 family, was first identified in chromosomal breakpoint of t(14;18) bearing human follicular B cell lymphoma (Bakhshi et al., 1985; Cleary and Sklar, 1985; Tsujimoto et al., 1985). The members of the Bcl-2 family can be divided in three groups according to their structural homology to the four Bcl-2 homology domains (BH1-4) and function (Figure 3).

The **antiapoptotic** members contain all four homology domains and include BCL-2, BCL-X_L (Boise et al., 1993), MCL-1 (Desagher et al., 1999; Wei et al., 2001) A1 (Choi et al., 1995), and BCL-W (Gibson et al., 1996). The first pro-apoptotic Bcl-2 family member, the Bcl-2 associated X protein (BAX) was identified by its binding to Bcl-2 (Oltvai et al.,1993) and forms together with BAK and BOK the **multi-domain pro-apoptotic** Bcl-2 family which contain the homology domains BH1-BH3. The localization of Bax and Bak differs,

while Bax is mainly cytosolic or loosely associated with the mitochondria, Bak is an integral part of the ER- and the mitochondrial membrane, bound to VDAC (Adams and Cory., 2007). The third Bcl-2 family subgroup contains the **BH3-only** members Bim, Bad, Bik, Bik, Bmf, HRK, Noxa, Puma. All members of this group are pro-apoptotic and share the signature BH-3 domain.

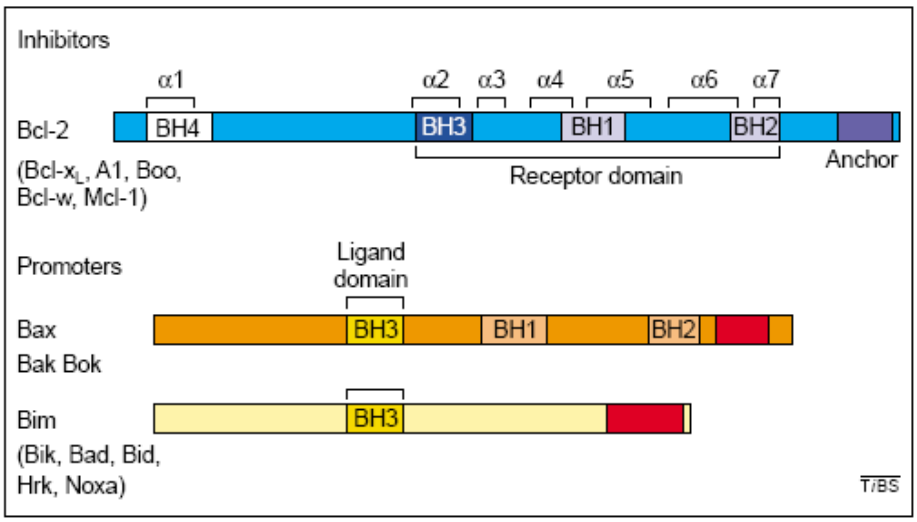

Figure 3: Bcl-2 family proteins and their subdivision. (From Adams and Cory, 2001)

Apoptosis induction via the intrinsic pathway is mainly regulated by Bcl-2 family members. After stress-induction, Bax and Bak are thought to travel to the mitochondria and by oligomerization and forming of a mitochondrial apoptosis-induced channel (MAC), perforate the outer mitochondrial membrane (Liu et al., 1996; Pavlov et al.,2001; Wei et al., 2001; De Giorgi et al., 2002; Guo et al., 2004). Bax and Bak are in most tissues largely redundant. Thus the absence of one protein has no effect on cell death, but the absence of both proteins inhibits apoptosis in many cell types (Wei et al, 2001, Dejean et al, 2005). Pro-survival Bcl-2-family proteins bind Bax and Bak, thereby inhibiting their translocation to the mitochondria and MAC formation (Pavlov et al., 2001; Guo et al., 2004; Martinez-Caballero et al.,2004). The BH3-only proteins act upstream of Bax and Bak, as they cannot induce apoptosis in cells lacking both Bax and Bak (Cheng et al.,

2001; Zong et al., 2001). Two models which describe the apoptosis induction by BH-3 only proteins have been proposed.

The **direct activation** model (Figure 4) suggests, that the activators tBid and Bim bind directly to Bax and Bak and therby activate them (Letai et al., 2002; Kuwana et al., 2005; Certo et al., 2006; Oh et al, 2006; Walensky et al., 2006). The other BH3-only members, the sensitizers, free tBid and Bim from the Bcl-2 family members, enabling the activation of Bax and Bak. Several findings make the direct activation model unlikely. No binding of Bak to any of the BH3-only members could be found and even in the absence of tBid and Bim apoptosis was not impaired (Willis et al., 2007).

The **indirect activation** model (Figure 4) proposes that the BH3-only family members bind to the pro-survival Bcl-2 proteins and thereby release Bax and Bak (Chen et al., 2005; Willis et al., 2005; Willis et al, 2007). The importance of single BH3-only family members depends on their ability to bind pro-survival proteins. Bim and tBid are able to bind all pro-survival Bcl-2 family members and are therefore more potent than the other BH3-only proteins which can only bind to a subset of the pro-survival proteins.

The concentration and the activity of BH3-only proteins changes under stress conditions, whereas the levels of Bax and Bak are unaltered. The activation of p53 induces the expression of Noxa and Puma (Jeffers et al., 2003; Villunger et al., 2003; Erlacher et al., 2005). Bim is induced downstream of the Akt pathway and its activity is regulated by phosphorylation (Dijkers et al., 2000). Phophorylation by Erk triggers Bim degradation, whereas phosphorylation by c-Jun N-terminal kinase potentiates its pro-apoptotic activity (Ley et al., 2003; Luciano et al., 2003; Akiyama et al., 2003; Putcha et al., 2003). The BH-3 only protein Bid needs to be proteolytically processed by caspases or granzyme B.

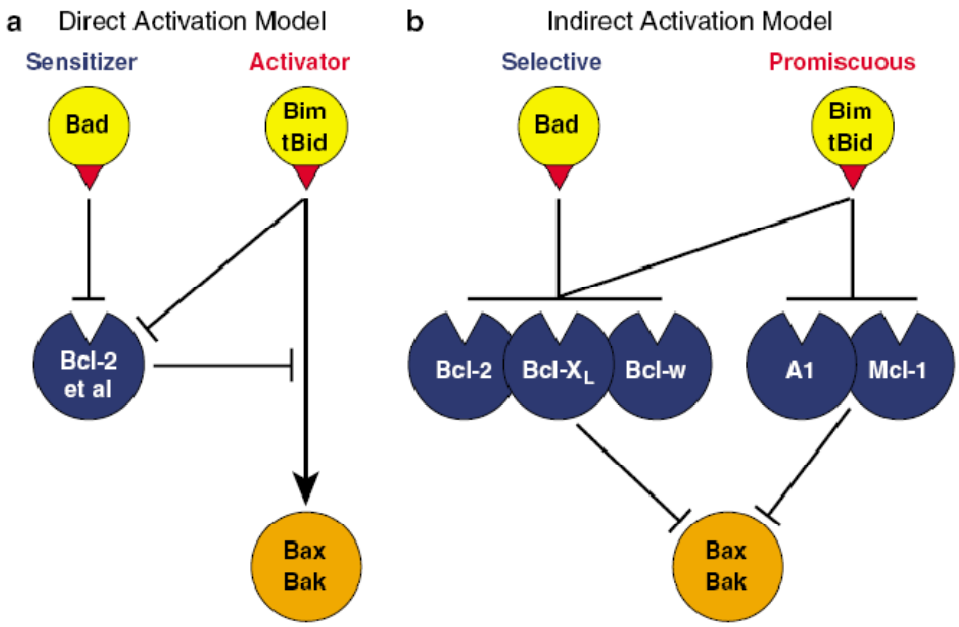

Figure 4: Contrasting direct and indirect activation models for Bax and Bak. (a) In the direct model (Letai et al., 2002), the putative activators Bim and tBid bind directly to Bax and Bak to drive their activation, whereas the sensitizers only bind to the pro-survival Bcl-2 homologs ('Bcl-2 et al.') via the BH3 domain (red triangle). (b) In the indirect activation model (Chen et al., 2005; Willis et al., 2005, 2007), the BH3-only proteins activate Bax and Bak not by binding to them directly, but instead by engaging the multiple pro-survival proteins that guard Bax and Bak. In this model, Bim and tBid are more potent than Bad and other BH3-only proteins owing to the greater range of pro-survival proteins that they can engage and neutralize (from Adams and Cory, 2007).

III.4. Nuclear Transport

III.4.1. Relevance of nuclear transport

The communication between nucleus and cytoplasm is a prerequisite for cell survival. Impaired nuclear transport is associated with various diseases like cancer, triple A syndrome, Alzheimer, primary biliary cirrhosis and viral infections (Worman and Courvalin, 2004, Kau et al., 2004, Cronshaw and Matunis, 2004; Jans, 2009). Thus, exchange of molecules between cytoplasm and nucleus has to be strictly regulated. The nuclear pore complex (NPC) together with numerous other components and factors ensures the controlled exchange of information between nucleus and cytoplasm.

III.4.2. Nuclear envelope and nuclear pore complexes

In eukaryotic cells, nucleus and cytoplasm are two compartments separated by a bilayered membrane, the nuclear envelope. The outer nuclear membrane (ONM) is continuous with the endoplasmic reticulum (ER) and studded with ribosomes (Gerace and Burke, 1988; D`Angelo and Hetzer, 2008). It serves as an anchoring site for structural elements of the cytoplasm like actin-filaments (Starr and Han, 2002; Padmakumar et al., 2004). The inner nuclear membrane (INM) contains proteins that bind to chromatin and lamina (Worman and Courvalin, 2000). The two membranes build a closed layer around the nucleus, only interrupted by (NPCs), which are inserted at sites were INM and ONM fuse. Being the sole gateway in and out of the nucleus, they function as gatekeepers, mediating the exchange of molecules between nucleoplasm and cytoplasm (Cook et al., 2007). Nuclear pore complexes are huge 120 MDa structures consisting of ~30 different proteins, the nuclear pore proteins (Nups), present in multiple copies (Cronshaw et al.,2002; Rout et al, 2000) (Figure 5). Each NPC has a diameter of about 120 nm, a depth of about 200nm and an opening diameter of about 50 nm. The NPC is an eightfold symmetrical structure which is arranged around a central channel and contains in its core framework the spokes ring which is sandwiched between a cytoplasmic - and a nuclear ring (Elad et al., 2009). From the cytoplasmic ring, eight filaments extend into the cytoplasm whereas the eight filaments emanating from the nuclear ring form the central basket and interconnect at their distal ends in the distal ring (Figure 5) (Ris, 1991; Jarnik and Aebi, 1991). In addition to the central channel, the existence of eight peripheral channels with a diameter of about 8nm has been proposed (Hinshaw et al, 1992) (Figure 8).

Nucleoporins can be classified into three groups according to their role in NPC structure or –function (Tran and Wente, 2006; Alber et al., 2007; DeGrasse et al., 2009). Nups in the first group are transmembrane nucleoporins which anchor the NPC to the NE. These Nups might be directly connected to the structural Nups of the second group. These form the nuclear scaffold and show two specific fold types, the ß-propellor and the α-solenoid. The third group contains the peripheral Nups, including the FG-

Nups, whose phenylalanine-glycine (FG) residues are separated by a polar spacer of variable length. FG-Nups are mobile, fill the central channel, have an unfolded structure and are responsible for interaction with transport receptors (Isgro and Schulten, 2007a,b, Denning, 2003, Peters, 2005).

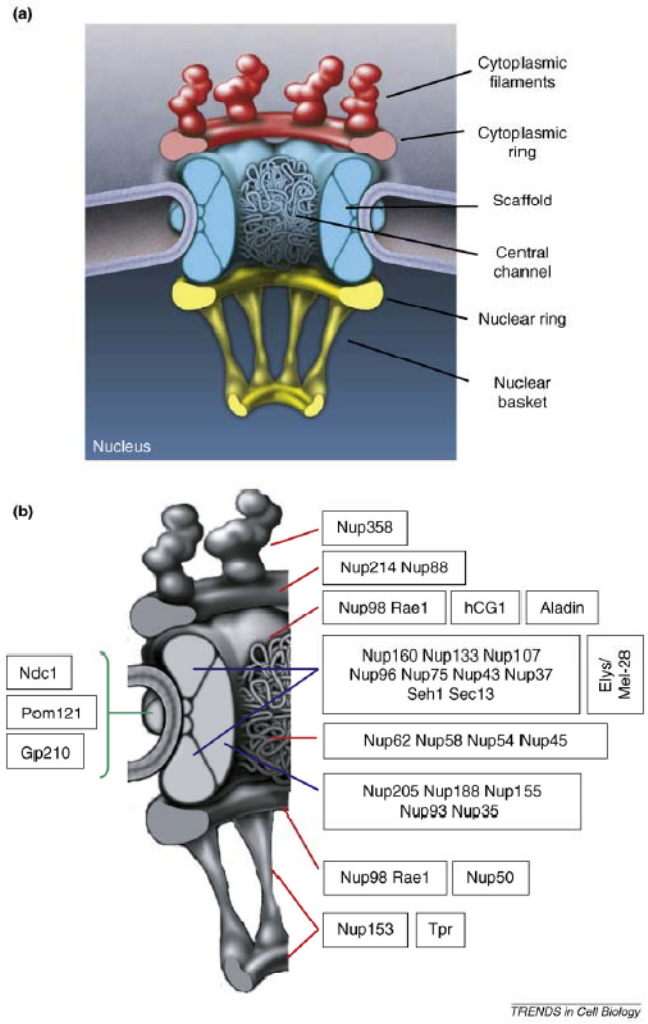

Figure 5: Nuclear pore complex (NPC) structure and composition. (a) Schematic illustration of the NPC structure. (b) Predicted localization of subcomplexes and nucleoporins within the NPC. The members of the Nup214 complex (Nup214, Nup88), Nup98 complex (Nup98, Rae1), Nup107–160 complex (Nup160, Nup133, Nup107, Nup96, Nup75, Nup43, Nup37, Sec13, Seh1), Nup62 complex (Nup62, Nup58, Nup54, Nup45) and Nup93–205 complex (Nup205, Nup188, Nup155, Nup93, Nup35) are enclosed in the same box. Green lines indicate the location of the three transmembrane nucleoporins, red lines indicate the location of peripheral components and blue lines indicate the location of scaffold subcomplexes. (from D`Angelo and Hetzer, 2008).

III.4.3. Mechanisms of nuclear transport

There are two different ways to pass the NPC. One is the diffusion of small molecules along the concentration-gradient, and the other is energy-dependent and requires the presence of transport receptors.

III.4.3.1. Passive nucleocytoplasmic diffusion

Molecules smaller than about 30-40kDa can pass the NPC via diffusion. So far it is not clear if small molecules pass the central channel or use the peripheral channels. There are different mechanisms under debate as to how passive diffusion and active transport take place at the same time and which routes they take. Naim et al., could show in 2007 that active and passive transport are largely uncoupled in HeLa cells. Peters in 2005 proposed that two routes exist in the central channel; active transport along the channel wall via facilitated transport and passive diffusion through a narrow tube in the middle of the central pore. Further the use of the eight peripheral channels, especially for ions smaller than 10kDa has been suggested (Bucholz et al., 2004; Shahin et al., 2001; Danker et al., 1999; Beck et al., 2004; Hinshaw et al., 1992; Stoffler et al., 2003; Akey and Radermacher., 1993).

III.4.3.2. Active transport mechanisms

Molecules which are too large to pass the NPC via diffusion have to be actively transported in or out of the nucleus. Therefore, they need a nuclear localization signal (NLS) or a nuclear export signal (NES). Classic NLSs contain either a monopartite NLS with 4-5 basic residues or a bipartite signal with a second basic cluster located 10-12 residues downstream of the first cluster (Stewart, 2007) Active nuclear import depends on receptor molecules which bind to the NLS of the cargo and mediate its transport through the NPC. The first identified nuclear importer was importin-ß (also Kap-ß) which belongs, together with importin-α (also Kap-α) and about 20 other molecules to the karyopherin-ß family (Figure 6) (Moroianu et al., 1999, Terry and Wente., 2009). Most members of the karyopherin family can bind directly to FG-repeat-containing Nups. Only importin-ß needs an adaptor molecule, importin-α, which mediates binding to FG-repeats.

In addition to karyopherins, import and export of molecules also depends on the small GTPase Ran. Ran is a member of the Ras superfamily of proteins and can be found in a GDP- or GTP-bound form. In the cytosol, due to the presence of RanGAP (GTPase activating protein), high amounts of RanGDP and low amounts of RanGTP are present. In the nucleus the concentrations are reversed: RanGDP is low and RanGTP is high due to presence of chromatin-bound Ran guanine nucleotide exchange factor (RCC1). This RanGTP gradient is essential for the directionality of transport: all importins implicated in nuclear export (exp1/crm1; CAS; exportin t; Msn5p) bind their cargoes preferentially in the presence of RanGTP (Kutay et al 1997; Farnerod et al., 1997; Stade et al., 1997).

Human	Cargo	Yeast	Cargo	Essential gene
Import				
Importin-β1	Many cargoes, cargoes with basic NLSs via karyopherin α, UsnRNPs via snurportin	Kap95	Many cargoes including those with basic NLS via karyopherin α	Yes
Karyopherin-β2	hnRNPA1, histones, ribosomal proteins	Kap104	Nab2, Hrp1	ts
Transportin SR1	SR proteins	Mtr10/Kap111	Npl3, Hrb1	ts
Transportin SR2	HuR	.....		
Importin 4	Histones, ribosomal proteins	Kap123	Ribosomal proteins, histones	No
Importin 5	Histones, ribosomal proteins	Kap121	Ribosomal proteins, histones, Pho4, others	Yes
Importin 9	Histones, ribosomal proteins	Kap114	TBP, histones, Nap1p	No
Importin 7	HIV RTC, Glucocorticoid receptor, ribosomal proteins	Nmd5/Kap119	TFIIS, Hog 1, others	No
		Sxm1/Kap108	Lhp1, ribosomal proteins	No
Importin 8	SRP19	.....		
Importin 11	UbcM2, rpL12	.....		No
.....		Kap122	TFIIA	
Export				
Crm1	Leucine rich NES cargoes	Crm1	Leucine rich NES cargoes	Yes
Exportin-t	tRNA	Los1	tRNA	No
CAS	Karyopherin α	Cse1	Karyopherin α	Yes
Exportin 4	eIF-5A	.....		
Exportin 5	microRNA precursors	.....		
Exportin 6	Profilin, actin	.....		
Exportin 7	p50Rho-GAP, 14-3-38	.....		
Import/Export				
Importin 13	Rbm8, Ubc9, Pax6 (import) eIF-1 A (export)	.....		
.....		Msn5	Pho4, others including phosphorylated proteins (import) Replication protein A complex (export)	No
Uncharacterized				
RanBP6	undefined	.....		
RanBP17	undefined	.....		
.....		Kap120	undefined	No

Figure 6: NES, nuclear export signal; NLS, nuclear localization signal. Members of the karyopherin-ß family from human and yeast are shown, and othologues as well as examples of their characterized cargoes are grouped. `Essential gene` indicates the phenotype of the yeast gene deletion. Dotted lines indicate orthologues that have not been identified. Although nmd5/Kap119 and Sxm1/Kap108 are shown as orthologues of importin-7, these proteins show a similar level of sequence relatedness to Importin 8. (From Pemberton and Paschal, 2005)

Several other nuclear localization signals and transport systems have been described (Moroianu, 1999), but only the classic NLS- and NES- pathway will be presented here. In the import pathway of classic NLS-containing molecules, importin-α mediates binding of the cargo to importin-ß which then binds to FG-Nups in the NPC via rapid, low affinity interaction (Figure 7) (Terry et al., 2007, Moroianu et al., 1999, Terry and Wente, 2009). Once in the nucleus, RanGTP interacts with the importin-ß in the cargo complex and so frees importin-α and the cargo molecule (Rexach and Blobel., 1995; Albertini et al., 1998; Pemberton et al., 1999). Nuclear export of molecules has either the purpose to transport cargo into the cytosol or to recycle import factors like importin-α (Figure 7). Therefore the export receptor, like CAS in the case of importin-α or Crm1 for NES containing cargoes, the cargo and RanGTP build a complex which is transported through the NE. For the recycling of importin-ß, RanGTP forms a complex with importin-ß, resulting in its transport into the cytosol.

At the cytoplasmic side of the NPC, all transport complexes are disrupted by hydrolysis of RanGTP to RanGDP by Ran GTPase activating protein (RanGap) which is localized at the cytoplasmic side of the NPC. The exclusive presence of RanGAP in the cytosol is ensured by two mechanism: 1) RanGAP is too large to diffuse back into the nucleus after its export and 2) modification by a small ubiquitin-like modifier (sumo-1) results in the targeting and binding to RanBP2 (Matunis et al., 1996; Mahajan et al., 1997; Yokoyama 1995; Bischoff et al., 1995). RanBP2 is a cytoplasmic Nup which forms the cytoplasmic fibers emanating from the NPC and is anchored to the NPC via Nup214 (Wu et al., 1995; Kraemer et al., 1994). As both recycling of transport receptors and export of cargo depletes 10^5 RanGTP-molecules/second from the nucleus, the import of RanGDP into the nucleus is a prerequisite for transport functionality (Görlich et al., 2003; Smith et al., 2002). RanGDP is imported into the nucleus by NTF2 which can interact directly with FG-repeat-containing Nups (Moore et al., 1994; Paschal and Gerace, 1995; Smith et al., 1998; Ribbeck et al., 1998).

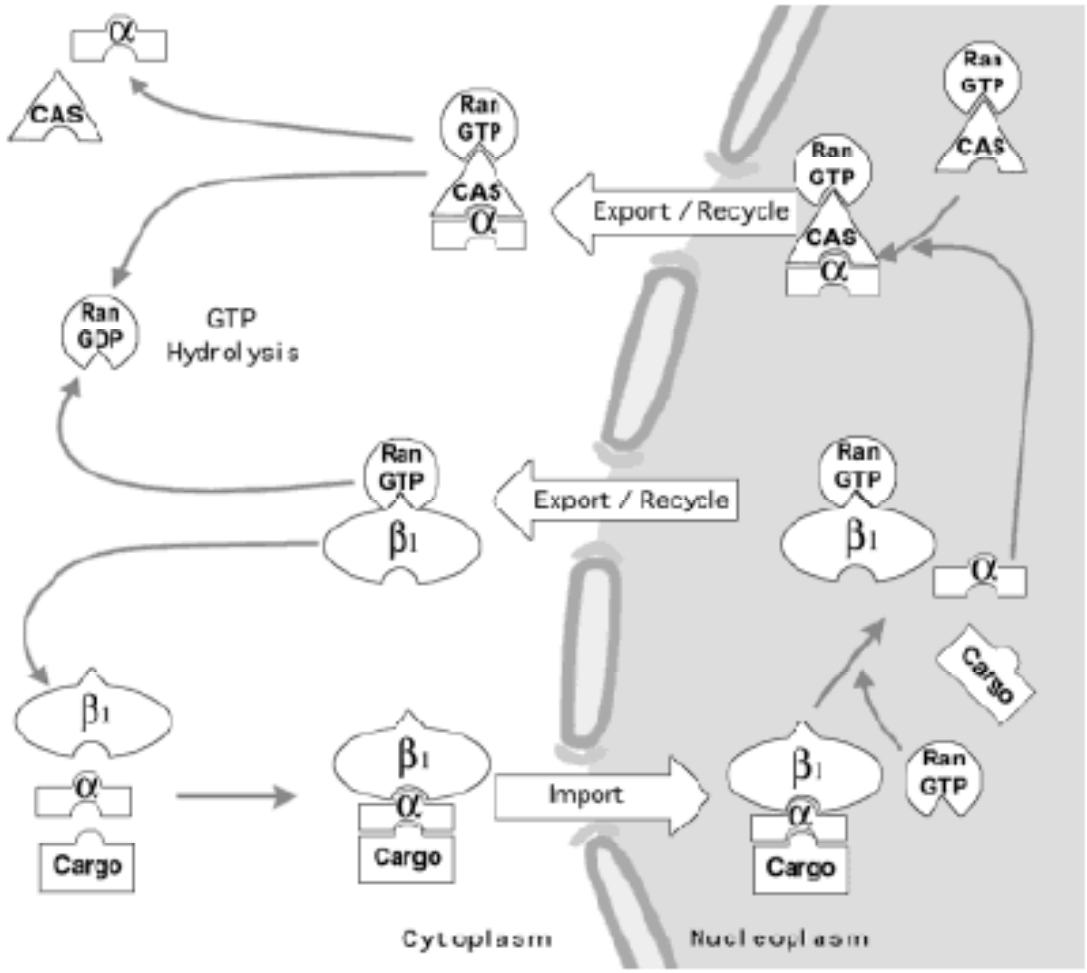

Figure 7: Model for nuclear import of classic NLS-containing proteins. The NLS-protein cargo binds in the cytoplasm to the karyopherin-αß heterodimer, which is stable because of low RanGTP levels. The resulting trimeric complex docks through karyopherin-ß to nucleoporins at the cytoplasmic fibers of the NPC. RanGTP then dissociates the karyopherin-αß complex and thus releases the α-subunit and it NLS-protein cargo into the nucleus. After the completion of the import reaction, karyopherin-α and karyopherin-ß/RanGTP are exported through separate pathways into the cytoplasm. Nuclear export of karyopherin-α is mediated by CAS, a member of the Karyopherin-ß family (adopted from Moroianu, 1999).

III.4.3.3. Proposed transport models

NPCs can perform 1000 translocation events per second, shuttling a mass of ~100MDa per second (Ribbeck and Görlich, 2001). Despite their high transport rate, NPCs are very selective, admitting passage only for molecules with a NLS or for small molecules. Different models have been proposed which explain the selectivity of nuclear transport, all taking into account that active transport occurs via facilitated diffusion which is achieved by interaction of the transport receptors with the FG-Nups.

The **`virtual gate model`** proposed by Rout et al., 2003 states that the pore forms an energetic barrier for the diffusing molecule, increasing with the molecules` size. Interaction with FG-repeats of the nucleoporins increases the probability of cargo-molecules for entering and passing the pore.

The **`oily-spaghetti model`** which was proposed by Macara, 2001 predicts that FG repeats fill and obstruct the pore. By transient binding to the FG-repeats the molecule can enter the pore. Once released from the nucleoporin it diffuses until it finds a new Nup to bind. The circle of binding and release enables the transporter with its cargo pass the nucleus via facilitated diffusion.

The **`selective phase model`** which was proposed by Ribbeck and Görlich indicates, that the FG-repeats form a sieve-like meshwork through weak hydrophobic interactions (Ribbeck, K. and Gorlich, D., 2001). Here the size-exclusion limit is defined by the pore size of the sieve-like net. The mesh-size is about 2.6 nm with some larger openings for passive diffusion of larger molecules. Transport of molecules through the physical barrier depends on the competitive binding of the transport receptor to FG repeats. This binding locally dissolves the meshwork, enabling the cargo-receptor complex to increase its solubility and pass the pore (Ribbek and Görlich, 2001; Mohr et al., 2009).

Peters, 2005 pronounced the **`reduction of dimensionality model`**. It predicts that a continuous FG surface exists from the cytoplasmic filaments to the nucleoplasmic basket. Transport receptors bind to the FG-repeats and

move through the NPC by two-dimensional walk. In the center of the channel, an unobstructed narrow tube exists, that permits the free passage of small molecules. This model is partially supported by Naim et al., 2007, who found that active transport and passive diffusion are segregated. Another possible explanation for the separation of the two transport modalities would be the existence of peripheral channels, which were originally proposed by Hinshaw et al., 1992 and later supported by work from the groups of Hans Oberleithner and Uli Aebi. Through this peripheral channels, passive diffusion of small molecules (< 10nm) takes place whereas active transport occurs through the central channel (Figure 8).

A) B)

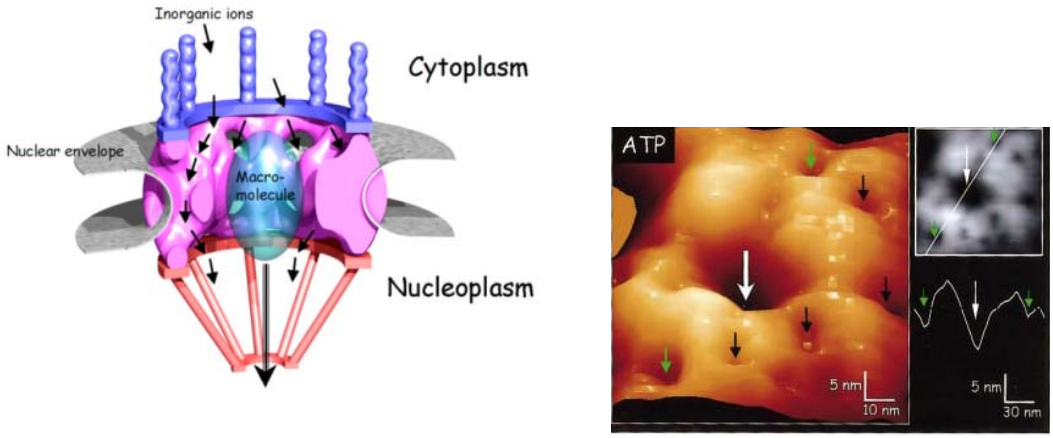

Figure 8: Nuclear Pore Complex A) Model of the NPC with a central channel for the transport of macromolecules and eight peripheral channels for the passive diffusion of small molecules. (from celldynamics.uni-muenster.de) B) AFM image of a nuclear pore and the surrounding peripheral channels. From Shahin et al., 2001

III.4.4. Alterations of nucleocytoplasmic transport

Nucleocytoplasmic transport and – permeability can be regulated and altered by many physiological and pathophysiological mechanisms (Terry et al., 2007). Not only can cargo molecules be modified, resulting in altered transport kinetics but also the nuclear pore complex is object of regulation. But structure and composition of nuclear pore complexes can be flexibly adjusted, enabling the NPC to fulfill specific demands concerning active- and passive transport mechanisms. Furthermore, modifications of Nups e.g. via phosphorylation, influences nuclear pore function. In the following sections, the physiological and pathophysiological alterations of nucleocytoplasmic transport are presented.

III.4.4.1. Stress- and pathogen-induced alterations of the nuclear pore

After infection with enteroviruses and rhinoviruses, Nup62, Nup153 and Nup98 are cleaved by viral protease $2A^{pro}$ (Belov et al, 2004. Gustin and Sarnow 2001, 2002) resulting in increased nuclear envelope permeability. At the execution of apoptosis, the cleavage of 7 out of the 30 Nups (Ferrando-May et al., 2001 and 2006) results in the irreversible disruption of the NPC and loss of permeability barrier function. Even prior to the fatal activation of caspases, the nuclear envelope is altered. Ferrando-May et al., 2001 showed that the nuclear envelope becomes permeable for 70kDa Dextran shortly after staurosporine (STS) treatment, independently of caspase activation. In addition, redistribution of Ran and importin-ß in STS treated cells could be observed. Further, early increase in nuclear envelope permeability has also been observed after cell death induction with H_2O_2 (Mason et al, 2005).

III.4.4.2. Posttranslational modifications of Nups

Phosphorylation of Nups is associated with the loss of protein-protein interaction, leading to nuclear envelope breakdown in mitosis (Courvalin et al., 1992, De Souza et al., 2004) and subsequent loss of permeability barrier function. Even prior to nuclear envelope breakdown in mitosis, phosphorylation of Nups and increased nuclear permeability have been observed (Lenart et al., 2003; Bardina et al., 2009). It has been suggested

that cardioviruses could thereby mimick the mitotic host cell mechanisms to alter nuclear envelope permeability in infected cells (Bardina et al., 2009). The results backing this hypothesis are so far not conclusive. Although addition of staurosporine, a broad spectrum kinase-inhibitor has been shown to reduce cardiovirus-induced increase in nuclear envelope permeability (Lidsky et al., 2006), increased phosphorylation of Nup62 after virus infection is not affected (Bardina et al., 2009). In addition to the effect on nuclear permeability, phosphorylation of Nups reduces active, importin-ß mediated transport but does not influence nuclear export (Kehlenbach and Gerace, 2000). Beside phosphorylation, modification of Nups by glycosylation has been shown. O-linked *N*-acetylglucosamine (O-GlcNAc). addition is more dynamic than phosphorylation and has been proposed to compete with phosphorylation, thereby controlling phosphorylation-induced alterations of the NPC (Miller et al., 1999).

III.4.4.2. Alteration of NPC composition

The residence time of 19 GFP-tagged nucleoporins at the NPC has been determined by fluorescent recovery after photobleaching (FRAP) (Rabut et al., 2004). This study revealed that the nuclear pore complex is a dynamic structure with residence time of the Nups varying from a few seconds to over 70h. Peripheral Nups like Nup153 and Nup50 are highly dynamic whereas scaffold Nups have long resident times. Nup153 and Nup214 have been found in two different regions of the NPC were they are thought to fulfill specialized transport functions (Fahrenkrog et al., 2002). In the slime mould *Aspergillus nidulans,* phosphorylation of peripheral, dynamic Nups by mitotic kinases leads to altered NPC composition (De Souza et al., 2004). The existence of tissue or development-dependent nucleoporins has been proposed. In testis, the abundance of the nuclear pore associated protein Npap60 is ten times higher than in other tissues (Fan et al., 1997). Also in pathogenesis, altered localization and interaction of Nups is observed. In myeloid leukemia, a chromosomal translocation fuses Nup214 to the DNA binding protein DEK and Nup98 to the transcription factor HOXA9, resulting in the nuclear localization of the complexes (Borrow et al., 1996; Fornerod, et al., 1995). Once in the nucleus, the FG-repeats of Nup214 and Nup98 are

supposed to interact and activate transcription factors like CREB binding protein (Kasper, 1999).

III.4.4.3. Modification of the transport machinery

Modification of cargo-molecules can either increase or decrease their affinity for transporter molecules like importin-α or importin-ß. For example, phosphorylation of SV40 large tumor-antigen results in enhanced recognition of nuclear import transporters and nuclear transport whereas phosphorylation of the transcription factor Pho4 decreases importin binding and nuclear import (Jans and Jans 1994; Kaffman et al., 1998). Phosphorylation of p53 results in its nuclear accumulation as export is inhibited (Zhang and Xiong, 2001). Targeting signals of cargo-molecules can be masked by the conformation of a protein. The nuclear localization signal of nuclear factor-κB (NF-κB) is masked in the p105 precursor form of the protein. Phosphorylation of NF-κB results in proteosomal degradation of the p105 precursor C-terminus, revealing the NLS and enabling nuclear import (Riviere et al., 1991). Nuclear transport can also be abrogated by masking the localization signal with another molecule. Binding of I-κB to NF-κB p65 blocks nuclear import by preventing importin- α and -ß recognition (Beg et al., 1992, Pemberton and Paschal, 2005). Defects in the regulation of this mechanisms result in severe deseases, like Hodgkin`s lymphoma or breast cancer. Hodgkin`s lymphoma is associated with extensive phosphorylation and degradation of I-κB, resulting in abnormally high levels of NF-κB p65 in the nucleus, because masking of p65 no longer takes place (Kau et al., 2004). The transport receptor CAS is involved in export and recycling of importin-α. It´s overexpression which is found in many tumors is supposed to increase nuclear import due to increased importin- α-levels in the cytoplasm (Brinkmann et al., 1995; Behrens et al., 2001).

III.4.4.4. Ca^{2+}-induced alterations of nuclear transport and nuclear envelope permeability

Work from various groups shows that nuclear transport and nuclear permeability are influenced by the Ca^{2+} level in the ER. Dunn and coworkers show a Ca^{2+}-sensitive, 5nm displacement of the central mass to the cytoplamic and the nucleoplasmic side of the nuclear pore complex (Moore-Nichols, 2002; Mooren et al., 2004). Further, it was reported that the distal ring of the nuclear basket acts as a Ca^{2+} sensitive iris-like diaphragm (Stoffler et al., 1999) (Figure 9). The reported effects of decreased ER Ca^{2+} -level on nucleocytoplasmic permeability and –transport are diverse. Some results show decreased nuclear permeability and -transport in the presence of low ER Ca^{2+}-level (Stehno-Bittel et al 1995, Greber and Gerace, 1995). This finding is supported by observations of Wang and Clapham in 1999 who used atomic force microscopy to show that depletion of ER Ca^{2+}-level results in decreased width of the nuclear pore channel. Further, decreased nuclear permeability and a visible occlusion of the central channel, due to low ER Ca^{2+}-level, was reported (Perez-Terzic, 1996).

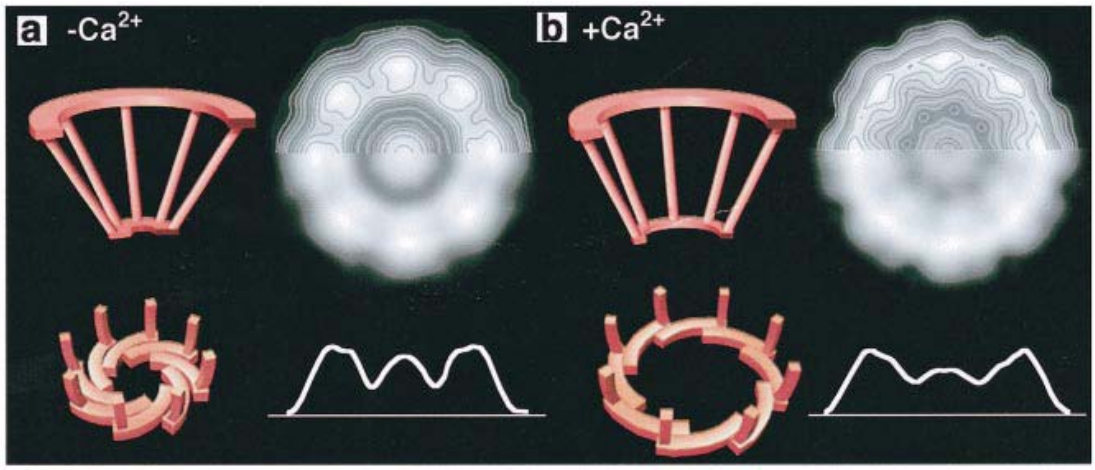

Figure 9: Tentative interpretation of the opening and closing of the nuclear baskets (i.e. the distal rings) in response to adding or removing Ca^{2+} as observed by time-lapse AFM (from Stoffler et al., 1999)

In contrast to the results presented above, increased nuclear permeability elicited by decreased ER Ca^{2+} level has also been shown. Measurements of nuclear envelope electrical resistance (NEER) performed with the nuclear

hourglass method revealed an increased nuclear permeability in the presence of low endoplasic reticulum Ca^{2+}-content (Shahin et al., 2001). In addition to the opposing effects of reduced ER Ca^{2+}-level on nuclear permeability, unaltered nuclear permeability and nuclear transport properties in response to decreased Ca2+ levels have also been reported (Wei et al., 2003; Enss et al, 2003; Strubing and Clapham, 1999).

IV. OBJECTIVES OF THE THESIS

This work is based on published and unpublished findings of our group. These data show:

- Caspase-dependent and caspase- independent alterations of the nucleocytoplasmic permeability barrier in STS induced cell death.
- Bcl-2 induced alterations of the nuclear permeability barrier.

The objective of this study is to further investigate the underlying mechanisms of STS-induced nuclear envelope alterations and to elucidate how and through which mechanisms Bcl-2 influences the nuclear permeability barrier.

AIMS:

(1) Apoptosis-induced alterations of the nucleocytoplasmic permeability barrier

- Employ the established confocal microscopy setup to investigate the influence of two different apoptotic stimuli on nuclear permeability.
- Investigate if the previously observed increase in nuclear envelope permeability in staurosporine-induced cell death is a general effect or stimulus dependent.
- Identify the caspase-independent mechanisms responsible for nuclear permeability alterations in cell death

(2) Effect of Bcl-2 overexpression on nuclear permeability

- Investigate the influence of Bcl-2 on nuclear permeability
- Elucidate the mechanisms responsible for Bcl-2 induced nuclear envelope alterations

V. MATERIAL AND METHODS

V.1. Cell culture

Cells were kept at 37°C, 5% CO2 in a humidified atmosphere. If not stated otherwise, all employed cell lines were cultured in high-glucose DMEM medium supplemented with 10% heat inactivated Fetal Bovine Serum, 100 units/ml penicillin, 100 µg/ml streptomycin and 1mM L-glutamine. Cells were passaged every second or third day to maintain a logarithmic growth phase. For imaging experiments – phenol red Gibco medium, Cat. No. 31053-028 was used with the same additions as to the normal medium

V.2. Preparation of lysates for caspase-activity, viability assay and western blot

Caspase assays, viability assays and western blots were performed using either transfected or non-transfected cells. For transfection experiments, cells were seeded two days prior to lysis. Otherwise, cells were seeded one day prior to lysis. In both cases, the cell density was the same. 2x10exp5 cells/3,5cm dish were plated in a total of 2 ml medium. If needed, one day after seeding, the cells were transfected with 0,6µg of Nup153-GFP and 0,4µg of 4xCherry encoding plasmid, described in *V.8. Transfection*. One ml medium was removed from the dishes, resulting in a remaining volume of 1ml. Then the cells were treated with either STS [0.5µM] or TRAIL [300ng/ml] for 1h, 2h, 4h and 6h. For caspase inhibition, 20µM zVAD was added 30 min prior to stimulus addition. Cells were lysed as follows: all following steps were performed on ice. 330µl 3xPBS was added to each 3,5cm dish, and the cells were scraped off and transferred to a 50ml falcon containing 2ml 1xPBS on ice. The cells were centrifuged for 5min at 1200rpm and 4°C. The supernatant was removed and the pellet dissolved in 200ml 1xPBS. From the cells suspension three different aliquots were taken: i) 10µl were transferred into an Eppendorf cup containing 10µl Fix-solution and stored at 4°C for later scoring at the fluorescence microscope. ii) 90l µl were transferred to a 1.5ml Eppendorf cup and centrifuged for 1min at 13000rpm. This aliquot was used

for measurement of caspase activity; iii) 100 µl were transferred to a 1.5ml Eppendorf cup and centrifuged for 1min at 13000rpm. This aliquot was used for western blot. After centrifugation, the supernatant of ii) was removed and the pellet resuspended in 40µl caspase buffer and frozen in liquid nitrogen. The pellet of iii) was resuspended in 40µl 95°C SDS lysis-buffer complemented with DTT and kept at 95°C for 10min until the pellet was completely dissolved. During the incubation the solution was mixed by vortexing and, if necessary, more buffer was added. Then the solution was centrifuged for 10 min at 13000 rpm and 4°C and the supernatant transferred to a fresh 1.5ml Eppendorf cup, frozen in liquid nitrogen and stored at -80°C.

V.3. Detection of DNA laddering

On th day preceeding the experiment HeLa 229 cells were seeded in 3.5cm dishes at a cell density of 2x10exp5 cells/well in 2ml volume. On the day of the experiments, 1ml medium was removed and either TRAIL (resulting in a final concentration of 300ng/ml) or STS (resulting in a final concentration of 0.5µM) was added. Inhibitors were added 30 min prior to the apoptosis stimulus. Lysis of cells was performed on ice. To each well, 330µl of 3xPBS were added; cells were scraped off using a rubber policeman and transferred to a 50ml falcon containing 2ml of 1xPBS. The cells were centrifuged at 2000rpm and 4°C for 5minutes. The supernatant was carefully removed, the pellet dissolved in 1ml lysis buffer and transferred to a 2ml Eppendorf cup and incubated with occasional vortexing over night at 37°C. On the next day, DNA was precipitated with 1000 µl Isopropanol which was slowly added while carefully shaking the Eppendorf cup. After 4h incubation at 4°C the solution was centrifuged at 13000rpm for 15min at 4°C. The resulting pellet was completely dissolved in 500µl 70% ice-cold ethanol and centrifuged for 15min at 4°C at 13000rpm. The supernatant was removed and the pellet was dried at 37°C.]Then the pellet was dissolved in 19µl TE-buffer and 1µl of freshly made RNase K -solution [20mg/ml] was added. The solution was mixed at 37° for 30min at 500rpm and then 2µl of orange loading buffer was added and the DNA solution separated on a 1.8% agarose gel at 70mV. The

DNA was visualized by ethidiumbromid staining. For solutions see *solutions and buffers*.

V.4. Measurement of Caspase3/7 activity

Caspase 3-like activity was determined by cleavage of the fluorogenic substrate DEVD-afc (DEVD-aminofluoromethyl- coumarin).

A standard curve was measured using the same plate in which the samples were to be measured. All standards were performed in duplicate. The AFC stock solution (500µM) was diluted 1:100 in caspase activity buffer (50 mM Hepes pH 7.5; 1% sucrose; 0.1% CHAPS) and a dilution series with caspase activity buffer was prepared in the same buffer as follows:

0 µM	100 µl buffer /well;
0.125 µM	97.5 µl + 2.5 µl diluted AFC /well
0.25 µM	95 µl + 5 µl diluted AFC /well
1 µM	80 µl + 20 µl diluted AFC /well
2 µM	60 µl buffer + 40 µl diluted AFC /well

The standard curve was measured at 37°C with the standard protocol.

For each sample to be measured 90 µl of substrate solution consisting of caspase-buffer complemented with 20 mM DTT and 44 µM DEVD-AFC (Stock: 10 mM, final concentration 40 µM) was prepared. In the same multiwell plate used for the standard curve, 10 µl of each sample were added and then 90 µl of reagent was added to each well. All samples were measured in triplicates. Air bubbles were removed prior to measurement. The samples were measured with the kinetic protocol at 37°C.

V.4.1. Calculation of caspase activity

From the standard curve (y = **a**x + b) the slope **a** in FU/μM (arbitrary fluorescence units per concentration) was obtained. The kinetic mode measures the time-dependent change of fluorescence due to the cleavage of the fluorogenic substrate in the samples. The value **z** given by the fluorimeter corresponds to the slope of the curve in FU/min.The relative enzymatic activity in μM/min was obtained by dividing the slope of the curve by the slope of the standard curve: rel. caspase units (μM/min) = **z**/**a.** The specific activity was then obtained by dividing the relative caspase activity through the protein concentration in the well in mg/ml and is expressed in nmol/mg min. The final result was obtained by multiplying the specific caspase activity with the dilution factor :10 (10μl sample +90μl solution).

V.4.2. Determination of condensed nuclei

Apoptosis was assessed by scoring apoptotic nuclei. Cells were incubated with 200ng/ml Hoechst 33342 and the percentage of condensed nuclei was determined by fluorescent microscopy.

V.5. Determination of serine protease activity by FLISP assay.

On the day preceeding the experiment 1.5x10exp5 cells/well were seeded in 12-well plates in a total volume of 1ml. On the day of the experiment medium was changed to 1ml medium without FCS. 400μM of either AEBSF or AEBSA were added to the cells 30 min prior to addition of 0.5mM STS. Cells were stimulated with STS for different time durations. All cells were harvested at the same time. Each time point was performed in duplicates. After incubation with STS, 500μl medium were removed from the wells and 10μM FLISP (Fluorescent Labeled Inhibitors of Serine Proteases) reagent (5μl of 50x stock) was added. Cells were incubated for two hours at 37°C. 12-well plates were agitated every 20min for optimal incubation. The supernatant was then transferred to a 50ml tube, the well was washed with warm PBS and the solution was also transferred to the Falcon tube. The cells were trypsinized and also transferred to the falcon tube. The cells were centrifuged

at 1400 rpm (295g) at RT for 5min. The supernatant was aspirated and the pellet resuspended in warm washing buffer and recentrifuged at 1300 rpm (255g) for 5 min. The washing step was repeated two times to completely remove unbound FLISP. The samples were centrifuged again and the pellet was dissolved in 200µl washbuffer. 150µl of the solution were transferred to a 96 well plate and FLISP signal was measured at a wallac plate reader at 485 excitation and 535nm emission wave length.

V.6. Ca^{2+} measurement with Fluo-4

V.6.1. Adaptation of HeLa K and K Bcl-2 cells to low external Ca^{2+}

Two days prior to Ca^{2+} measurement, HeLa K and KBcl-2 cells were plated in 96 well plates at a density of 1.5*10exp5cells/ml in 100µl/well. The following day, the medium of HeLa K cells was changed to low Ca^{2+} buffer. As a control the other HeLa K and Hela KBcl-2 cells were incubated in normal buffer (s.buffers and solutions). On the day of the experiment a 1:1 solution of Fluo4 (1mM) and 20% pluronic acid was prepared. 8µl of this solution were then added to 1ml low – or normal Ca^{2+} buffer, resulting in a final concentration of 4µM Fluo4-AM. After washing the cells carefully! two times with the appropriate buffer (low - or normal Ca^{2+}), 100µl of Fluo-4-AM/Pluronic solution were added. Cells were incubated for 60 min at RT in the dark. Cells were washed two times with either low – or normal Ca^{2+} buffer containing 1mM probenecid and then incubated for 30 min at RT for de-esterification. Directly before measurement, the buffer in all wells was replaced with 150µl low Ca^{2+} medium with probenecid.

The protocol *calcium anfang* was used to measure basal Ca^{2+} signal, then the plate was removed from the reader, 50µl of buffer were replaced with 50µl Thapsigargin-solution (final concentration 5µM) and kinetic of ER Ca^{2+} release was assessed with the *nach-zugabe* protocol. The plate was removed from the plate reader and the medium in all wells was replaced by 150µl normal Ca^{2+} medium to measure capacitive Ca^{2+} influx with the *nach zugabe* protocol.

V.6.2. Measurement of Ca^{2+}-level in HeLa 229 cells treated with STS and TRAIL

On the day preceeding the experiment, cells were seeded in 96-well plates at a density of 1.5*10exp5/ml using 100µl/well. On the day of the experiment a 1:1 solution of Fluo4 (1mM) and 20% pluronic was prepared. 8µl of this solution were then added to normal Ca^{2+} buffer, resulting in a final concentration of 4µM Fluo4-AM. After washing the cells carefully two times with normal Ca^{2+} buffer, 100µl of Fluo-4-AM/Pluronic solution was added to each well. After incubation for 60 min at RT in the dark, cells were washed two times with normal Ca^{2+} buffer with 1mM probenecid and then incubated for 30 min at RT for de-esterification. Directly before measurement, the buffer in all wells was changed to 150µl fresh normal Ca^{2+} medium with probenecid.

The protocol *calcium anfang* was used to measure basal Ca^{2+} signal, then the plate was removed from the reader, 50µl of buffer were replaced with 50µl Thapsigargin-solution (final solution 5µM) and kinetic of ER Ca^{2+} release was assessed with *nach-zugabe* protocol.

V.7. SDS-Page and Western Blot

V.7.1. Determination of protein concentration

Protein concentration was determined with the BCA Protein Assay Reagent (Pierce). A standard curve as described in the manufacturer`s protocol was measured in 96-well plate. In the same plate, 5µl of each sample were mixed in a well with 95µl of a BCA solution consisting of 1 part solution A and 50 parts of solution B, both provided by the manufacturer. After incubating the samples for 30min at 37°C, protein concentration was determined by measuring the amount of emitted light from each well at 550nm in a fluorescent plate reader. The protein concentration of the samples was then calculated by using the standard curve.

V.7.2. SDS-Page according to Thomas Kornberg

SDS-PAGE of nuclear pore complex proteins was performed according to Thomas and Kornberg. (Thomas and Kornberg, 1975). 80-100µg protein in 10x sample buffer (final concentration 1x) and 1x loading buffer (s. buffers and solutions), were loaded on the SDS – gel after boiling for 5minutes. The gel had a ratio of acrylamide (Rothiphorese Gel A):bisacrylamide (Rothiphorese Gel B) of 30:0.15, and was run at a constant voltage of 40 V until samples left the stacking gel. Then the voltage was switched to 120 V.

Two markers for protein sizes were used: a broad-range biotinylated marker (Biorad) and a prestained Protein Molecular Weight Marker (Fermentas).

V.7.3. Western blot

After electrophoresis was completed, the protein was blotted on a nitrocellulose membrane over night in a wet blot device. The transfer stack was build as follows: First a packing sponge was put on the black cathode side followed by three layers of Whatman 3MM paper and the gel. On the gel, the nitrocellulose membrane was placed, followed again by three sheets of Whatman 3MM paper and a packing sponge. All parts of the stack were soaked with blotting buffer (s.buffers and solutions). The gel was run for 45 min at 400 mA and 300 W, then 3,8ml of 10% SDS were added and the gel was run overnight at 350mA and 300W. On the next day, the membrane was washed in tab water and stained with Ponceau red (0.2% Ponceau S, 5% acetic acid) to control the transfer of proteins from the gel to the membrane. While the staining was still visible, the marker lane was cut off the membrane, as it does not need a primary antibody (biotinylated). After that, the membrane was washed several times in TNT (s. buffers and solutions) followed by incubation for at least two hours at room temperature in TNT with 5% milk powder to block unspecific antibody binding. The membrane was incubated with the primary antibody in 5% MP/TNT for 24-72 hours at 4°C. After washing the membrane several times with TNT, the second antibody was added in 5%MP/TNT for at least one hour at room temperature. The marker was incubated with streptavidin - HRP 1:5000 in TNT. After incubation, membrane and marker lane were washed several times in TNT,

incubated with freshly made developing solution (s. buffers and solutions) for 3 min and HRP signal was detected by exposure of the membrane to x-ray films.

V.8. Transfection

Transfection of all cells was performed with EFFECTENE.

In all experiments, the medium in the dishes was replaced by fresh medium 4-10 hours after transfection

V.8.1. Co-transfection of 4xCherry and Nup153-GFP

HeLa 229 cells were transfected with a total of 1µg DNA, Effectene and Enhancer was used according to the manufacturers protocol as for a total amount of 0.8µg. Effectene: 8*0.8µg= 6.4µl; Effectene: 10*0.8µg=8µl.

Protocol for one IBIDI-dish containing 3ml medium:

140 µl EC –buffer

0,4µg plasmid DNA encoding for 4xCherry

0,6µg plasmid DNA encoding for Nup153-GFP or mutant Nup153-GFP

6,4 µl Enhancer

→ vortex ~ 1s; incubate ~ 4 min at RT

8µl Effectene

→ vortex ~ 5s; incubate ~ 8 min at RT

200µl medium from the IBIDI containing the cells to be transefected were added to the transfection mixture and then the whole solution was added to the IBIDI dish.

For the transfection of many dishes, a mastermix was prepared. To this mix, some medium was added and the solution was equally divided among the dishes.

In all experiments, the medium in the dishes was replaced by fresh medium 4-10 hours after transfection

V.8.2. Co - transfection of plasmid DNAs encoding for 4xCherry and GFP-NLS

HeLa 229 cells were transfected with a total of 0.6 µg DNA, Effectene and Enhancer was used according to the manufacturers protocol as for a total amount of 0.6µg. Effectene: 8*0.6µg= 4.8µl; Effectene: 10*0.6µg=6µl.

Protocol for one IBIDI-dish with 3ml medium:

140 µl EC –buffer

0,4µg plasmid DNA encoding for 4xCherry

0,2µg plasmid DNA encoding for GFP-NLS

4.8 µl Enhancer

→ vortex ~ 1s; incubate ~ 4 min at RT

6µl Effectene

→ vortex ~ 5s; incubate ~ 8 min at RT

200µl medium from the IBIDI containing the cells to be transefected were added to the transfection mixture and then the whole solution was added to the IBIDI dish.

For the transfection of many dishes, a mastermix was prepared. To this mix, some medium was added and the solution was equally divided among the dishes.

In all experiments, the medium in the dishes was replaced by fresh medium 4-10 hours after transfection

V.8.3. Co-transfection of plasmid DNAs encoding for 4xCherry and SERCA

HeLa 229 cells were transfected with a total of 1 µg DNA, Effectene and Enhancer was used according to the manufacturers protocol as for a total amount of 0.6µg. Effectene: 8*1µg= 8µl; Effectene: 10*1µg=10µl. Cells were either transfected with 0.3µg plasmid DNA encoding for 4xCherry and 0.7µg plasmid DNA encoding for SERCA or with 0.3µg plasmid DNA encoding for 4xCherry and 0.7µg plasmid DNA encoding for empty vector pcDNA3.1.

Protocol for one IBIDI-dish with 3ml medium:

140 µl EC –buffer

0,3µg plasmid DNA encoding for 4xCherry

0,7µg plasmid DNA encoding for empty vector pcDNA3.1 or SERCA

8 µl Enhancer

→ vortex ~ 1s; incubate ~ 4 min at RT

10µl Effectene

→ vortex ~ 5s; incubate ~ 8 min at RT

200µl medium from the IBIDI containing the cells to be transefected were added to the transfection mixture and then the whole solution was added to the IBIDI dish.

For the transfection of many dishes, a mastermix was prepared. To this mix, some medium was added and the solution was equally divided among the dishes.

In all experiments, the medium in the dishes was replaced by fresh medium 4-10 hours after transfection

V.9. Determination of nuclear 4xCherry

V.9.1. Determination in live cells:

Localisation of nuclear 4xCherry in the nucleus was determined by fluorescence microscopy. Only cells showing at least the same 4xCherry signal in the nucleus as in the cytosol were scored as having a nuclear 4xCherry localization. Localization of 4xCherry in all cells except in SERCA overexpressing cells and the respective controls, was detected in live cells, 24h-48h after transfection. To this end cells were seeded and transfected in IBIDI dishes, according to the described transfection protocol and 24h-48h after transfection nuclear 4xCherry was detected. After scoring, cells were still viable for several days in the incubator.

V.9.2. Determination in fixed cells in combination with SERCA-specific immunostaining

For detection of the effect of SERCA overexpression on nuclear permeability, cells were seeded in 12-well plates containing 16mm coverslips. On the next day, Hela KBcl-2 cells were transfected with plasmid DNA encoding for either SERCA and 4xCherry or with plasmid DNA encoding for 4xCherry and empty vector pcDNA3.1. HeLa K cells were transfected with plasmid DNA encoding for 4xCherry and empty vector pcDNA3.1 (as described in V.8. Transfection). 24h-48h after transfection, cells were fixed overnight in 4%PFA. Fixation overnight is necessary to maintain proper 4xCherry localization. Then cells were washed for at least 20min in PBS immunostaining with anti-SERCA specific antibody was performed. If not stated otherwise, all steps were performed at RT. Cells were blocked with 50mM NH_4Cl for 20 minutes, washed two times 5 minutes in PBS and permeabilized in 0.1% Triton for 5 minutes. Cells were washed 3 times for 5 min in PBS and blocked with 1%BSA/PBS for at least 30 minutes. After blocking, cells were incubated overnight at 4°C with anti-SERCA antibody (IID8), diluted 1:750 in blockingbuffer. On the next day, cells were washed three times, (for 5, 10, 15 minutes) with PBS and then incubated with secondary antibody, alexa488 anti-mouse, diluted 1:400 in blockingbuffer for at least 1h. After washing the cells three times, (for 5, 10, 15 minutes) with PBS, cells were labeled with 200ng/ml Hoechst for 10min. The slides were mounted in Aquapolymount and dried at 4°C over night. 4xCherry specific fluorescence in cells overexpressing SERCA was detected and compared to signal in cells without SERCA overexpression in Hela K and HeLa KBcl-2 cells.

V.10. Live cell imaging

V.10.1. Preparation of cells

Two days prior to the experiment, HeLa 229 cell were seeded in IBIDI dishes with a density of 1*10exp5cells/dish in 2ml total volume. On the next day, cells were transfected with the proper constructs as decribed in *V.5. Transfection.* On the day of the experiment, the culture medium was replaced with the same medium lacking phenol red to reduce background

fluorescence. Addition of 150ng/ml Hoechst to the culture resulted in fluorescent labeling of the chromatin. The IBIDI dishes were then transferred to the microscope stage and placed in a heated, CO_2 controlled chamber, to achieve proper incubation conditions. To this end, temperature was adjusted to 38.1 °C at the controller device. The cells were left undisturbed for 1h (prior to imaging of apoptosis) or at least two hours (prior to imaging of mitosis). The two hour preincubation at the microscope stage in the case of mitosis experiments was necessary in order to increase the number of cells which undergo cell division within the first hours after starting the experiment. A shorter preincubation resulted in a delayed entry into mitosis and thus longer imaging times.

V.10.2. Confocal microscopy settings

Confocal time lapses were acquired at a LSM Zeiss 510 Meta using a Plan-Apochromat 63x /1.4 oil objective. The following laser settings were employed:

405nm: 0.1% transmission

488nm: 5% transmission

543nm: 6% transmission

These conditions of low laser intensity ensured optimal cell viability. To compensate for the resulting low signal intensities, high detector sensitivities were used. The signal to noise ratio was relatively low but nevertheless sufficient for proper quantitation of the time series.

Pinhole settings:

As the 405nm laser line is the most phototoxic irradiation, the intensitiy was kept to a minimum (see above). To obtain enough signal at the detector, a maximum pinhole diameter was chosen, allowing to minimize phototoxicity. For analogous reasons, it was not possible to use the optimal pinhole size of one Airy unit for excitation with the 488nm (GFP) and 543nm (4xCherry) laser lines. In this case, a pinhole diameter of about two Airy units was chosen for both detection channels, ensuring the same slice thickness. The

aim of the confocal setup was to image only regions contained within the nuclear volume excluding emission from the cytoplasm below or above the nucleus. The chosen pinhole settings resulted in a slice thickness of 1.5 µm which is still clearly below the diameter of the nucleus of 10-20µm. A z-stack of three slices with a spacing of 0.6 µm was recorded. This allowed to compensate for deformations of the live cells during the experiment and resulted in at least one slice representing an equatorial section of the nucleus.

V.10.3. Data acquisition

For each experiment, 10-13 cells were imaged at a 5x zoom in a time interval of about eight minutes. If necessary, a delay between the acquisition rounds was defined to keep this time frame constant. After the first imaging cycle, the apoptotic stimulus was added. During the autofocusing procedure the nuclei were scanned in the Hoechst channel over a z-range of 30 µm with a specific z-step interval (here: 0.6 µm) resulting in a defined number of scans (5 in this case). The autofocus routine detects the center of mass of the Hoechst signal and centers the nucleus within the recorded frame. To give good results this procedure required a specific cell density: if two cells were too close, the autofocus routine would center on the brighter nucleus, which might be not the one originally chosen.

V.10.4. Data evaluation

The images taken during each time series were saved in one file according to the sequence in which they were recorded (Cell no. 1, first cycle; cell no. 2 first cycle;…..cell no. 1 second cycle; cell no. 2 second cycle; etc.) To obtaine a proper time course of each individual cell the raw data were concatenated. The resulting image stacks consisted of three channels: blue for Hoechst-DNA; red for 4xCherry and green for Nup153-GFP or GFP-NLS. Further, for each time point three z-slices were recorded. For each time point, the optimal z-plane, was chosen for evaluation (command: *gallery→ time+Z →subset*). The open source software Image J was the used to combine the resulting substacks (e.g. slice 1-3 and slice 4-20 of the one cell) (command:

plugins → stacks → stack builder). For each time point all three channels were evaluated separately.

V.10.4.1. Determination of nuclear rim fluorescence

The nuclear rim fluorescence was visualized by transfecting the cells with plasmid DNA encoding for either wt - or caspase-uncleavable Nup153-GFP. Data evaluation was performed with image J. To this end, for each time point of the Nup153-GFP-series, all parts of the rim structure which were in focus were marked as shown in Figure 10 and the intensity in the resulting region of interest (ROI) was measured.

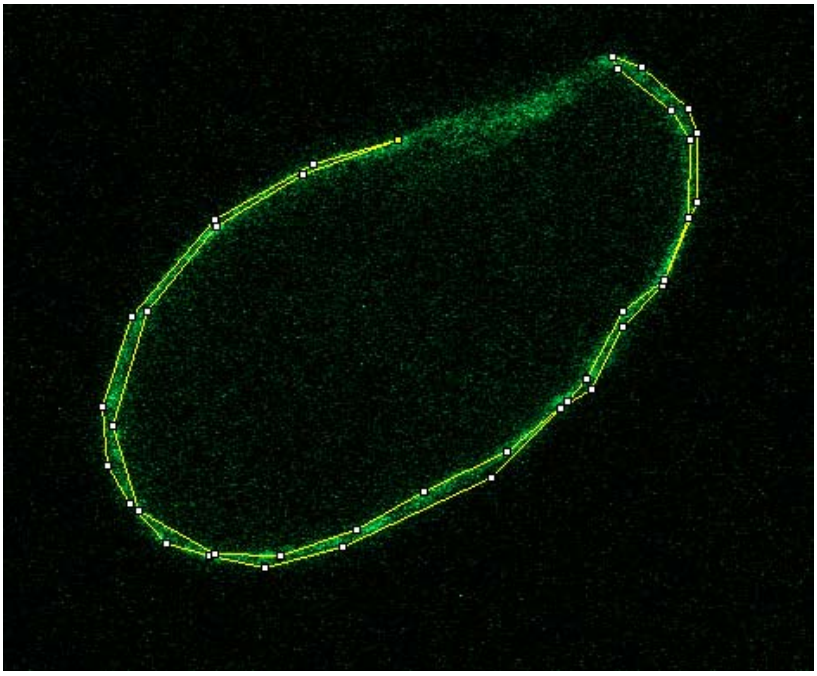

Figure 10: In focus regions of the Nup153-GFP labeled rim were marked and the intensity in the ROI was measured.

V.10.4.2. Determination of Hoechst and 4xCherry signal

The intensities of the Hoechst signal and the nuclear 4xCherry signal were measured using identical ROIs. First, the inner border of the nuclear rim was marked using the Nup-153-GFP channel. This ROI was then transferred to the Hoechst and the 4xCherry channels and the intensities of the respective signals were measured (Figure 11)

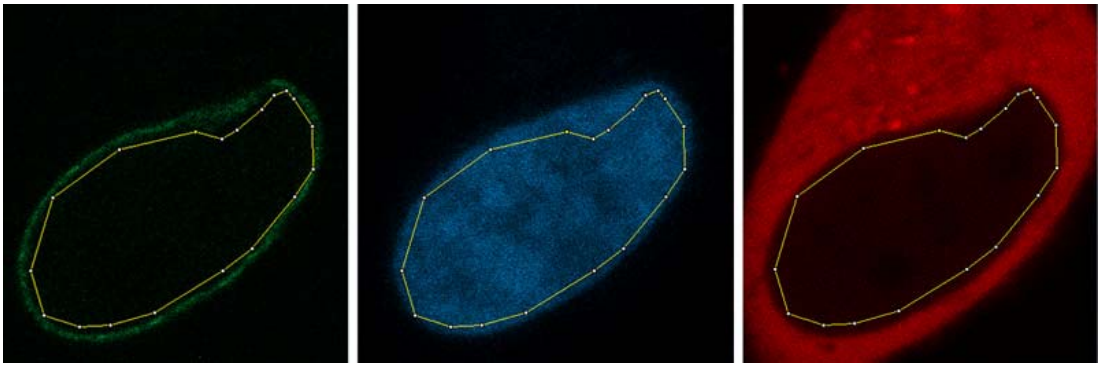

Figure 11: A ROI along the inner border of the nuclear rim was drawn (left image) and then transferred to the other two channels where the respective intensities were measured.

V.11 Material

V.11.1. Cell lines

HeLa 229 cells (human cervix carcinoma) were a kind gift of the Karolinska Institute (Stockholm, Sweden).

Hela K cells (human cervix carcinoma) and MEF 3T9 WT cells and MEF Bax/Bak DKO cells (mouse embryonic fibroblasts) were a kind gift from Prof. Christoph Borner from Freiburg.

Hela KBcl-2 cells were achieved by stable transfection of HeLa K cells with pcDNA3-mbcl2 (Patricia Grote, Dissertation).

V.11.2. Medium

DMEM high glucose (41966-029) cell culture medium and media supplements as penicillin, streptomycin and L-glutamine were purchased from Life Technologies. Cell culture flasks and dishes were purchased from Costar GmbH. Fetal calf serum was obtained from Biochrom AG

V.11.3. Buffers and solutions

V.11.3.1. Ca^{2+} Buffer

Normal Ca^{2+} buffer:

		1l	200ml
Hepes	20 mM	4,8 g	0.96g
NaCl	140 mM	8,2 g	1.64g
KCl	5 mM	0,4 g	0.08g
MgSO4 x7H2O	1 mM	0,24 g	0.048g
CaCl2	1 mM	0,15 g	0.03g
NaH2PO4	1 mM	0,12 g	0.024g
Glukose	5.5 mM	0,99 g	0.198g

Adjust pH 7,4 with NaOH; sterilize by filtration

Low Ca^{2+} buffer:

		1l	200ml
Hepes	20 mM	4,8 g	0.96g
NaCl	140 mM	8,2 g	1.64g
KCl	5 mM	0,4 g	0.08g
MgSO4 x7H2O	1 mM	0,24 g	0.048g
CaCl2	1 mM	0,15 g	0.003g
NaH2PO4	1 mM	0,12 g	0.024g
Glukose	5.5 mM	0,99 g	0.198g

Adjust pH 7,4 with NaOH; sterilize by filtration

V.11.3.2. Solutions for western blot

Blotting buffer:

11.4 g Tris

57.2 g glycine

ad 4 liters VE

Developer solution:

Solution A: 4.4ml H2O

500µl 1M Tris-HCl pH 8.5

50µl 250mM Luminol, resuspend well

22µl 90mM Coumaric acid, resuspend well

Solution B: 4.5ml H2O

500µl 1M Tris-HCl pH 8.5

3µl 30% H_2O_2 (SIGMA)

Directly before use mix 2.5ml of A with 2.5ml of B. Separate solutions are stable for 24h.

V.11.3.3. Solutions for cell lysates, caspase activity and DNA laddering

1xPBS/3xPBS:

For 12ml 1xPBS/ 4 ml 3xPBS

120µl Roche (100x solution = 1 pellet in 500µl MQ)

12µl DTT 1M

Add~ 11,9ml /~3,9ml PBS

Caspase activity buffer:

50 mM Hepes pH 7.5

1% sucrose

0.1% CHAPS

Sterilize by filtration

Caspase lysis buffer:

25mM Hepes pH7,5 1.25ml from 1M

5mM MgCL2 2.5ml of 0.1M

1mM EGTA 0.5ml of 0.1M

0.5% Triton X 100 0.25ml of 100%

Ad 50ml MQ, sterilize by filtration

SDS lysis buffer:

0,5% SDS	0,25ml of 20%SDS
0,05M TRIS-HCL pH 7,5	0,5ml of 1M

ad 10ml MQ

directly before use: add 1µl von DTT 1M to 1ml Buffer and heat at 95°C

DNA lysis buffer:

100 mM Tris-HCl, pH8.5,	2ml of 1M Stock
5 mM EDTA,	770µl of 130mM Stock
0.2 M NaCl,	4ml of 1M Stock
0.2% SDS,	200µl of 20% Stock

Ad MQ 20ml

directly before use add 0.2 mg/ml proteinase K

Fix-solutions:

For 96-well plates:

1ml Formaldehyde

0.5ml PBS

5µl Hoechst

50µl of soultion to 100µl in well

For lysate fixation:

600µl Formaldehyde

1200µl PBS

3µl Hoechst

Mix 1:1 with lysate

V.11.4. DNA constructs and transfection reagents

pNup153-GFP was kindly provided by Dr. Jan Ellenberg (Heidelberg).

pcDNA3.1-4xCherry was constructed by Karin Schäuble during her diploma thesis.

pcDNA3-mbcl2 was kindly provided by Prof. Christoph Borner (Freiburg)

pSERCA2 was kindly provided by L. Scorrano (University of Padua).

pNup153-D349N-GFP (caspase non-cleavable mutant of Nup153-GFP) was constructed by Patricia Grote.

Cells were transfected using EFFECTENE from Qiagen; cat No. 301425

V.11.5. Chemicals

Bachem Biochemica GmbH, Heidelberg, Germany: z-Val-Ala-DL-Asp-fluoromethyl-ketone (zVAD-fmk).

Bender & Hobein GmbH, Heidelberg, Germany: Pierce BCA protein assay reagent.

BioRad Laboratories GmbH, Munich, Germany: biotinylated SDS-Page standards

Biomol, Hamburg, Germany: Asp-Glu-Val-Asp-aminotrifluoromethylcoumarine (DEVD-afc).

Merck, Darmstadt, Germany: acetonitrile, β-mercaptoethanol, dithiothreitol (DTT), formaldehyde, sucrose. BAPTA/AM Cat.No. 196419, Calpeptin Cat. No. 03-34-0051

Molecular Probes Europe BV, Leiden, Netherlands: Hoechst 33342, Fluo-4, AM F14201, Probenecid P36400, Pluronic® P3000MP F-127.

Polysciences: Aquapolymount, Cat No. 18606

Roche, Germany: complete protease inhibitor mix.

Roth GmbH & Co., Karlsruhe, Germany: acetic acid glacial, glycine, ethanol, 4-(2-hydroxyethyl)piperazine-1-ethanesulfonic acid (HEPES), ponceau S, rotiphorese gel 30, sodium chloride, Tris.

Serva, Heidelberg, Germany: acrylamid-bis (37.5:1) 30 % (w/v), ammonium persulfate, coomassie brillant blue G250, glycerol, paraformaldehyde, silicone oil, sodium dodecylsulfate (SDS), 1,2-Bis(dimethylamino)ethane (TEMED).

Sigma-Aldrich Chemie GmbH, Deisenhofen, Germany: 7-amino-4-trifluoromethyl-coumarin (AFC), bovine serum albumin (BSA), 3-[(3-cloamidopropyl)-dimethylammonio]-propanesulfate (CHAPS), cycloheximide (CHX), digitonin, creatine phosphokinase, dimethylsulfoxide (DMSO), ethidium bromide, ethylendiamine tetraacetic acid (EDTA), ethylglycol-bis(_-aminoethylether) tetraacetic acid (EGTA), glycine, glycerol, luminol, normal goat serum, phosphocreatine, proteinase K, tris-(hydroxymethyl)-aminomethan (Tris), Triton X-100, trypan blue 0.4 %, Tween 20.

V.11.6. Antibodies

Anti-SERCA antibody (IID8) was obtained from Alexis. Catalogue number: Alx-804-048

VI. RESULTS

VI.1. Apoptosis induced alterations of the nucleocytoplasmic permeability barrier.

In order to investigate apoptosis-associated alterations of the nuclear permeability barrier and to characterize the temporal dynamics, a time lapse confocal microscopy approach was chosen. To this end, HeLa 229 cells were transfected with different constructs. Firstly Nup153-GFP, a fluorescently labeled nuclear pore protein that is cleaved by caspases in apoptosis (Ferrando-May et al., 2001). This cleavage detaches the GFP moiety from the nuclear rim, resulting in decreased nuclear rim fluorescence. The second marker construct is a tetrameric mCherry construct (4xCherry) which localizes to the cytosol in healthy cells (Karin Schäuble, Diploma thesis, 2006). This construct serves as a permeability marker as it has no nuclear localization signal and is not able to pass the nuclear envelope by diffusion due to its size of 106 kDa. 24hours after transfection, the chromatin was labeled with Hoechst and the dishes with the living cells were placed in a heated and CO_2 controlled imaging chamber under the microscope (see Material and Methods). To ensure comparable conditions in all experiments, the cells were cotransfected with 4xCherry and one Nup153-GFP construct, even if only one reporter was to be analyzed. Confocal live cell imaging was performed over a period of several hours and cells were treated with one of the two apopotic stimuli TRAIL or STS. The fluorescence intensity at the nuclear rim (Nup153-GFP) and the 4xCherry fluorescence signal in the nucleus was quantitated and displayed over time.

VI.1.1. Mitosis induces complete disruption of the nuclear envelope, resulting in the temporal loss of its permeability barrier function

To validate the experimental system and to exclude phototoxicity due to imaging over severl hours, changes of nuclear integrity and permeability were followed in mitotic cells. To this end, cells were transfected with Nup153-GFP and 4xCherry, labeled with Hoechst and imaged for up to 36

hours (Figure 12). Chromatin structure visualized by Hoechst, 4xCherry fluorescence in the nucleus and nuclear rim fluorescence were detected as described in Material and Methods. In prophase, the nuclear envelope is degraded, resulting in the total loss of Nup153-GFP-fluorescence. Furthermore, the absence of the nuclear envelope enables the permeability marker 4xCherry to freely diffuse into the nucleus (Figure 12B). The chromatin condenses, resulting in a increased Hoechst signal. As mitosis proceeds, chromosomes are arranged in the equatorial plane of the cell (metaphase, Figure 12C) and the sister chromatids are separated and pulled to opposite poles of the cell (anaphase Figure 12D). Finally, the two daughter cells are formed and the nuclear envelope is rebuilt resulting in restored Nup153-GFP signal at the nuclear rim of both daughter cells (Figure 12E). In parallel, the permeability barrier function of the nuclear envelope is restored and the 4xCherry again localizes to the cytoplasm (Figure 12E). In summary, this set of experiments shows on the one hand that the chosen reporters are suited to detect dismantling of the nuclear envelope and the breakdown of the nuclear permeability barrier. On the other hand they confirm that the illumination and incubation conditions chosen allow for cell division and thus are compatible with cell viability.

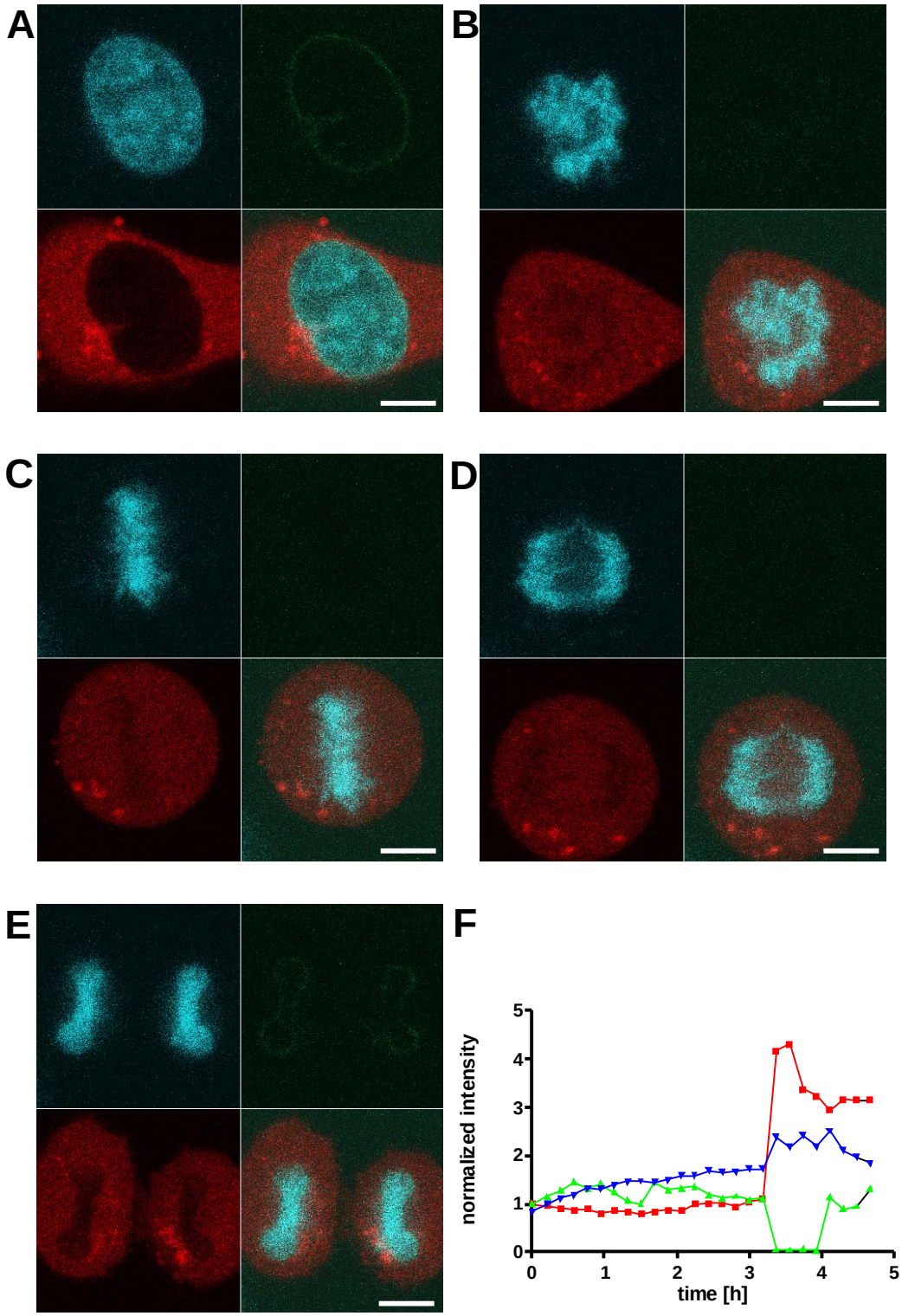

Figure 12: Nuclear envelope dismantling in mitosis. A) –E) confocal images of a mitotic HeLa 229 cell transfected with Nup153-GFP (green) and 4xCherry (red). Chromatin is labeled with Hoechst (blue). A) In S-phase, the cell shows a clear nuclear rim staining, the chromatin is homogeneously distributed and the 4xCherry is located in the cytosol. B) In prophase, chromatin reorganizes into chromosomes

and the nuclear envelope is degraded, resulting in the complete loss of nuclear rim fluorescence and loss of nuclear permeability barrier function. C) In metaphase, chromatin is arranged at the equatorial plane, D) In anaphase, the sister chromatids are pulled to opposite poles. E) In telophase, the two daghter cells are separated. Around each nucleus a new nuclear membrane is build from fragments of the parent cell`s nuclear membrane. The Nup153-GFP signal is again visible. In parallel, the permeability barrier function of the nuclear envelope is restored, resulting in the exclusion of 4xCherry from the nucleus. F) Evaluation of the cell in A) – E). Blue: Hoechst intensity; Green: Nup153-GFP intensity at the nuclear rim; Red: 4xCherry signal in the nucleus.

VI.1.2. Data visualization

Data for nuclear envelope permeability (red channel), for nuclear pore integrity (green channel) and for chromatin condensation (blue channel) were obtained from confocal time series as described in Material and Methods. From these data, the backround signal was subtracted. To account for bleaching, the resulting values were then corrected by dividing by the equation: $e^{(-k*t)}$ (with k being the bleaching constant and t the time) and finally normalized to the starting intensity.

The bleaching constants k were obtained by imaging untreated cells under the same conditions. For each channel and time point, the measured mean grey value (M_t) was normalized to the value of the first time-point (M_1): (M_t/M_1). The LNs of the obtained values were plotted over time. The slope of the regression line is the bleaching constant k.

Chromatin condensation is a hallmark of apoptosis and was therefore employed to define the time point of apoptosis execution. Chromatin condensation was determined as strong increase in Hoechst signal (Figure 13 A,B, blue trace). The time point of chromatin condensation was set when Hoechst fluorescence increased abruptly by a factor of at least 1.07. All following time points had to display at least the same value.

As the kinetics of cell death differ between individual cells, plotting of averaged traces was problematic. In Figure 13 the traces of two different cells (A,B) and the two respective averaged graphs (C,D) are shown in order to illustrate this point.

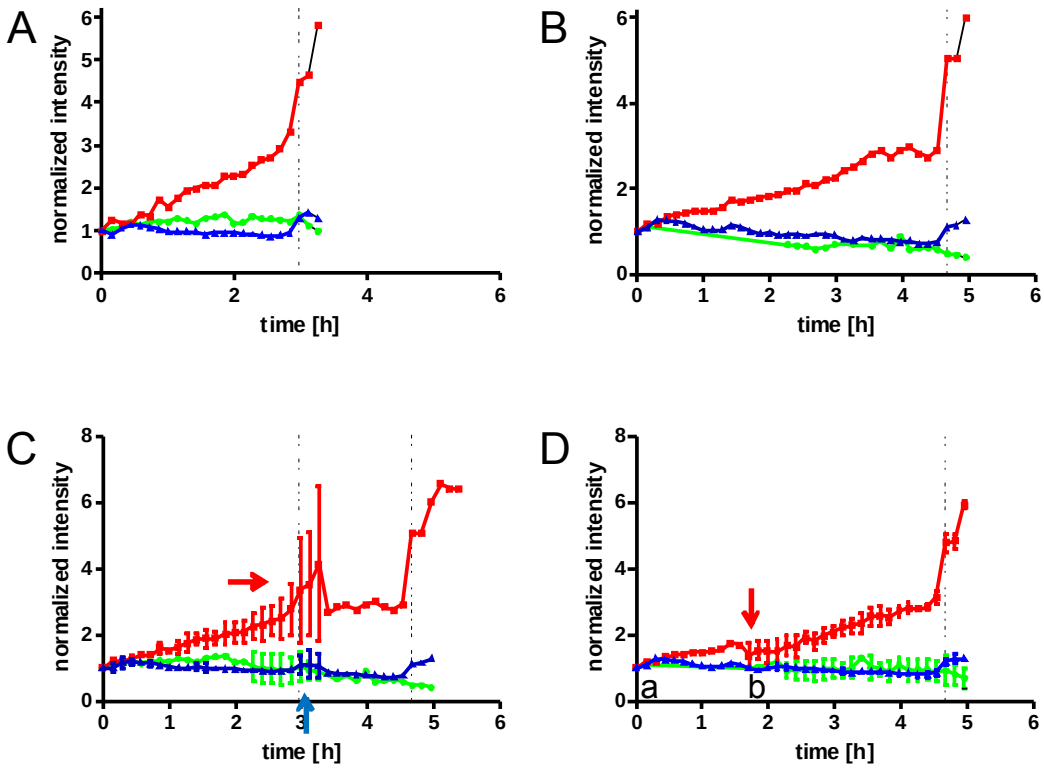

Figure 13: Data evaluation is problematic due to varying apoptosis kinetics. Traces of two different cells with different kinetics are shown. A) undergoes apoptosis after 3h (marked by chromatin condensation, jump increase in blue trace), whereas the cell in B) shows chromatin condensation only after 4.5 hours. C) and D) depict two suboptimal averaging solutions

The cells in Figure 13 A) and B) show the same early, steady increase in 4xCherry signal and a late, abrupt increase of 4xCherry signal (red traces) at chromatin condensation (jump-increase in blue trace). The kinetics, however, are different. Apoptosis proceeds faster in cell A) than in cell B). This can be judged by the different time points when chromatin condensation occurs: in cell A) after about 3h (blue trace, dotted line), whereas in cell B) chromatin condensation occurs after about 4.5h. In 13 C) cells are averaged from the start of the experiment. With this method, two different time points of chromatin condensation occur, resulting in a falsified time course of 4xCherry

signal (red arrow; Figure C) and Hoechst signal (blue arrow, Figure C). In D) cells were averaged in such a way that the time points of chromatin condensation of both cells were superimposed. Although this averaged graph better resembles to the two single graphs, a problem arises due to the different durations of the two apoptosis time courses (A; B). Since the data of the individual traces are normalized to the fluorescence signal at the beginning of the experiment which is set as 1, the value of the later starting point of the second cell falsifies the effect of 4xCherry increase (red arrow, Figure 13 D).

A solution for this problem was found by splitting the x-axis (Figure 14). On the left x-axis, the traces are displayed from the start of the experiment and only time points prior to chromatin condensation are depicted. On the right x-axis the time points corresponding to chromatin condensation are superimposed: two time points prior to chromatin condensation and two time points after chromatin condensation are plotted. Instead of the actual time values, the x-axis shows the numbering of the time points with 0 beeing the time point of chromatin condensation. The distance between time points is eight minutes, as every eight minutes an image of each cell is taken.

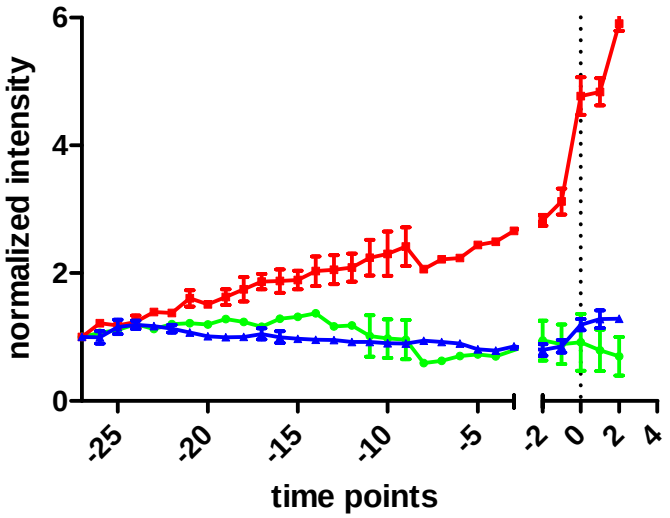

Figure 14: Final averaging and plotting of data. The x-axis is splitted. On the right x-axis the two cells are superimposed to chromatin condensation, on the left, the traces are averaged until the onset of chromatin condensation

The number of time points given on the x-axis correlates with the duration of the apoptotic process and depends on the stimulus used. The number of time points plotted on the x-axis was determined by the time span in which 90% of the cells are apoptotic. In TRAIL–induced apoptosis, 90% of the cells die after 96 minutes, so 12 time points, with an interval of about eight minutes between each data point prior to chromatin condensation are plotted. In STS treated cells, 90% of the cells undergo apoptosis within 216 minutes. Hence, 27 time points prior to chromatin condensation are depicted (Figure 14). On the left x-axis, the averaged traces of all measured cells until the onset of chromatin condensation are shown. On the right x-axis, the traces are superimposed at the time point of chromatin condensation, visualized by abrupt increase in Hoechst signal, as time point 0 (Figure 14, dotted line). Two time points prior to- and after chromatin condensation are displayed.

VI.1.3. STS and TRAIL trigger a similar caspase-mediated collapse of the nuclear envelope barrier but differ in early permeability barrier function.

To visualize apoptosis-induced effects on chromatin and nuclear envelope function, confocal live cell imaging experiments using two different apoptotic stimuli, TRAIL, 300ng/ml (Figure 15 A)) and STS, 0.5µM (Figure 15 B) were conducted. The fluorescence signal of the nuclear rim in cells transfected with wild type Nup153-GFP or caspase - uncleavable Nup153-GFP (mutNup) in the presence or absence of the caspase inhibitor zVAD was detected as described in Material and Methods and displayed over time. In addition, changes in Hoechst fluorescence, monitoring alterations of chromatin structure were analyzed (Figure 15). In both apoptotic models chromatin condenses, visualized by abrupt increase in Hoechst signal (Figure 15, blue trace, dotted line). In parallel, Nup153-GFP is cleaved, resulting in decreased nuclear rim fluorescence (Figure 15, black traces). This effect is caspase-dependent in both models of apoptosis, as the caspase - uncleavable mutant Nup153-GFP is not cleaved, resulting in unaltered nuclear rim fluorescence at chromatin condensation (Figure 15 E),F), green traces). In the presence of the caspase inhibitor zVAD neither chromatin condensation (not shown) nor

cleavage of Nup153-GFP occurs (Figure 15 E),F), red traces) in both investigated models of apoptosis.

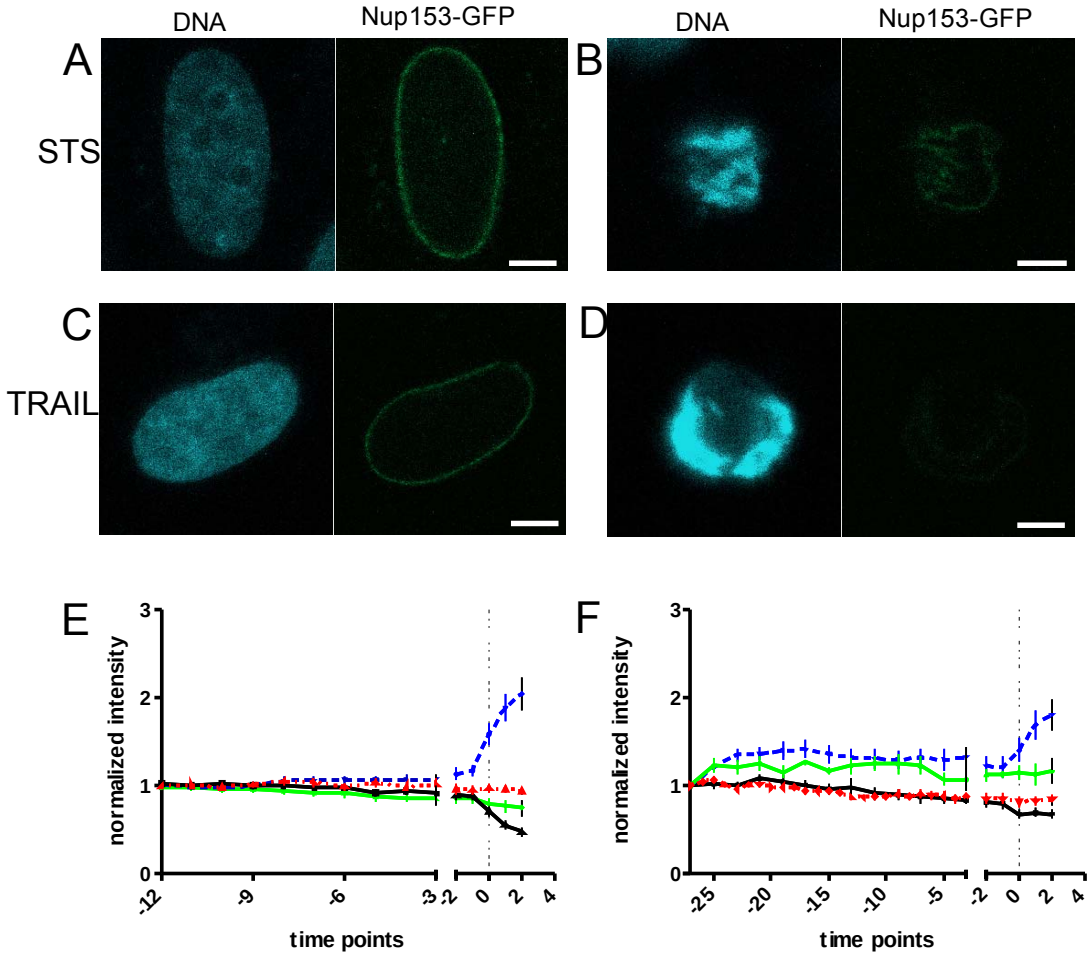

Figure 15: Chromatin condensation and cleavage of Nup153-GFP occurs simultaneously in both models of apoptosis. A) - D) HeLa 229 cells transfected with Nup153-GFP and 4xCherry (not shown), chromatin is labeled with Hoechst A), B) confocal images of a cell treated with 0.5µM STS. C),D) confocal images of a cell treated with 300ng/ml TRAIL. A), C) and B),D) show cells prior to apoptosis induction and at the time point of chromatin condensation, respectively. E),F) for each graph at least 13 cells from different, independent experiments, treated with either STS or TRAIL were evaluated and averaged. Wt Nup153-GFP (black traces); chromatin (blue traces), caspase uncleavable mutant Nup153-GFP (green traces) and Nup153-GFP in the presence of zVAD (red traces) are depicted. At the time point of chromatin condensation (dotted line, time point 0), wt Nup153-GFP but not the mutant Nup153-GFP is cleaved in both models of apoptosis. In the presence of zVAD, neither chromatin condensation (not shown) nor caspase-mediated cleavage of wt Nup153-GFP (red traces) occurs.

In addition to live cell imaging experiments, caspase - dependent cleavage of Nup153-GFP in both apoptotic models was also shown by western blot (Figure 16). Here, cleavage of the endogenous wtNup153 and Nup153-GFP can be detected at two hours after treatment. Addition of zVAD to cells treated for 6h with either STS or TRAIL completely inhibits Nup153 and Nup153-GFP cleavage.

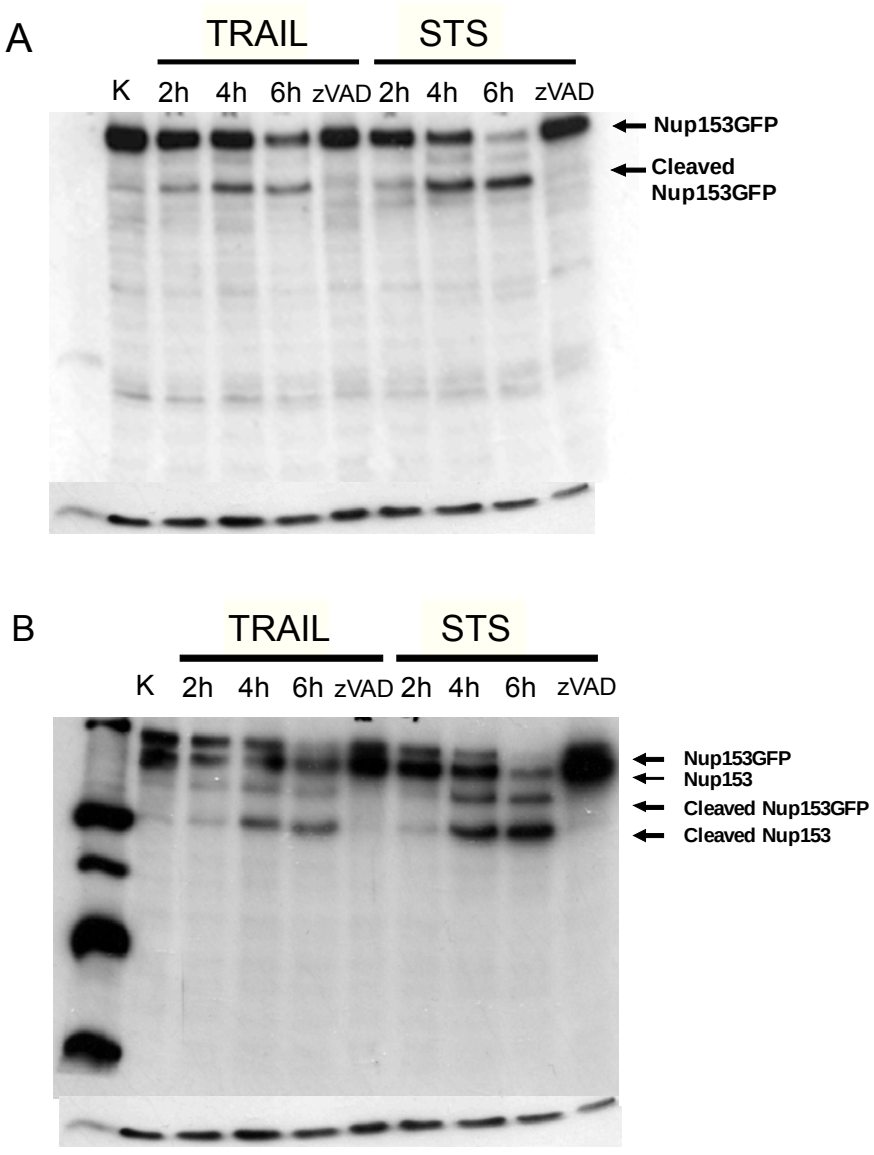

Figure 16: Caspases mediate cleavage of Nup153. HeLa 229 cells were transfected with Nup153-GFP, and treated with STS for different time spans in the absence or presence of zVAD. After lysis, equal amounts of protein were added on a SDS-gel. The resulting blot was first incubated with anti-GFP antibody (1:1000, over night) (A), and then incubated with anti-Nup153 antibody (1:50, over night) (B). In both apoptotic models Nup153 and Nup153-GFP are cleaved. Addition of zVAD to the sample treated for 6h with STS abolishes Nup153 and Nup153-GFP cleavage

Furthermore, caspase activity was assessed by cleavage of caspase3/7 in a fluorimetric assay, and caspase mediated chromatin condensation was detected by DNA laddering (Figure 17). Both employed stimuli induce a time dependent activation of caspases (Figure 17B), chromatin condensation (Figure 17C) and DNA laddering (Figure 17A). Addition of 20µM zVAD abolishes caspase activation and all associated effects as DNA laddering and appearance of apoptotic nuclei (Figure 17).

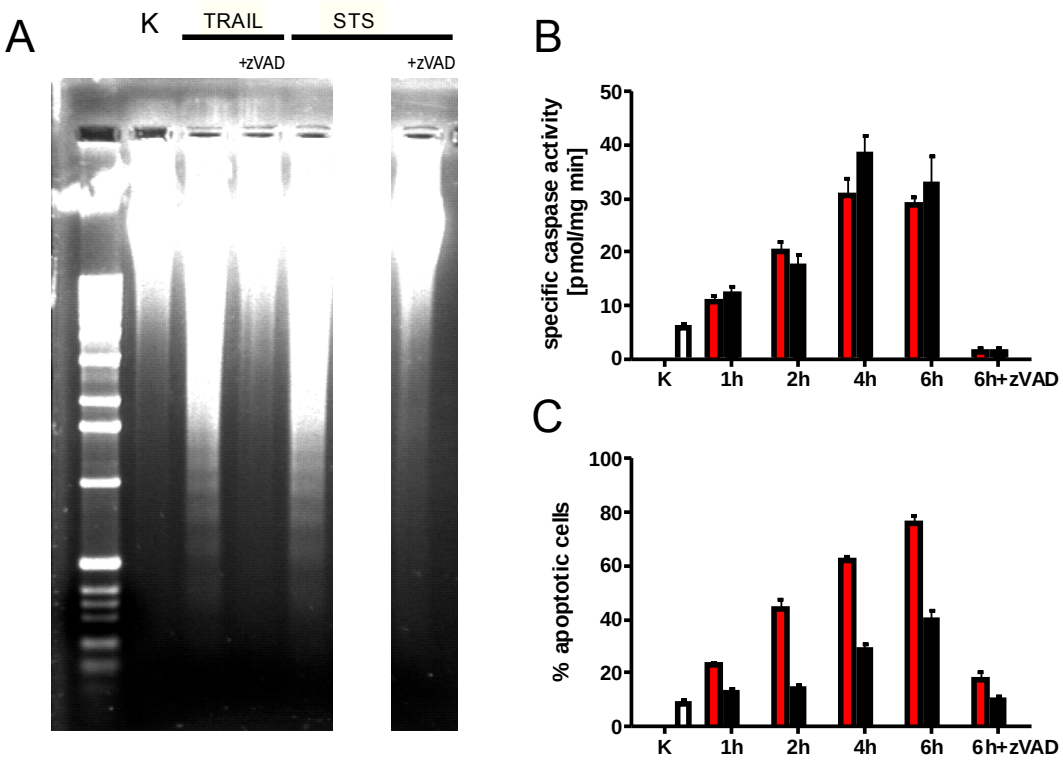

Figure 17. Active caspases induce DNA laddering in both apoptotic models. A) HeLa 229 were treated with STS and TRAIL in the presence or absence of zVAD. B),C) HeLa cells were transfected with Nup153-GFP and 4xCherry and caspase3/7 activity after treatment with STS (black bars) or TRAIL (red bars) was detected by cleavage of the fluorogenic substrate DEVD-afc. In C) the percentage of apoptotic nuclei was determined by labeling with Hoechst and counting.

To detect nuclear permeability alterations, confocal live cell imaging with HeLa 229 cells using two different apoptotic stimuli, STS and TRAIL, was performed (Figure 18). Cells were transfected with Nup153-GFP and 4xCherry, labeled with Hoechst and the fluorescence intensity of 4xCherry in the nucleus was detected as described in Material and Methods.

In both apoptotic models, an abrupt increase in nuclear 4xCherry signal in the nucleus could be detected, simultaneously to caspase-mediated disruption of the nuclear pore and chromatin condensation. Prior to this final disruption of the nuclear permeability barrier, however, a distinct difference in kinetics of nuclear permeability dysfunction between TRAIL and STS-treated cells could be seen. While cells induced with TRAIL show unaltered nuclear 4xCherry fluorescence prior to chromatin condensation (Figure 18 D-F and G, black trace), STS-induced cell death elicits an early, steady leakage of 4xCherry into the nucleus (Figure 18, A-C and G, red trace).

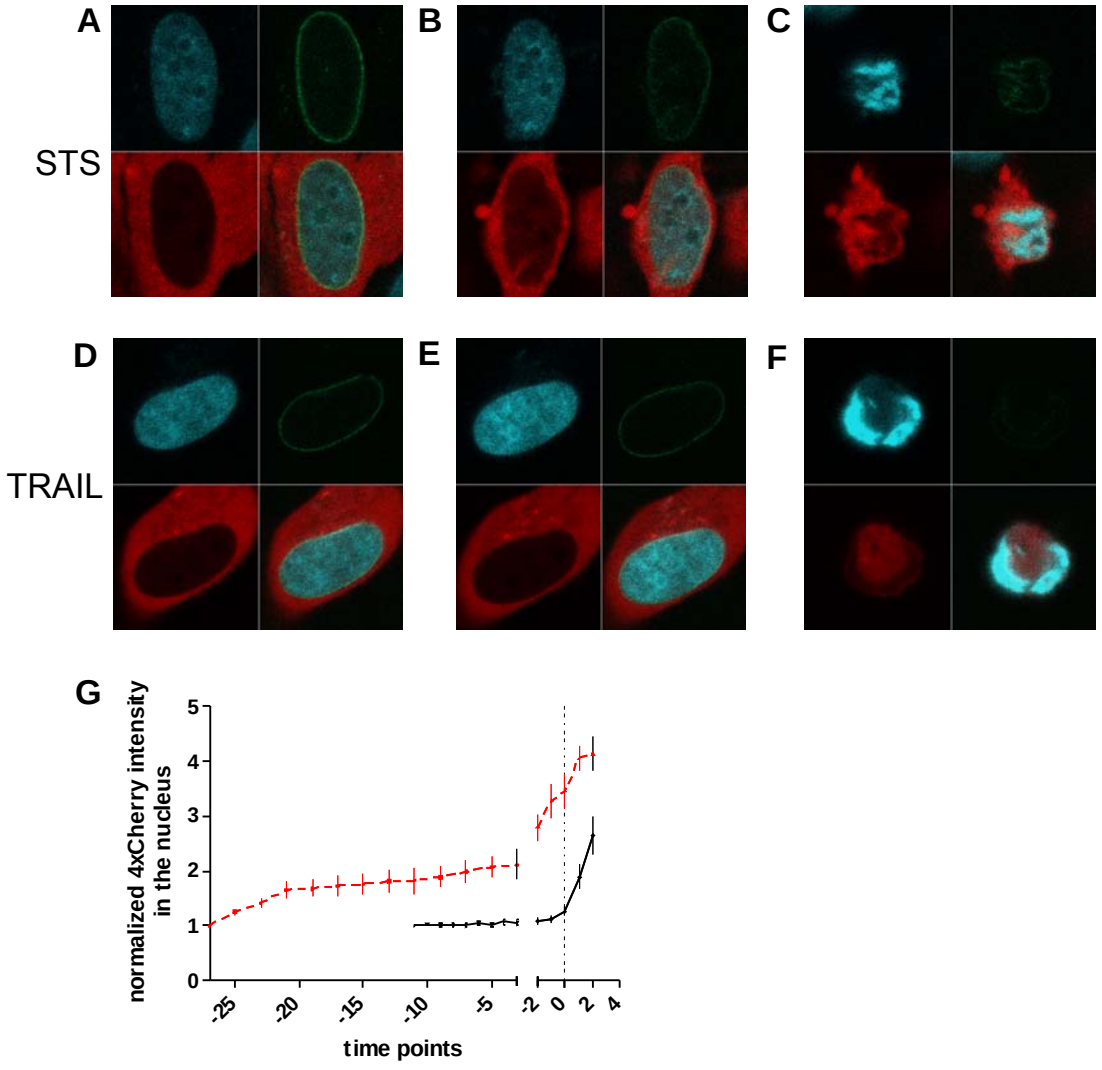

Figure 18: Changes in nuclear permeability are stimulus dependent. A) - F) HeLa 229 cells transfected with Nup153-GFP (green) and 4xCherry (red), chromatin is labeled with Hoechst A) - C) confocal images of a cell treated with 0.5µM STS A) prior to experiment B)1h after start of experiment C) and at time point of chromatin condensation. D) - F) confocal images of a cell treated with 300ng/ml TRAIL D) prior to experiment E) 1h after start of experiment F) and at time point of chromatin

condensation. G) averaged traces of at least 13 cells from independent experiments. The nuclear 4xCherry signal is depicted in STS treated– (red trace) and TRAIL treated cells (black trace).

VI.1.4. STS-induced nuclear leakage is caspase independent

The finding that nuclear permeability increases early and gradually and prior to caspase activation in STS-treated cells, raises the question about the underlying mechanisms. As caspase-mediated cleavage of the nuclear pore has been shown to occur in both models of apoptosis (Figure 15, 16, 17), the possible role of caspases in mediating the STS-induced increase in nuclear envelope permeability was investigated. To this end, HeLa 229 cells were transfected with Nup153-GFP and 4xCherry and treated with STS or TRAIL in the presence or absence of caspase inhibitors (Figure 19). Treatment of the cells with TRAIL in the presence of the caspase inhibitor zVAD, completely abolishes chromatin condensation and all other apoptotic changes, including increase in nuclear permeability (Figure 19A, black trace). At the time point of chromatin condensation, nuclear envelope cleavage, and loss of permeability barrier occur in TRAIL treated cells, no changes are visible in caspase-inhibited TRAIL-treated cells. Preincubation of STS treated HeLa cells with zVAD also abolishes chromatin condensation and nuclear envelope disruption (Figure 16), but it does not alter the early nuclear leakage of 4xCherry into the nucleus (Figure 19B, black trace).

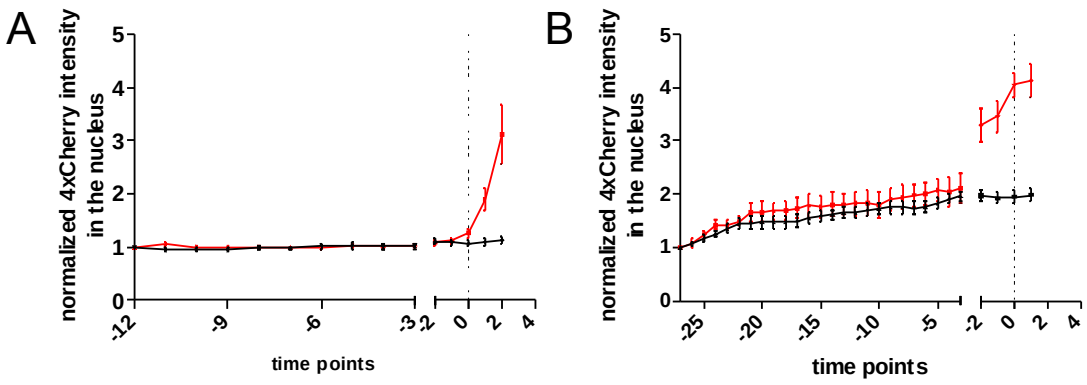

Figure 19: Caspase inhibition does not alter the early, STS-induced nuclear leakage. A),B) evaluated traces from cells treated either with TRAIL - (A) or STS (B). The nuclear 4xCherry signal was detected in the presence (black traces) or absence (red traces) of the caspase inhibitor zVAD (20µM).

VI.1.5. Influence of serine proteases and calpains on STS- induced nuclear leakage

As caspases are admittedly responsible for the late disruption of nuclear permeability barrier but not for the STS- induced early nuclear leakage, the influence on nuclear envelope permeability of other proteases was investigated. Serine proteases have been implicated in the execution of apoptosis in the absence of caspases (Egger et al.,2003) and in inhibition of STS-induced chromatin fragmentation (O`Connell et al., 2006). In addition unpublished data from our group indicated an influence of serine proteases on nuclear permeability (Dissertation Grote, 2007). In addition, the involvement of calpains in early STS-induced nuclear leakage was investigated, as calpains have recently been shown to mediate early increase in nuclear envelope permeability in excitotoxicity (Bano et al., 2009).

VI.1.5.1 Serine proteases are active in STS- induced cell death.

Before testing the influence of serine protease inhibition on STS- induced nuclear permeability, serine protease activation and the influence of serine protease inhibition on chromatin fragmentation in STS induced cell death was investigated. Serine protease activity was measured using a fluorescent inhibitor of serine proteases (FLISP). Upon binding to active serine proteases, the inhibitor emits an increased fluorescence (Figure 20B). Fragmentation of chromatin by caspases can be visualized by a ladder – like distribution of chromatin fragments on an agarose gel. To test whether serine protease inhibition might inhibit caspases and therefore chromatin condensation, a DNA laddering assay in the presence of the serine protease inhibitor AEBSF or the caspase inhibitor zVAD, was performed (Figure 20A). To this end, HeLa 229 cells were incubated with STS for 4h and chromatin fragmentation was visualized by DNA- laddering as described in material and methods (Figure 20 A).

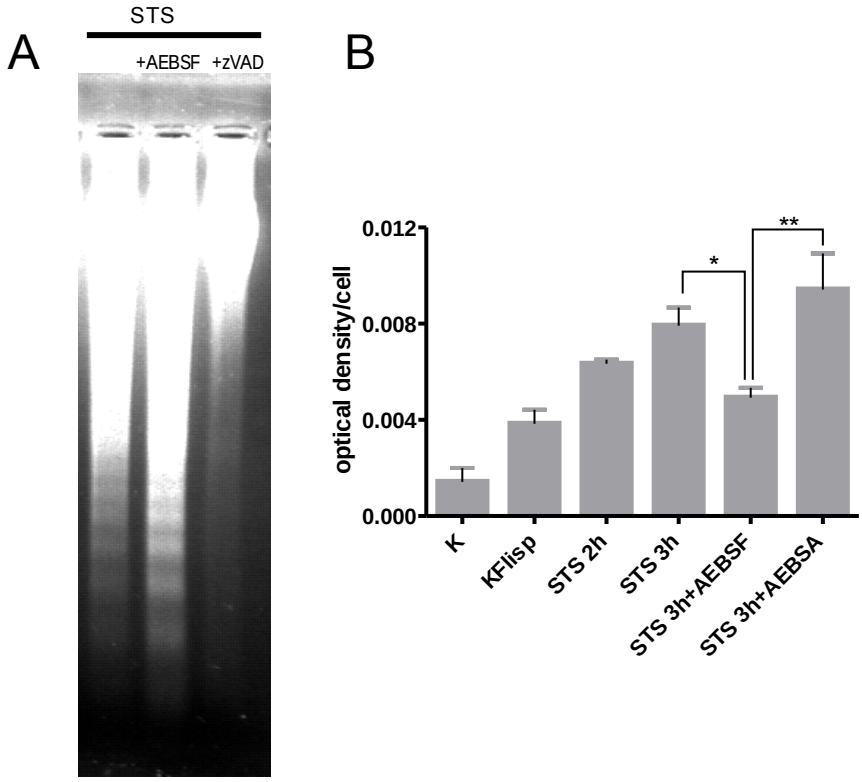

Figure 20) Serine proteases are active in STS – induced cell death. A) DNA-laddering assay of HeLa 229 cells treated with STS in the presence of AEBSF or zVAD. In cells trated with STS alone as well as in the presence of AEBSF chromatin fragmentation occurs. Preincubation of the cells with zVAD completely abolishes chromatin fragmentation. B) FLISP-assay to detect active serine proteases. HeLa 229 cells were treated with STS for different time spans in the presence or absence of the serine protease inhibitor AEBSF or the non-functional analog AEBSA. The cells were then incubated with the FLISP substrate and the resulting fluorescence signal was detected.

As can be seen by the increased fluorescence signal in STS- treated cells in Figure 20B), serine proteases are activated in STS- induced cell death. Preincubation with the serine protease inhibitor AEBSF, but not with its inactive analog AEBSA resulted in a significantly decreased fluorescence signal. Furthermore, caspase activity was not affected by the serine protease inhibitor at the concentration employed here as shown by the unaltered induction of DNA laddering (Figure 20A).

VI.1.5.2 Neither calpains nor serine proteases influence nuclear permeabilization in STS-induced cell death.

To test whether calpain inhibiton might influence the activity of other proteases, like caspases, caspase-activity was measured by cleavage of the fluorescent caspase 3/7 substrate DEVD-afc. Inhibiton of calpains did not affect caspase activity or reduced cell death (Figure 21). This ensures that all potential effects of calpains on nuclear permeability are not elicited by parallel inhibition of caspases.

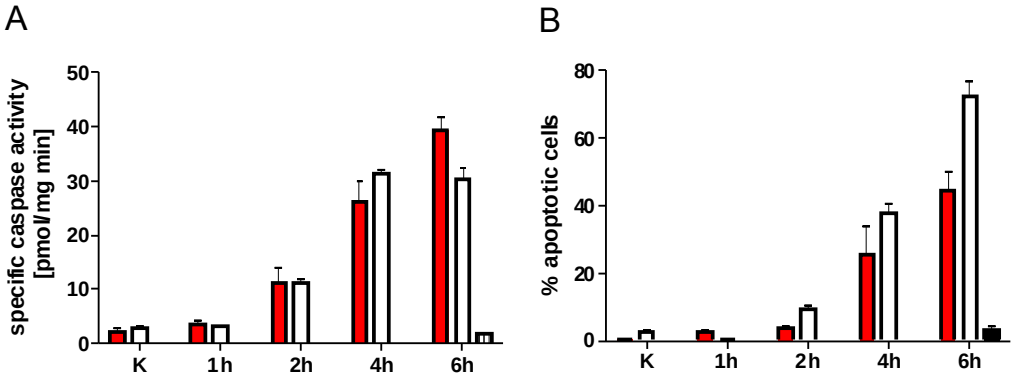

Figure 21: Inhibition of calpains does not influence caspase activity and even enhances cell death. HeLa 229 cells were treated with STS for the indicated time points in the presence (white bars) or absence of calpeptin (red bars). A) Caspase activity was measured by cleavage of DEVD-AFC. No differences in caspase activation could be detected. zVAD addition completely abolishes caspase activity (black bar). B) In the same lysates used for caspase activity measurement, the percentage of apoptotic cells was determined by counting condensed nuclei. Calpain inhibition even increases the amount of condensed nuclei. Error bars show SEM.

To elucidate the role of serine proteases and calpains on nuclear envelope permeability, HeLa 229 cells were transfected with the permeability marker 4xCherry and the caspase sensor Nup153-GFP and confocal live cell imaging experiments with the serine protease inhibitor AEBSF or the calpain inhibitor Calpeptin were performed in staurosprine- treated cells. The kinetics of STS-induced nuclear leakage in the presence of Calpeptin or AEBSF were detected (Figure 22).

In the presence of AEBSF, chromatin condensation, caspase activation and loss of permeability barrier function are unaltered (Figures 20 and 22A).

Although serine proteases are activated in STS-induced cell death (Figure 20), their inhibition did not diminish the early increase in nuclear envelope permeability (Figure 22A, grey trace). Inhibition of calpains did not alter caspase-mediated cleavage of nuclear pore proteins, chromatin condensation and subsequent loss of permeability barrier function (Figure 22B). It also did not affect STS-induced nuclear leakage, on the contray nucleoytoplasmic permeabilization was even increased (Figure 22B, green trace). In addition the percentage of apoptotic nuclei was augmented (Figure 21B). Taken together, the data on calpain- and serine protease inhibition show that neither is responsible for the STS-induced early nuclear leakage.

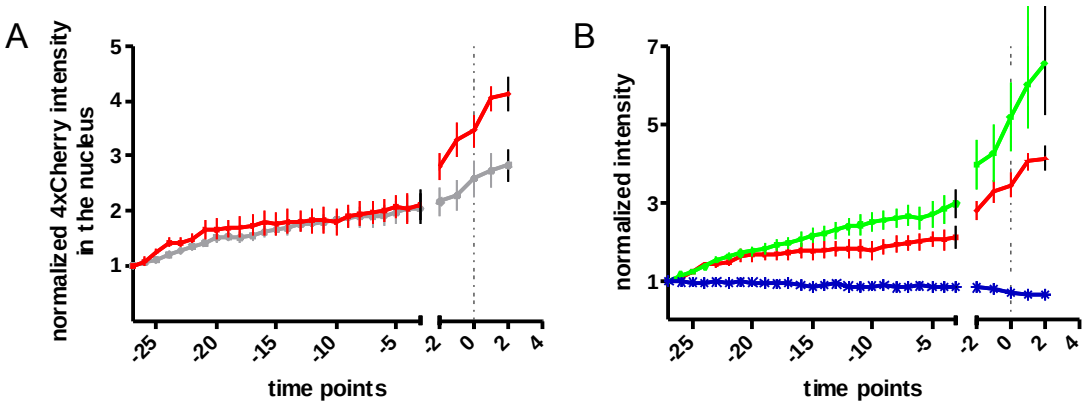

Figure 22: Calpains and serine proteases are not involved in early STS-induced nuclear leakage. Normalized 4xCherry intensity in the nucleus over time. Averaged traces of at least 13 cells from different, independent eperiments are plotted. A) The early nuclear leakage in STS induced cell death (red trace) is unaltered by addition of AEBSF (grey trace). B) Addition of the calpain inhibitor calpeptin even increases nuclear envelope permeability (green trace). As in control cells, caspase mediated Nup153-GFP cleavage occurs parallel to chromatin condensation (blue trace). Error bars show SEM.

VI.1.6. STS-induced alterations of nuclear envelope permeability are mediated by ER Ca^{2+} level

VI.1.6.1. STS-induced early nuclear leakage is abolished by addition of the Ca^{2+} chelator BAPTA/AM

As all tested protease inhibitors had no diminishing effect on apoptotic nuclear envelope permeabilization, another, non-protease mechanism was investigated. Ca^{2+} is known to regulate the nuclear pore complex structure and nuclear transport by altering the filling state of the ER (Feldherr and Akin,

Mooren et al. 2004; Enns et al., 2003). The effect of Ca^{2+} on nuclear envelope permeability was investigated by confocal live cell imaging of HeLa cells in the presence of the Ca^{2+} chelator BAPTA/AM. Therefore, the cells were co-transfected with Nup153-GFP and 4xCherry and 40 min prior to STS addition, the cells were incubated with BAPTA/AM.

Addition of BAPTA/AM completely abolishes early nuclear leakage in STS-treated cells (Figure 23, blue trace). Caspase-activation, chromatin condensation, nuclear pore cleavage and the subsequent loss of nuclear permeability barrier function are unaltered in the presence of BAPTA/AM (Figure 23 and Figure 24).

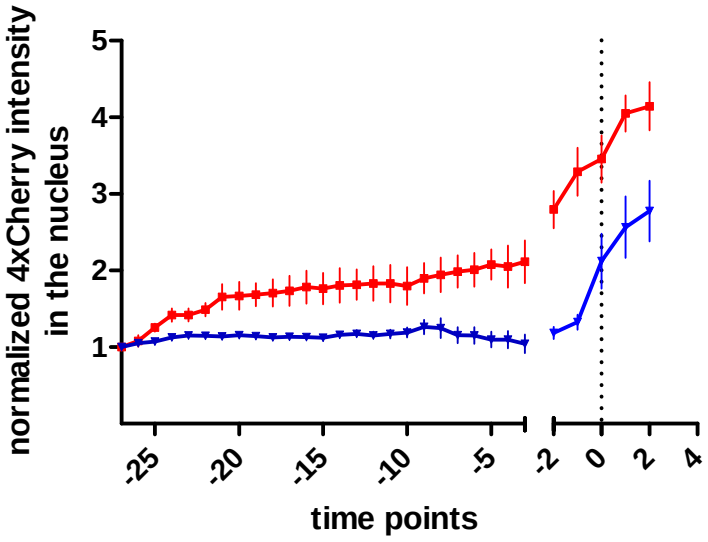

Figure 23: Ca^{2+} mediates early STS-induced nuclear leakage. Averaged traces of at least 13 cells from different, independent experiments, in the presence (blue trace) or absence (red trace) of BAPTA/AM. Addition of BAPTA/AM completely abolishes early STS-induced nuclear leakage. Loss of permeability barrier function at the time point of chromatin condensation (dotted line) due to caspase activation still occurs in the presence of BAPTA/AM, visualized by the abrupt increase in nuclear 4xCherry fluorescence. Error bars present SEM

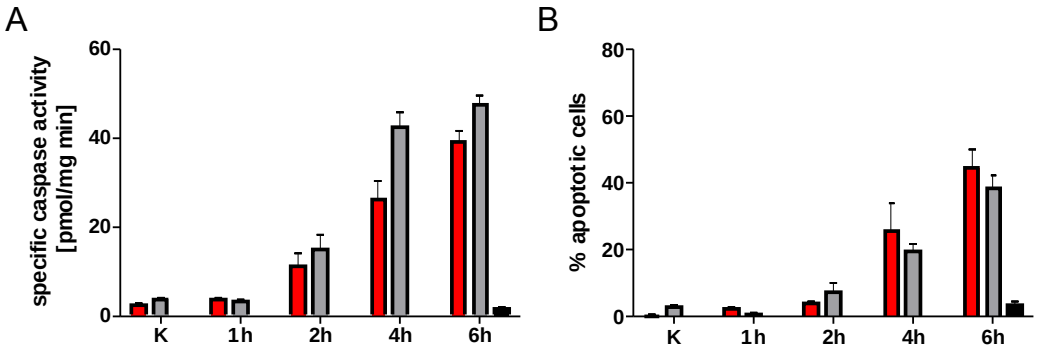

Figure 24: Caspase activation and apoptosis occur in the presence of BAPTA/AM. HeLa 229 cells were treated with STS for the indicated time points in the presence (grey bars) or absence of BAPTA/AM (red bars). A) Caspase activity was measured by cleavage of DEVD-AFC. No differences in caspase actvation could be detected. zVAD addition completely abolishes caspase activity (black bar). B) In the same lysates used for caspase activity measurement, the percentage of apoptotic cells was determined by counting condensed nuclei. Error bars show SEM.

VI.1.6.2. STS reduces ER Ca^{2+} level

The amount of Ca^{2+} in the ER has been shown to alter nuclear permeability (Enns et al., 2003; Mooren et al., 2004, Scorrano et al., 2003). To further specify the role of Ca^{2+} in STS-induced increase in nuclear envelope permeability, Ca^{2+} - loading of the ER was determined in control cells, STS- and TRAIL- treated HeLa 229 cells. The apoptosis inducer TRAIL was used as a reference stimulus. TRAIL does not elicit early nuclear leakage and should therefore not elicit ER Ca^{2+} -level alterations. Endplasmic reticulum Ca^{2+}-level were assessed with the fluorescent Ca^{2+} sensor Fluo-4. After treatment with either STS or TRAIL for 1h, ER Ca^{2+}-level were determined with a fluorescence plate reader. Therefore, Thapsigargin, which is an inhibitor of the sarcoplasmic/endoplasmic calcium-ATPase SERCA was added and the amount of released Ca^{2+} from internal stores was assessed. The Thapsigargin-induced increase in Fluo-4 fluorescence is a measure for the amount of Ca^{2+} released from the ER.

HeLa 229 cells treated with STS for 1h show reduced ER Ca^{2+} level, whereas cells treated with TRAIL for 1h have unaltered ER Ca^{2+} level (Figure 25).

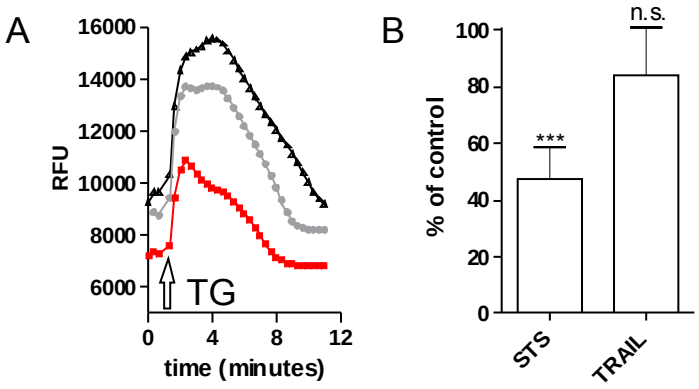

Figure 25: STS reduces ER Ca^{2+} level. A) Representative traces of HeLa 229 cells incubated with Fluo-4 and treated with 0.5µM STS or 300ng/ml TRAIL. The basal Ca^{2+} level of control - (black trace), STS-treated - (red trace), and TRAIL-treated cells (grey trace) was detected by a fluorescence plate reader. The increase in Fluo-4 fluorescence after thapsigargin addition was detected. B) Quantification of three independent experiments. All experiments were performed in triplicates. The difference between basal level and peak level corresponds to the amount of released ER Ca^{2+}. The released Ca^{2+} was expressed as percent of the Ca^{2+} amount released by control cells. Statistics: one way ANOVA compared to control with Bonferroni post-test. *** $p < 0.001$

VI.1.7. Active nuclear transport is unaffected by alteration of ER Ca^{2+} level.

Alterations in ER Ca^{2+} not only influence passive diffusion but also have an impact on active transport (Greber and Gerace, 1995). To investigate, whether altered Ca^{2+} content and the early increase in nuclear envelope permeability affect active nuclear transport in STS-induced cell death, Hela 229 cells were transfected with the permeability marker 4xCherry and a marker for active nuclear transport: GFP-NLS. GFP-NLS is a construct of about 24 kDa which is small enough to pass the nuclear envelope by passive diffusion, but due to its nuclear localization signal (NLS) is actively imported into the nucleus in healthy cells, resulting in a exclusively nuclear localization. If active nuclear transport is impaired, GFP-NLS is no longer imported into the nucleus and distributes over the whole cell. Confocal live cell imaging of cells treated with STS was performed and the GFP-NLS signal in the cytoplasm was measured. As a comparison cells were treated with TRAIL. Since in this model nuclear envelope permeability and Ca^{2+} content are

unchanged until final caspase-mediated execution of apoptosis, no alteration in active transport functionality was expected (Figure 26).

Active nuclear transport is functional in both models of apoptosis until caspase activation, chromatin condensation and loss of nuclear envelope permeability. Only directly before caspase activation and final disruption of the NPC does increased leakage of GFP-NLS into the cytosol occur in STS treated cells. This indicates that at this stage the rate of actively imported GFP-NLS molecules no longer compensates for the the rate of passive efflux. Although early nuclear leakage and decreased ER Ca^{2+} level occur in STS-induced apoptosis, active nuclear transport is largely unaffected. These results lead to the conclusion that active and passive transport are largely uncoupled.

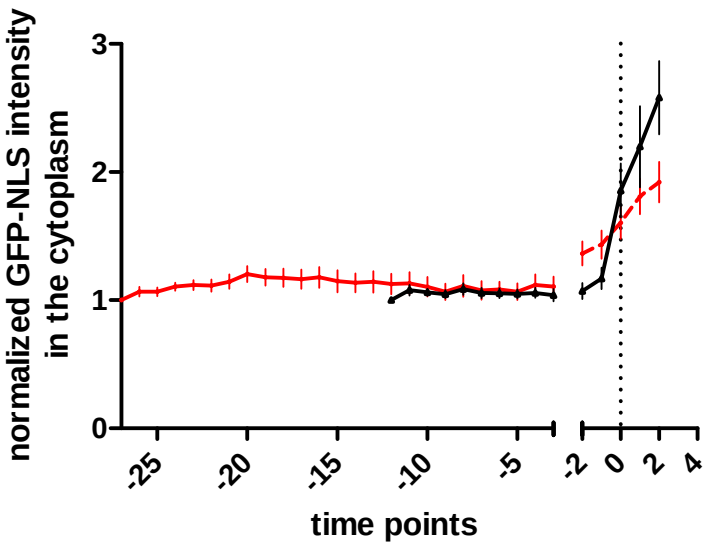

Figure 26: Active nuclear transport is unaffected by alterations of ER Ca^{2+}. Cytosolic GFP-NLS fluorescence in cells treated with TRAIL (black trace) and STS (red trace) was detected and plotted against time. For each apoptotic stimulus, 15 cells from different, independent experiments were evaluated and averaged. Error bars show SEM

VI.2. Effect of Bcl-2 on nuclear envelope permeability

VI.2.1. Nuclear permeability is increased in cells overexpressing Bcl-2

Recent work from our group has indicated that HeLa K and SW480 cells which overexpress Bcl-2 have a higher constitutive nuclear permeability (Patricia Grote, Dissertation 2007). The finding of increased nuclear permeability in Bcl-2 overexpressing cells was highly unexpected as Bcl-2, being an anti-apoptotic protein, was initially expected to have an opposing effect as compared to apoptosis-inducing agents. To validate the observed effect of Bcl-2 on nuclear permeability, HeLa K and Hela KBcl-2 cells, stably overexpressing Bcl-2, were transfected with the permeability marker 4xCherry. 24h after transfection, the distribution of 4xCherry was detected by fluorescence microscopy. Only cells showing at least the same fluorescence of 4xCherry in the nucleus as in the cytoplasm were counted as exhibiting nuclear 4xCherry. The preliminary results from our group could be confirmed. In Hela KBcl-2 cells, the percentage of cells with nuclear 4xCherry is significantly increased compared to WT HeLa K cells (Figure 27).

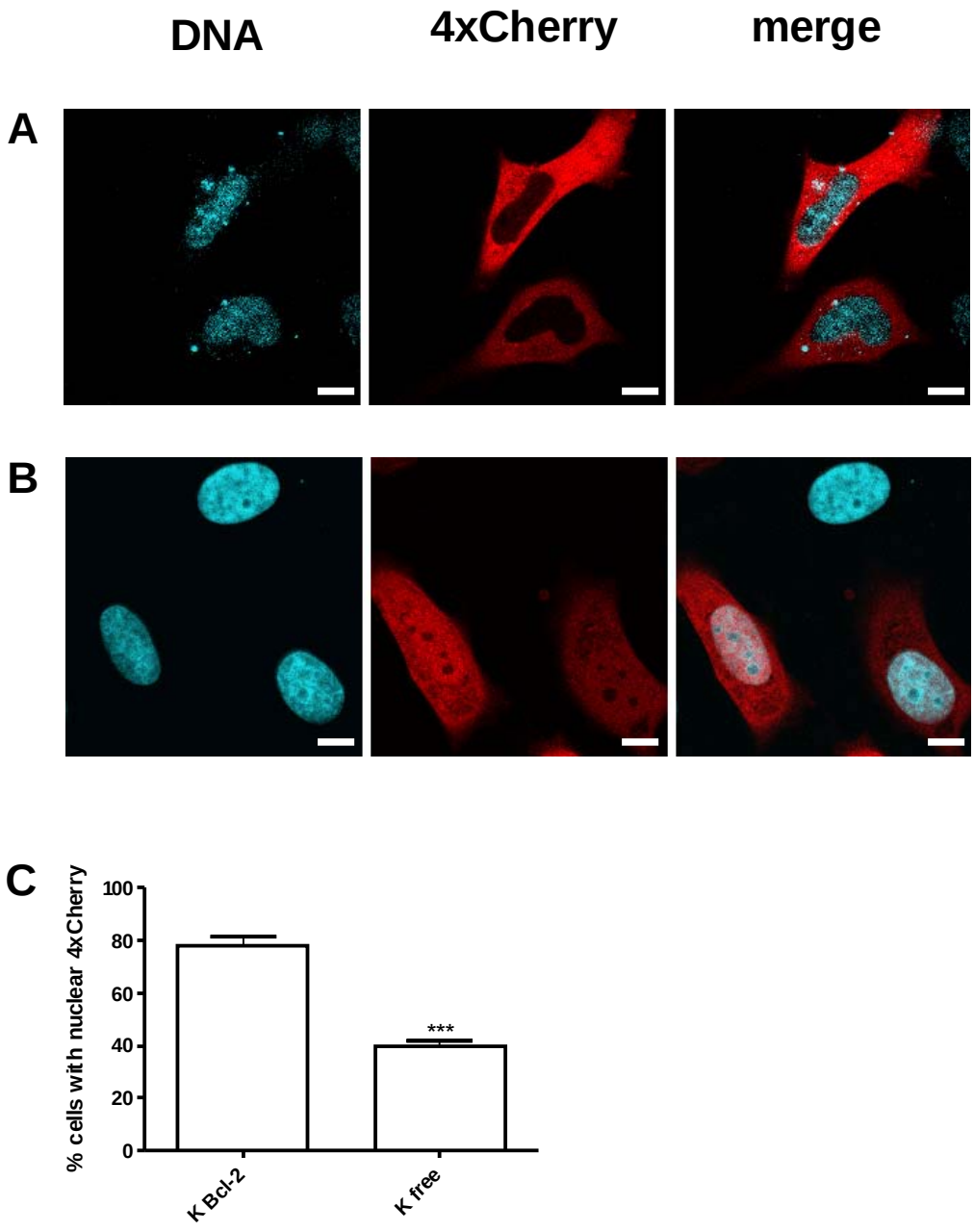

Figure 27: Bcl-2 overexpression increases nuclear permeability. HeLa K - and Hela KBcl-2 cells were transfected with the permeability marker 4xCherry and co-labelled with the chromatin intercalating dye Hoechst 33342. Representative confocal images of HeLa K - (A) and K Bcl-2 cells (B) are shown. C) Cells expressing homogeneously distributed 4xCherry were counted as cells with nuclear 4xCherry localization. For each cell line three independent experiments were performed. In each experiment at least 300 cells per cell line were counted. Scale bar: 10µm. Statistics: see complete Figure 28)

VI.2.2. Overexpression of the Ca^{2+}-ATPase SERCA reduces nuclear envelope permeability

A first hint concerning the mechanism underlying Bcl-2 - induced increase in nuclear permeability was obtained during a previous PhD thesis Patricia Grote, Dissertation). Here, it was shown that the Bcl-2 dependent increase in nuclear permeability could be counteracted by overexpression of the sarcoplasmic/endoplasmic Ca^{2+}-ATPase SERCA. SERCA is an ER Ca^{2+} pump and increases Ca^{2+} levels in the ER. To verify this result, HeLa K and HeLa K-Bcl-2 cells were transfected with the permeability marker 4xCherry; in addition Bcl-2 overexpressing cells were cotransfected with a DNA construct encoding SERCA. The percentage of cells expressing nuclear 4xCherry fluorescence was determined 24 h after transfection in cells overexpressing SERCA by fluorescent microscopy. Overexpression of SERCA in HeLa K-Bcl-2 cells resulted in significantly decreased nuclear envelope permeability (Figure 28). This finding indicates an involvement of Ca^{2+} in regulation of the nuclear envelope permeability.

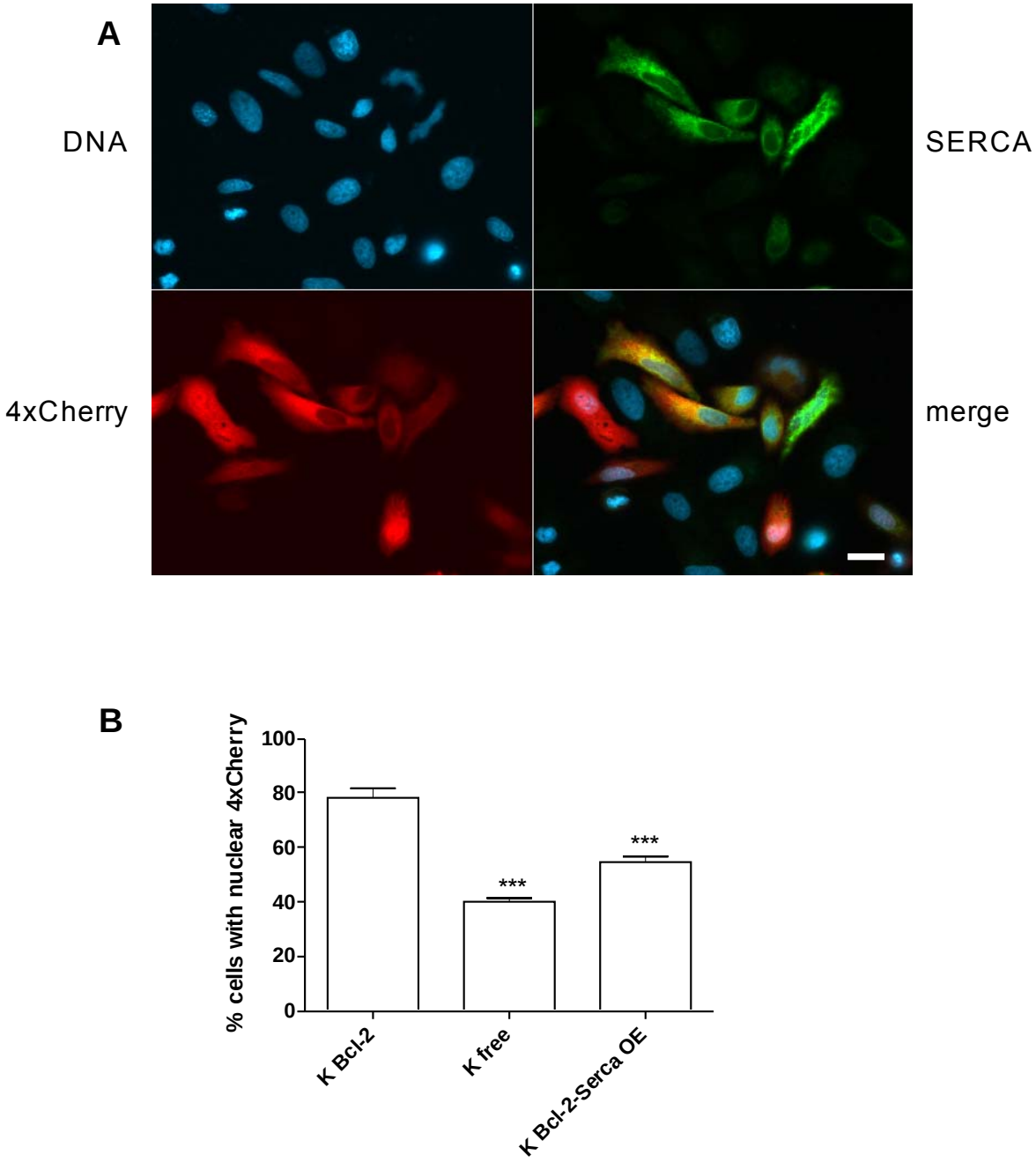

Figure 28: SERCA overexpression reduces nuclear envelope permeability. A) Fluorescent images of HeLa K - and Hela KBcl-2 cells transfected with the permeability marker 4xCherry and SERCA. Cells expressing homogeneously distributed 4xCherry were counted as cells with nuclear 4xCherry localization. Scale bar: 20µm. B) quantification of experiments as in A). For each cell line three independent experiments were performed. In each experiment at least 300 cells per cell line were counted. Statistics: one way ANOVA with Bonferroni post-test; $p>0.05$; *** < 0.001.

VI.2.3. Cells overexpressing Bcl-2 show reduced ER Ca^{2+} level

As the increased nuclear permeability in Bcl-2 overexpressing cells can be reversed by overexpression of the ER Ca^{2+} pump SERCA, an involvement of Ca^{2+} seems likely. To test this hypothesis the ER Ca^{2+} content was measured in control and Bcl-2 overexpressing HeLa K cells. In addition, control HeLa K cells were incubated in low Ca^{2+} medium (0.1mM) for 18h to reduce the ER Ca^{2+} content. This slow down regulation of ER Ca^{2+} levels should mimic the supposed effect of Bcl-2 overexpression on ER Ca^{2+} levels. Cells were labeled with Fluo-4-AM, a cell permeable form of the fluophore Fluo-4 for one hour at room temperature. The cells were then washed and the basal Fluo-4 signal was measured in a Tecan plate reader in low Ca^{2+} medium. After three time points the SERCA inhibitor thapsigargin was added and the Ca^{2+} released from the ER was measured by the increase in Fluo-4 signal. When the Ca^{2+} signal had abated to the basal level, the medium was replaced by normal, Ca^{2+} containing medium (1mM) and the capacitive uptake of Ca^{2+} was detected by Fluo4 signal intensity (Figure 29). Decreased capacitive uptake has been reported in cells with diminished ER Ca^{2+} content (Pinton et al., 2000). Indeed, cells overexpressing Bcl-2 show reduced ER Ca^{2+} level and reduced capacitive Ca^{2+} influx as compared to control, non-overexpressing cells.

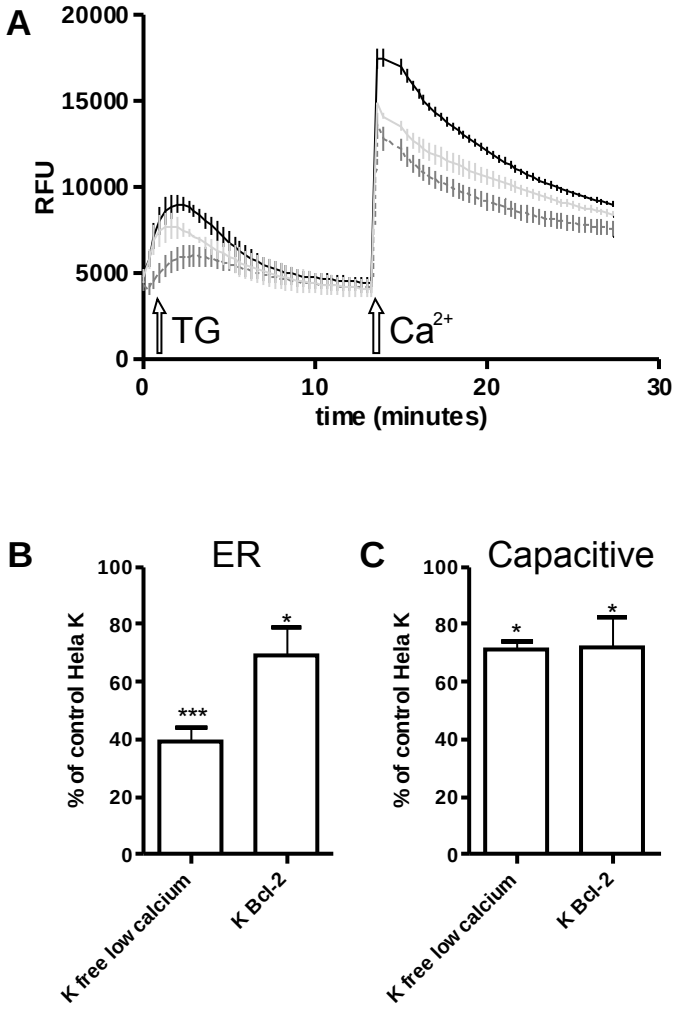

Figure 29: Bcl-2 overexpression reduces ER Ca^{2+} levels. HeLa K and Hela KBcl-2 cells were either kept in normal or low Ca^{2+} medium, then labeled with Fluo4 and the fluorescence was detected with a plate reader. A) averaged traces of five independent experiments. Time points of thapsigargin – and Ca^{2+} addition are indicated. B) quantification of ER Ca^{2+} release after TG addition in % of amount released by control cells. C) quantification of capacitive Ca^{2+} in % of amount released by control cells. Statistics: T-test; $p< 0.05$.

VI.2.4. Ca^{2+} mediates increase in nuclear permeability.

To emphasize the importance of Ca^{2+} on nuclear envelope permeability, HeLa K cells were adapted to low Ca^{2+} concentrations. If indeed reduced ER Ca^{2+} level are responsible for the Bcl-2 induced increase in nuclear permeability, then the effect on nuclear permeability should be mimicked by adapting cells to low Ca^{2+}-conditions.

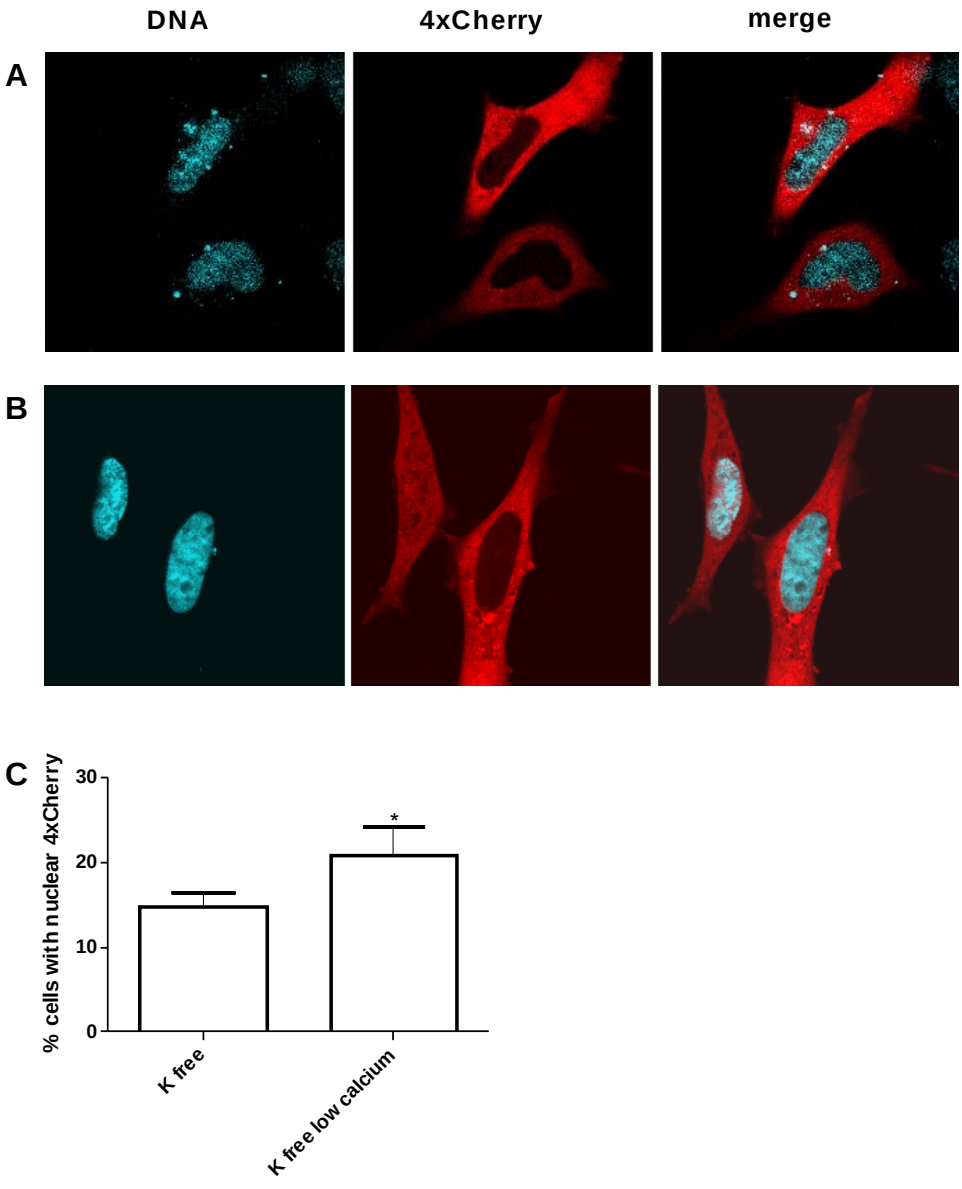

Figure 30: Adaptation to low Ca^{2+} mimics effect of Bcl-2 overexpression on nuclear permeability. HeLa K cells were kept either in normal Ca^{2+} - (A) or in low Ca^{2+} buffer (B) and then transfected with 4xCherry. C) Cells showing homogeneously distributed 4xCherry signal were counted as cells with nuclear 4xCherry localization. Statistics: T-test; $p< 0.05$.

To verify this hypothesis, HeLa K cells were incubated in low Ca^{2+} -medium (0.1mM) and after 6h transfected with the permeability marker 4xCherry. To exclude an influence of the buffer, control cells were incubated and transfected under the same additions as with low-buffer only with normal Ca^{2+} -concentrations (1mM). Cells were labeled with Hoechst and the percentage of cells with nuclear 4xCherry was determined by fluorescence microscopy. Indeed, counting of about 1000 cells reveals a significant increase in nuclear envelope permeability in cells maintained in low Ca^{2+} buffer (Figure 30).

Taken together, the results on Bcl-2 induced increase in nuclear permeability strongly indicate that alterations of ER Ca^{2+} -level are involved in this effect.

VII. DISCUSSION

This work was aimed at elaborating a detailed knowledge on the regulation of the nuclear envelope permeability barrier in cell death. To this end, two apoptosis inducing agents, STS and TRAIL, were employed. In both models the underlying mechanisms mediating the influence on nuclear envelope permeability were investigated. In the first part, the influences of both apoptosis-inducing agents on nuclear envelope alterations will be discussed. The second part deals with the role of Bcl-2, an anti-apoptotic molecule, on nuclear envelope permeability. This discussion presents possible explanations for the similar effects of both pro- and anti-apoptotic pathways on nuclear permeability. This includes the involvement of Ca^{2+} and a putative Ca^{2+}-sensing nucleoporin, gp210.

VII.1. Apoptosis-induced alterations of the nucleo-cytoplasmic permeability barrier.

Apoptosis-induced alterations of the nuclear envelope have been reported for several years. With a confocal imaging setup established in our group, the influence of apoptotic stimuli on nuclear permeability and structural alterations of the nuclear envelope were investigated in live cells. Two different treatments were used to detect general and stimulus dependent alterations of the nucleocytoplasmic permeability barier. TRAIL-induced apoptosis is receptor mediated and caspase-dependent whereas staurosporine, a broad spectrum kinase inhibitor, induces apoptosis via the intrinsic pathway.

VII.1.1. Caspase-dependent mechanisms

In this work, a general caspase-dependent aspect of cell death could be observed. Caspases are activated in both models of apoptosis. These are necessary for chromatin fragmentation as confirmed by DNA laddering experiments (Figure 17). At the execution of apoptosis, cleavage of nuclear pore protein Nup153-GFP by caspases could be seen in live cell imaging experiments and in western blots (Figures 15 and 16). This effect is in

accordance with data from other groups which also reprted a caspase dependent cleavage of Nups (Faleiro et al., 2000; Ferrando-May et al., 2000; Patre et al, 2006). To test the function Nup153-GFP as caspase sensor, kinetics of cell death were investigated in cells expressing a caspase uncleavable mutant Nup153GFP. As expected, no cleavage of Nup153GFP occurred. This allowed the conclusion, that Nup153-GFP is suitable as caspase sensor. Further, the results indicate that cleavage of Nup153-GFP is not necessary for execution of cell death as chromatin condensation still occurs and the cells eventually die. As Nup153-GFP is located in the periphery of the nuclear pore complex, this result is not unexpected. In TRAIL-induced cell death, the nuclear permeability barrier function is unaltered until chromatin condensation and the caspase-mediated disruption of the nuclear envelope. Only then, the loss of permeability barrier function could be detected. TRAIL induced cell death is purely caspase-dependent as inhibition of caspases inhibits all features of cell death in TRAIL induced apoptosis. TRAIL was used as a reference stimulus to staurosporine (STS). The mechanisms through which STS induces apoptosis are still under debate. Caspase-dependent aspects of STS-induced cell death have been shown by various groups in numerous cell types (Zhang et al., 2004; O`Connell et al., 2006, Patre et al., 2006). Data in this work also show a caspase-dependant aspect of STS-induced apoptosis. Similar as in TRAIL induced apoptosis, caspases mediate chromatin condensation and disruption of the nuclear pore complex (NPC) (Figure 14). Beside these caspase-dependent effects, caspase-independent alterations of the nuclear permeability barrier in STS-induced cell death could be observed in this work. Prior to caspase-mediated nuclear pore cleavage and the concomitant increase in nuclear permeability, a steady increase in nuclear envelope permeability in STS-induced cell death could be detected. This increase could not be abrogated by addition of the broad spectrum caspase inhibitor zVAD-fmk. Caspase independent pathways for STS-induced cell death have been shown in certain cell types; so does zVAD-fmk addition not inhibit DNA laddering in acute lymphoid leukemia cells (Belmokhtar, 2001) and HL-60 cells (O`Connell et al., 2006).

VII.1.2. Influence of serine proteases on nuclear envelope permeability

In the next step, the mechanisms responsible for the caspase-independent increase in nuclear permeability were investigated. Unpublished data from our group show an involvement of serine proteases in regulating the nuclear permeability barrier. Addition of the serine protease-inihibitor AEBSF to semi-permeabilized HeLa cells, inhibited the permeabilizing activity of apoptotic Jurkat T-cell extracts (Patricia Grote, Dissertation). Furthermore, serine proteases have been shown to be involved in STS-induced cell death (O`Connell et al., 2006). To elucidate the influence of serine protease inhibition on the STS-induced, early and caspase-independent increase in nuclear permeability, live cell imaging experiments were performed. Further, the effect of the serine protease inhibitor AEBSF on chromatin fragmentation was observed. The results clearly revealed that serine protease inhibition has no effect on early STS-induced nuclear leakage and does furthermore not interfere with DNA fragmentation (Figure 20). The latter result is in contrast to data published by other groups. O`Connell et al, 2006 and Zang et al., 1999 showed that inhibition of serine proteases by TPCK but not caspase inhibition by zVAD prevented chromatin condensation, and activation of L-DNaseII. These differing findings might very well be due to the use of different cell lines (Hela in this work and HL-60 in O`Connell et al.,2006). Moreover, AEBSF which has been used in the present work is a more potent serine protease inhibitor than TPCK, which was used in O`Connell et al.,2006. Controversing effects of serine proteases can also be found in other publications (Egger et a, 2003; de Bruin et al., 2003). While in some cell lines and with certain stimuli activation of serine proteases occurs in parallel to caspase-dependent mechanisms, in other cell lines serine proteases only play a role in the absence of caspases.

VII.1.3. Influence of calpains on nuclear envelope permeability

Ca^{2+} dependent proteases, calpains, have recently been shown to influence the nuclear permeability barrier of neuronal cells in excitotoxicity (Bano et al. 2009). In the present work, the impact of calpain inhibition on nuclear permeability was investigated by confocal live cell imaging. Interestingly, preincubation of HeLa cells with the calpain inhibitor Calpeptin did not decrease the early STS-induced nuclear leakage but even enhanced nuclear envelope permeability. This effect of calpain inhibition is surprising in the light of the results presented by Bano et al, 2009, which report a protective role of calpain inhibition on nuclear permeability function. In accordance to their findings, other groups have also correlated calpain activation with caspase-dependent and- independent pro-apoptotic functions in cell death. For example calpain-mediated cleavage of the pro-apoptotic Bcl-2 family member Bid enables it`s binding to pro-survival Bcl-2 family members. This results in the release of Bax and Bak which can induce apoptosis at the mitochondria (Gil-Parado et al, 2002). Further, calpains have been reported to facilitate caspase-3 activation by initial cleavage of the pro-enzyme (Blomgren et al., 2001). Furthermore calpain I cleaves and releases apoptosis inducing factor (AIF) from the mitochondria, which leads to caspase independent fragmentation of the DNA (Polster et al., 2005; Yuste et al, 2005; Norberg et al, 2008). In contrast to these pro-apoptotic effects of calpains, anti-apopotic functions of calpains have been proposed. Calpain mediated cleavage of p53 reduces DNA damage-induced cell death (Kubbutat and Vousden, 1997) and Calpain4-/- mice are more susceptible to STS- and TNF-α-induced cell death. Interestingly, Yin et al., 2010 showed that calpain inhibition enhances STS-induced cell death. In the light of the reported anti-apoptotic function of calpains, it is possible that calpains fulfill an anti-apoptotic function in STS-induced cell death. This correlates to the finding presented in this work showing that calpain inhibition even increases the STS-induced nuclear leakage (Figure 22B). A potential acceleration of STS-induced cell death by calpains is also possible, although this aspect was not addressed here.

VII.1.4. Ca2+-level are important for mediation of STS induced cell death

It has been shown that increased mitochondria- or cytosolic-Ca^{2+} concentrations are involved in STS induced cell death. So causes exposure of PC12-cells to staurosporine an increase in mitochondrial- and cytosolic Ca^{2+} levels which then leads to cytochrome c release, caspase-3 activation and DNA fragmentation (Kruman et al., 1998; Seo and Seo, 2009). To test whether Ca^{2+} is involved in STS-induced early nuclear permeability increase, confocal live cell imaging with HeLa cells pretreated with the Ca^{2+} chelator BAPTA-AM were conducted. The effect is striking: early nuclear leakage is completely abolished in STS-treated cells in the presence of BAPTA-AM (Figure 23) while caspase activation, chromatin condensation and loss of permeability barrier function still occur. As reduced Ca^{2+} level in the ER have been shown to influence nuclear permeability (Greber and Gerace, 1995, Shahin et al., 2001, see introduction), it was investigated whether treatment of cells with STS affects ER Ca^{2+} level. TRAIL stimulation served as a control here since no alterations of the permeability barrier prior to chromatin condensation occur. The ER Ca^{2+} level were detected by Fluo-4, which is a fluorescent Ca^{2+} indicator based on BAPTA. Indeed, treatment of cells for one hour with STS but not with TRAIL, significantly decreases ER Ca^{2+} -content (Figure 25).

The reduced ER Ca^{2+} levels and the concomitant early nuclear leakage in STS-induced cell death may represent mechanisms to enhance apoptosis (see VII.3).

VII.2. Effect of Bcl-2 overexpression on nuclear permeability

VII.2.1. Bcl-2 and increased nuclear permeability

Bcl-2 overexpressing cells are at least partially protected against stauroporine-induced cell death (Hanson et al., 2008). Several mechanisms have been proposed as to how Bcl-2 confers resistance to apoptotic stimuli. Inhibition of mitochondria permeabilization and thereby blocking the release of pro-apoptotic factors has long been proposed as one of the main anti-apoptotic mechanisms of Bcl-2 pro-survival proteins (Adams and Cory, 2007). Another mechanism as to how pro-survival Bcl-2 family members inhibit apoptosis involves the regulation of ER Ca2+-content (Rong and Distelhorst, 2008). In our group it was hypothesized, that the rescuing effect of Bcl-2 on staurosporine-induced cell death might be due to decreased nuclear envelope permeability. Preliminary experiments done in our group and experiments performed in this work, however, gave unexpected results:the presence of higher levels of Bcl-2 did protect from apoptosis, however the cells displayed a constitutively increased nuclear envelope permeability already prior to apoptosis induction. As this effect of increased permeability could only be detected when Bcl-2 was overexpressed at the ER or the nuclear envelope but not at the mitochondria, an involvement of ER Ca^{2+} level was suspected. ER Ca^{2+} levels have been reported to be influenced by Bcl-2. Overexpression of Bcl-2 reduces ER Ca^{2+} content (Pinton et al., 2000; Foyouzi-Youseffi et al., 2003). This reduction of ER Ca^{2+} level is hypothesized to be responsible for decreased sensitivity against certain apoptotic stimuli like ceramide and staurosporine (Annis et al., 2001). After apoptosis induction, less Ca^{2+} is released from the ER resulting in a decreased uptake of Ca^{2+} in the mitochondria (Annis et al., 2001, Pinton et al, 2001; Rudner et al., 2001).

VII.2.2. Ca^{2+} mediates Bcl-2 induced nuclear permeability increase

To investigate if Bcl-2 overexpressing cells show reduced ER Ca^{2+} level, measurements with fluorescent Ca^{2+} indicator Fluo-4 were performed. In parallel, control cells were adapted to low Ca^{2+} medium to mimic the effect of Bcl-2 on ER Ca^{2+} level. It could be shown that Bcl-2 overexpression and long term Ca^{2+} depletion both significantly reduce ER Ca^{2+} level and also reduce capacitive Ca^{2+} influx. Capacitive Ca^{2+} influx has been proposed to be an adaptive response to decreased ER Ca^{2+} level (Pinton et al., 2000).

The effect of Ca^{2+}-level on nuclear envelope permeability was investigated by usage of the permeability marker 4x Cherry. To this end, control, Bcl-2 overexpression and Ca^{2+} depleted cells were transfected with 4xCherry and the percentage of cells with nuclear 4xCherry was determined. Beside Bcl-2 overexpressing cells, also control cells adapted to low Ca^{2+} medium show increased nuclear permeability (Figures 27 and 30), strengthening the hypothesis that decreased ER Ca^{2+}-level are responsible for increased nuclear permeability. To further validate these results, the effect of ER Ca^{2+} replenishment by overexpression of the Ca^{2+} ATPase SERCA was investigated. Cells overexpressing Bcl-2 and SERCA show reduced nuclear permeability compared to cells only overexpressing Bcl-2 (Figure 29). Taken together, the data show that Bcl-2 induced alterations of nuclear permeability are Ca^{2+} mediated.

VII.3. Bcl-2 and STS both reduce ER Ca^{2+} level and increase nuclear envelope permeability.

The data presented in this work show that Bcl-2 overexpression as well as Staurosporine-induced apoptosis both decrease ER Ca^{2+}-level and increase nuclear envelope permeability. These findings are unexpected as Bcl-2 is a pro-survival member of the Bcl-2 family and a proto-oncogene whereas the broad-spectrum kinase inhibitor STS induces apoptotic cell death in a wide variety of cell lines (see Sarkar et al., 2009 for references). At the first glance it seems unlikely, that both pathways should elicit the same mechanisms.

Furthermore, increased nuclear envelope permeability is constitutiv and stimulus independent in the Bcl-2 paradigm, whereas in the apoptotic setting an exogenous stimulus elicits an acute increase in nuclear envelope permeability.

Although being widely used, the mechanisms through which STS exerts its effect are widely unknown. It is generally assumed that mitochondria are involved in mediating STS-induced cell death (Gil et al., 2003; Chandele et al., 2004; Wang et al., 2008). The disruption of mitochondria membrane potential and modulation of cell cytoskeleton have been proposed to play key roles in STS-induced cell death. Activation of caspases has long been assumed to be a prerequisite for STS induced cell death. Work done in different groups, however, has demonstrated that beside the caspase-dependent pathway also a caspase-independent pathway exists (Zhang et al., 2003). The involvement of Ca^{2+} in mediating staurosporine-induced cell death has been shown (Kruman et al., 1998; Seo and Seo, 2009). In the results presented in this work decreased ER Ca^{2+} -level have been shown. This corresponds to published data, showing increased mitochondrial Ca^{2+} uptake, very likely released from the ER, in STS-induced apoptosis (Kruman et al., 1999; Minagawa et al., 2005). It has been proposed that increased nuclear envelope permeability is important for the nuclear entry of pro-apoptotic factors that are normally restricted to the cytosol and therefore elicits cell death (Faleiro et al., 2000; Ferrando-May et al., 2001; Roehrig et al., 2003). In further support of the hypothesis that increased nuclear

permeability favors apoptosis progression, Ca^{2+} chelation by BAPTA results in prolonged nuclear permeability barrier function which might possibly increase resistance of HeLa cells to STS. The possible cytoprotective effect is further supported by the finding in this work that BAPTA addition slightly decreased the percentage of apoptotic nuclei (Figure 24B). Although this effect is not statistically significant, it warrants further investigation. In addition, a cytoprotective function of calpain inhibition has been discussed (VII.3.1.) based on the observed increase in nuclear permeability and the enhanced cell death in the presence of calpain inhibitors (Figure 22B and 21B). Taken together, the Ca^{2+}-mediated increase in nuclear envelope permeability in STS-induced apoptosis detected in this work is very likely a mechanism to elicit cell death.

As Bcl-2, being a pro-survival factor, would be expected to decrease apoptosis-associated nuclear permeability, the observed Ca^{2+}-mediated increase in nuclear permeability is more difficult to explain.

There are at least three proposed mechanisms as to how Bcl-2 decreases ER Ca^{2+} level. One mechanism proposes that Bcl-2 forms ion-transmitting pores in the ER membrane. This hypothesis is based on the structural resemblance of Bcl-2 and Bcl-x_L to pore forming bacterial-toxins and on the ability of Bcl-2 to form pores in artificial lipid membranes in vitro (reviewed in Sharpe et al., 2004). Work done by Chami et al., 2004 however, showed that the pore-forming regions of Bcl-2 are not necessary for reduced ER Ca^{2+} level. The second hypothesis proposes increased leakage of Ca^{2+} from the ER through binding of Bcl-2 to inositol 1,4,5-trisphosphate receptors (IP3Rs). White and co-workers (Li et al., 2007; White et al., 2005) report an increased sensitivity of IP3Rs to IP3 when Bcl-2 is bound, resulting in decreased ER Ca^{2+} level. Furthermore, induction of hyper-phosphorylation of IP3Rs by Bcl-2 in the absence of Bax/Bak, resulted in decreased ER Ca^{2+} level (Oakes et al., 2005). The third mechanism is a reduction of ER Ca^{2+} level by decreasing the levels of sarcoplasmic/endoplasmic Ca^{2+} -ATPase (SERCA) through direct interaction of Bcl-2 with SERCA (Dremina et al., 2004, 2006). For Bcl-x_L, another pro-survival member of the Bcl-2 family, reduced endoplasmic Ca^{2+} level have only be seen in the presence of Bax inhibitor-1 (BI-1) (Xu et

al., 2008). BI-1 is an evolutionary conserved, transmembrane protein that resides in the ER in both animal and plant cells (Xu and Reed, 1998). When overexpressed it has cytoprotective functions in animal or plant cells and reduces ER Ca^{2+} content (Kawai et al., 1999; Bolduc et al., 2003; Xu et al 2008).

As Bcl-2 is an oncogene, one reason for Bcl-2-induced increase in nuclear envelope permeability might be the increased need of rapidly proliferating cells for nuclear-cytoplasmic exchange. This hypothesis is unlikely as the tumorigenic effect of Bcl-2 is not caused by increased proliferation but decreased apoptosis.

It might be possible that Bcl-2-induced increase in nuclear permeability conveys additional, non-mitochondria related, protection against apoptotic stimuli. Alterations of nuclear permeability have been shown in non-apoptotic situations. So is nuclear envelope permeability increased in prophase and late anaphase of the mitotic cycle (Lenart et al., 2003; Bardina et al, 2009; Akin and Feldherr, 1990). Furthermore, an increase in nuclear permeability and relocation of normally cytosolic proteins to the nucleus has also been observed in the closed mitosis of some yeast (De Souza et al., 2004). In support of the non-pathogenic alterations of nuclear envelope permeability, Buchholz and coworkers have observed a transient increase in nuclear permeability after treatment with aldosterone (Buchholz et al., 2004). In all these examples, increased nuclear permeability might be necessary for facilitated exchange of transport factors important for enhanced transcriptional activity. In light of the presented published data, it is tempting to speculate that Bcl-2-induced increased permeability, which has been demonstrated in this work, is relevant for enhanced transcription of pro-survival factors. Therefore increased nuclear permeability is not in contrast to Bcl-2´s anti-apoptotic function at the mitochondria but may convey additional protection towards pro-apoptotic cues by supporting high levels of gene expression including transcription of pro-survival factors.

From the data discussed above, one can conclude that despite employment of the same mechanism, Ca^{2+}-mediated increase in nuclear envelope

permeability, the underlying purpose is different. While in STS-induced apoptosis increased nuclear permeability may serve as a pro-apoptotic mechanism increasing transport of pro-apoptotic factors, Bcl-2 may increase nuclear permeability to enhance transcription of pro-survival proteins.

VII.3.1. Dependency of Bcl-2 mediated ER Ca^{2+} -level reduction on other proteins

Work done in the group of Carl White demonstrates that Bcl-x_L -induced decrease in ER Ca^{2+} content depends on the presence of certain IP3R isoforms. Their results show that Bcl-x_L elicits reduced ER Ca^{2+} level only in the presence of IP_3R isoform-3. This reduction does not occur in the presence of IP_3R isoforms-1 and -2 (Li et al., 2007) alone. The necessity of IP_3R isoform-3 for reduced Ca^{2+} level could explain unpublished data obtained in the course of this PhD project. Bax/Bak DKO MEFS do not show increased nuclear permeability although Bcl-2 which is no longer sequestered by Bax/Bak, could stimulate Ca^{2+} release from the ER (data not shown). As Bcl-2 is a close relative of Bcl-x_L it could be dependent on the same IP_3R isoform. The possible absence of IP_3R isoform-3 in the MEFs used in this work could inhibit depletion of ER Ca^{2+}-content and therefore might explain the unaltered nuclear permeability. However, Ca^{2+}-levels and IP_3R isoform-3 levels have not been measured in these cells. Another explanation why Bax/Bak DKO MEFs do not display increased nuclear permeability might be the dependence of Bcl-2 on Bax-inhibitor-1 (BI-1) for altering ER Ca^{2+} -content as has been shown for the related Bcl-x_L (Xu et al., 2008). BI-1 is an evolutionary conserved, transmembrane protein that resides in the ER in both animal and plant cells (Xu and Reed, 1998). When overexpressed it has cytoprotective functions in animal or plant cells and reduces ER Ca^{2+} content (Kawai et al., 1999; Bolduc et al., 2003; Xu et al 2008). In the absence of BI-1 Bcl-XL failed to reduce ER Ca^{2+}-level. Again, the presence of BI-1 in Bax/Bak DKO MEFs has not been investigated in this work.

VII.4. Detection of reduced ER Ca^{2+} -level by the nuclear pore complex.

The lumen of the ER and the nuclear envelope are contiguous (Unwin and Milligan, 1982). As nuclear pore complexes are integral parts of the nuclear envelope, changes in nuclear cistern Ca^{2+} concentrations are likely to be detected by the NPCs. Depletion of ER Ca^{2+} has been shown to have variable effects on nuclear envelope permeability. While some groups propose decreased nuclear envelope permeability after Ca^{2+} depletion (Greber and Gerace, 1992; Perez-Terzic et al., 1996), others report increased nuclear permeability (Shahin et al., 2001; Scorrano et al., 2003) whereas a third group does not detect an effect of Ca^{2+}-depletion on nuclear envelope permeability (Enss et al.,2003; Wei et al., 2003) (see introduction).

Different mechanisms as to how ER Ca^{2+} -level could influence nuclear pore structure and nuclear envelope permeability have been proposed. Firstly, reduced Ca^{2+}-level in the perinuclear space could disrupt interaction of the NPC with unknown factors that are important for NPC function (Greber and Gerace, 1995). Secondly, decreased nuclear permeability due to Ca^{2+} depletion in the ER has been reported to be a part of the stress response due to accumulation of misfolded proteins which occur in the absence of ER Ca^{2+}, (Wileman et al., 1991; Lodish et al., 1992, Greber and Gerace, 1995). A very interesting possibility as to how Ca^{2+} regulates nuclear permeability, involves nuclear pore protein gp210 (Greber and Gerace, 1995). Glycoprotein 210 is an integral membrane protein which contains a small cytoplasmic tail on the C-terminus and one transmembrane region. Most of it`s mass (>95%) is located in the perinuclear space (Wozniak et al., 1989; Greber and Gerace, 1990). Gp210 contains in its perinuclear region sequences homologous to the conserved Ca^{2+} binding EF-hand motif (Greber and Gerace, 1995; Kretsinger, 1976; Strynadka and James, 1989). The involvement of gp210 in nuclear transport has been demonstrated by Greber and Gerace in 1992. Incubation with an antibody directed against the luminal domain of gp210 resulted in reduced active transport and passive permeability.

DISCUSSION

To test whether gp210 mediates the effect of reduced Ca^{2+} level in ER / perinuclear space on nuclear permeability, experiments with two different siRNAs directed against gp210 were performed. Although both siRNAs have been shown to reduce gp210 level (Mansfeld et al., 2006; Stavru et al.; 2006) in HeLa cells, no reduction of gp210 levels in either western blot or immunofluorecence could be achieved here. In the same setting, downregulation of LaminA/C was succesfull. Because of time reasons, the role of gp10 in mediating the Ca^{2+} effect at the NPC could not be pursued further.

VIII. Perspectives

This work demonstrates regulation of nuclear envelope permeability by ER Ca^{2+} -level in two opposing cellular contexts apoptosis and anti-apoptosis.

VIII.1. Staurosporine-induced alteration of nuclear envelope permeability

It would be interesting to identify the component of the nuclear envelope responsible for detecting altered ER Ca^{2+}-level. As gp210 has been proposed to be this component, live cell imaging of gp210 knockdown cells should be performed to gain information about the relevance of gp210 in mediating the effect of reduced Ca^{2+} level at the nuclear pore complex. The problems with published siRNA sequences against gp210 have been discussed. As a first step, at least two functional siRNAs should be constructed, which then could be used alone or in combination to down regulate gp210 expression. Another problem which needs to be addressed is the limited cell number that can be investigated by live cell imaging. Therefore either a stable downregulation with very high efficiency or immunostaining with gp210 antibody and counting permeability in cells without gp210 has to be performed. A further problem is the functionality of the gp210 antibody. All used antibodies were functional only for western blot but not immunofluorescence.

Another aspect of STS-induced leakage which should be investgated further is the influence of calpain-inhibition and Ca^{2+} chelation. As has been outlined in the discussion part, calpains may exhibit pro-survival properties and could, when inhibited, lead to enhanced cell death. An indication supporting this hypothesis was given by the even increased early nuclear leakage in STS-induced cell death and increased percentage of apoptotic nuclei under calpain inhibition (Figures 22B and 21B). To test the influence of calpains on cell death, it would be necessary to perform viability assays in the presence or absence of calpain-inhibitors.

In contrast to calpain inhibition, chelation of Ca^{2+} completely abolished early nuclear permeability increase in STS-induced apoptosis. The possible

beneficiary effect on cell viability is indicated by counting apoptotic cells in the presence of BAPTA, which showed decreased cell death (Figure 24B). To further strengthen this finding, viability assays with or without Ca^{2+} chelation should be performed.

VIII.2. Bcl-2-induced alteration of nuclear envelope permeability

In the course of the work on this project, the effect of Bcl-2 knock-down was tested in preliminary experiments. To this end, ER Ca2+ level and nuclear envelope permeability were investigated in Bcl-2 -/- MEFs (a kind gift of Prof. Christoph Borner). It was expected, that decreased Bcl-2 levels should result in higher or at least equal endoplasmic Ca2+ level and and decreased nuclear envelope permeability. Preliminary experiments gave inconclusive results. While some experiments revealed decreased nuclear permeability in Bcl-2 KO cells, other data showed increased permeability (data not shown). Measuring of Ca^{2+} level was very difficult as MEFs are very sensitive to washing steps; even under very careful handling, especially MEF Bcl-2 KO cells lost contact to the surface. As this resulted in different cell densities in the different wells, comparison of measured Ca^{2+} levels was problematic. The few obtained data, support decreased peak values of endoplasmic Ca2+ release after thapsigargin addition in Bcl-2 KO cells. Although the peak value is lower without Bcl-2, the overall amount of released Ca^{2+} is higher than in control cells, due to sustained Ca^{2+} release. Possibly Bcl-2 KO cells do not initially release more ER Ca^{2+} after thapsigargin stimulation but may nonetheless have higher ER Ca^{2+} level. The effect of Bcl-2 knockdown has to be further investigated as the results are needed to clarify Bcl-2`s role on ER Ca2+ level and nuclear permeability. In parallel the effect of Bax/Bak double knockout on nuclear permeability should be investigated.

Further, the relevance of different IP3R isoforms and BI-1 protein for reduction of ER Ca^{2+} level has been mentioned. Bax/Bak double Knockout MEFs do not show reduced ER Ca^{2+} levels. To enlighten the role of IP3R isoform-3 and BI-1 protein in reducing Ca2+ level in the ER and the

continous nuclear envelope lumen, expression of these proteins in the different cell lines should be investigated.

IX. References

Adams, J. M. and S. Cory (2007). "Bcl-2-regulated apoptosis: mechanism and therapeutic potential." Current Opinion in Immunology 19(5): 488-496.

Adams, J. M. and S. Cory (2007). "The Bcl-2 apoptotic switch in cancer development and therapy." Oncogene 26(9): 1324-1337.

Akiyama, T. P. B., Tsuyoshi Miyazaki, et al. (2003). "Regulation of osteoclast apoptosis by ubiquitylation of proapoptotic BH3-only Bcl-2 family member Bim." EMBO J. 22(24).

Alber, F., S. Dokudovskaya, et al. (2007). "The molecular architecture of the nuclear pore complex." Nature 450(7170): 695-701.

Albertini, M., L. F. Pemberton, et al. (1998). "A Novel Nuclear Import Pathway for the Transcription Factor TFIIS." J. Cell Biol. 143(6): 1447-1455.

Andrabi, S. A., N. S. Kim, et al. (2006). "Poly(ADP-ribose) (PAR) polymer is a death signal." Proceedings of the National Academy of Sciences 103(48): 18308-18313.

Annis, M. G. N. Z., Weijia Zhu1, Linda Z Penn4, Guido Kroemer3, Brian Leber1,2 and David W Andrews1 (2001). "ER localized Bcl-2 prevents apoptosis when redistribution of cytochrome c is a late event." oncogene 20(16).

Assefa, Z., G. Bultynck, et al. (2004). "Caspase-3-induced truncation of type 1 inositol trisphosphate receptor accelerates apoptotic cell death and induces inositol trisphosphate-independent calcium release during apoptosis." J. Biol. Chem. 279: 43227.

Baffy, G., T. Miyashita, et al. (1993). "Apoptosis induced by withdrawal of interleukin-3 (IL-3) from an IL-3-dependent hematopoietic cell line is associated with repartitioning of intracellular calcium and is blocked by enforced Bcl-2 oncoprotein production." J. Biol. Chem. 268: 6511.

Bakhshi, A., J. P. Jensen, et al. (1985). "Cloning the chromosomal breakpoint of t(14;18) human lymphomas: clustering around Jh on chromosome 14 and near a transcriptional unit on 18." Cell 41(3): 899-906.

Baliga, B. C., P. A. Colussi, et al. (2003). "Role of Prodomain in Importin-mediated Nuclear Localization and Activation of Caspase-2." Journal of Biological Chemistry **278**(7): 4899-4905.

Bano, D., D. Dinsdale, et al. (2009). "Alteration of the nuclear pore complex in Ca2+-mediated cell death." Cell Death Differ 17(1): 119-133.

Bardina, M. V., P. V. Lidsky, et al. (2009). "Mengovirus-Induced Rearrangement of the Nuclear Pore Complex: Hijacking Cellular Phosphorylation Machinery." J. Virol. 83(7): 3150-3161.

Bauer, M. K. A., A. Schubert, et al. (1999). "Adenine Nucleotide Translocase-1, a Component of the Permeability Transition Pore, Can Dominantly Induce Apoptosis." J. Cell Biol. 147(7): 1493-1502.

Beg, A. A., S. M. Ruben, et al. (1992). "I kappa B interacts with the nuclear localization sequences of the subunits of NF-kappa B: a mechanism for cytoplasmic

etention." Genes & Development 6(10): 1899-1913.

Behrens P, B. U., Fogt F, Wernert N, Wellmann A. (2001). "Implication of the proliferation and apoptosis associated CSE1L/CAS gene for breast cancer development." Anticancer res 21(4A): 2413-1417.

Belmokhtar, C. A. H., Josette and Bendirdjian, Evelyne Ségal- (2001). "Staurosporine induces apoptosis through both caspase-dependent and caspase-independent mechanisms." Oncogene 20(26): 3354-3362.

Belov, G. A., P. V. Lidsky, et al. (2004). "Bidirectional Increase in Permeability of Nuclear Envelope upon Poliovirus Infection and Accompanying Alterations of Nuclear Pores." J. Virol. 78(18): 10166-10177.

Bezprozvanny, I. (2005). "The inositol 1,4,5-trisphosphate receptors." Cell Calcium 38: 261.

Bischoff, F. R., Krebber H, Smirnova E, Dong W, and Ponstingl H (1995). "Co-activation of RanGTPase and inhibition of GTP dissociation by Ran-GTP binding protein RanBP1." EMBO J 14(4): 705-715.

Blomgren, K., C. Zhu, et al. (2001). "Synergistic Activation of Caspase-3 by m-Calpain after Neonatal Hypoxia-Ischemia." Journal of Biological Chemistry 276(13): 10191-10198.

Boatright, K. M. and G. S. Salvesen (2003). "Mechanisms of caspase activation." Current Opinion in Cell Biology 15(6): 725-731.

Boehning, D., R. L. Patterson, et al. (2003). "Cytochrome c binds to inositol (1,4,5) trisphosphate receptors, amplifying calciumdependent apoptosis." Nat. Cell Biol. 5: 1051.

Boise, L. H., M. González-García, et al. (1993). "bcl-x, a Bcl-2-related gene that functions as a dominant regulator of apoptotic cell death." Cell 74(4): 597-608.

Bolduc N, O. M., Pitre F, Brisson LF. (2003). "Molecular characterization of two plant BI-1 homologues which suppress Bax-induced apoptosis in human 293 cells." Planta 216(3).

Borrow, J. A. M. S., Vincent P. Stanton Jr., Reinhard Becher, Tucker Collins, Amy J. Williams, Ian Dubé, Fay Katz, Yok L. Kwong, Christine Morris, Kazuma Ohyashiki, Keisuke Toyama, Janet Rowley & David E. Housman (1996). "The t(7;11)(p15;p15) translocation in acute myeloid leukaemia fuses the genes for nucleoporin NUP96 and class I homeoprotein HOXA9." nature genetics 12: 159-167.

Brinkmann U, B. E., Gallo M, Pastan I. (1995). "Cloning and characterization of a cellular apoptosis susceptibility gene, the human homologue to the yeast chromosome segregation gene CSE1." Proc Natl Acad Sci U S A 92(22): 10427-10431.

Buchholz, I. E. K., C. Schafer, A. Schlune, V. Shahin and H. Oberleithner (2004). "Transient Permeability Leak of Nuclear Envelope Induced by Aldosterone " Journal of Membrane Biology 199(3): 135-141.

REFERENCES

Certo, M., V. D. G. Moore, et al. (2006). "Mitochondria primed by death signals determine cellular addiction to antiapoptotic BCL-2 family members." Cancer Cell 9(5): 351-365.

Chami, M., A. Prandini, et al. (2004). "Bcl-2 and Bax Exert Opposing Effects on Ca2+ Signaling, Which Do Not Depend on Their Putative Pore-forming Region 10.1074/jbc.M409663200." J. Biol. Chem. 279(52): 54581-54589.

Chen, L., S. N. Willis, et al. (2005). "Differential Targeting of Prosurvival Bcl-2 Proteins by Their BH3-Only Ligands Allows Complementary Apoptotic Function." Molecular Cell 17(3): 393-403.

Cheng, E. H. Y. A., M. C. Wei, et al. (2001). "BCL-2, BCL-XL Sequester BH3 Domain-Only Molecules Preventing BAX- and BAK-Mediated Mitochondrial Apoptosis." Molecular Cell 8(3): 705-711.

Choi SS, P. S., Kim UJ, Shin HS. (1997). "Bfl-1, a Bcl-2-related gene, is the human homolog of the murine A1, and maps to Chromosome 15q24.3 " mammalian genome 8(10).

Cleary ML and Sklar, J. (1985). "Nucleotide sequence of a t(14;18) chromosomal breakpoint in follicular lymphoma and demonstration of a breakpoint-cluster region near a transcriptionally active locus on chromosome 18." Proc Natl Acad Sci U S A 82(21): 7439–7443.

Colussi, P. A., N. L. Harvey, et al. (1998). "Conversion of Procaspase-3 to an Autoactivating Caspase by Fusion to the Caspase-2 Prodomain." Journal of Biological Chemistry **273**(41): 26566-26570.

Courvalin, J. C., K. Lassoued, et al. (1990). "The 210-kD nuclear envelope polypeptide recognized by human autoantibodies in primary biliary cirrhosis is the major glycoprotein of the nuclear pore." The Journal of Clinical Investigation 86(1): 279-285.

Courvalin, J. C., N. Segil, et al. (1992). "The lamin B receptor of the inner nuclear membrane undergoes mitosis-specific phosphorylation and is a substrate for p34cdc2-type protein kinase." Journal of Biological Chemistry 267(27): 19035-19038.

Cronshaw, J. M. and M. J. Matunis (2004). "The nuclear pore complex: disease associations and functional correlations." Trends in Endocrinology & Metabolism 15(1): 34-39.

Cronshaw, J. M., A. N. Krutchinsky, et al. (2002). "Proteomic analysis of the mammalian nuclear pore complex." J. Cell Biol. 158(5): 915-927.

D'Angelo, M. A. and M. W. Hetzer (2008). "Structure, dynamics and function of nuclear pore complexes." Trends in Cell Biology In Press, Corrected Proof.

de Bruin, E. C., D. Meersma, et al. (2003). "A serine protease is involved in the initiation of DNA damage-induced apoptosis." 10(10): 1204-1212.

De Giorgi, F., L. Lartigue, et al. (2002). "The permeability transition pore signals apoptosis by directing Bax translocation and multimerization." FASEB J. 16(6): 607-609.

REFERENCES

De Souza, C. P. C., A. H. Osmani, et al. (2004). "Partial Nuclear Pore Complex Disassembly during Closed Mitosis in Aspergillus nidulans." Current Biology 14(22): 1973-1984.

DeGrasse, J. A., K. N. DuBois, et al. (2009). "Evidence for a Shared Nuclear Pore Complex Architecture That Is Conserved from the Last Common Eukaryotic Ancestor." Molecular & Cellular Proteomics 8(9): 2119-2130.

Degterev, A., J. Hitomi, et al. (2008). "Identification of RIP1 kinase as a specific cellular target of necrostatins." **4**(5): 313-321.

Degterev, A., M. Boyce, et al. (2003). "A decade of caspases." Oncogene **22**(53): 8543-8567.

Dejean, L. M., S. Martinez-Caballero, et al. (2005). "Oligomeric Bax Is a Component of the Putative Cytochrome c Release Channel MAC, Mitochondrial Apoptosis-induced Channel." Mol. Biol. Cell 16(5): 2424-2432.

Denault, J.-B. and G. S. Salvesen (2002). "Caspases: Keys in the Ignition of Cell Death." Chemical Reviews **102**(12): 4489-4500.

Denning, D. P., S. S. Patel, et al. (2003). "Disorder in the nuclear pore complex: The FG repeat regions of nucleoporins are natively unfolded 10.1073/pnas.0437902100." Proceedings of the National Academy of Sciences of the United States of America 100(5): 2450-2455.

Dijkers, P. F., R. H. Medema, et al. (2000). "Expression of the pro-apoptotic Bcl-2 family member Bim is regulated by the forkhead transcription factor FKHR-L1." Current Biology 10(19): 1201-1204.

Distelhorst, C. W., M. Lam, et al. (1996). "Bcl-2 inhibits hydrogen peroxideinduced ER Ca2+ pool depletion." Oncogene 12: 2051.

Dremina, E. S., V. S. Sharov, et al. (2004). "Anti-apoptotic protein Bcl-2 interacts with and destabilizes the sarcoplasmic/ER Ca2+-ATPase (SERCA)." Biochem. J. 383: 361.

Dremina, E. S., V. S. Sharov, et al. (2006). "Displacement of SERCA from SR Lipid Caveolae-Related Domains by Bcl-2:□ A Possible Mechanism for SERCA Inactivation†." Biochemistry 45(1): 175-184.

Duchen, M. R. (2000). "Mitochondria and Ca2+in cell physiology and pathophysiology." Cell Calcium 28(5-6): 339-348.

Egger, L., J. Schneider, et al. (2003). "Serine proteases mediate apoptosis-like cell death and phagocytosis under caspase-inhibiting conditions." Cell Death Differ 10(10): 1188-1203.

Elad, N., T. Maimon, et al. (2009). "Structural analysis of the nuclear pore complex by integrated approaches." Current Opinion in Structural Biology 19(2): 226-232.

Enss, K., Danker T, Schlune A, Buchholz I and Oberleithner H (2003). "Passive Transport of Macromolecules through Xenopus laevis Nuclear Envelope." Journal of Membrane Biology 196(3): 147-155.

REFERENCES

Espert, L., M. Denizot, et al. (2006). "Autophagy is involved in T cell death after binding of HIV-1 envelope proteins to CXCR4." The Journal of Clinical Investigation **116**(8): 2161-2172.

Fahrenkrog, B., B. Maco, et al. (2002). "Domain-specific antibodies reveal multiple-site topology of Nup153 within the nuclear pore complex." Journal of Structural Biology 140(1-3): 254-267.

Faleiro, L. and Y. Lazebnik (2000). "Caspases Disrupt the Nuclear-Cytoplasmic Barrier." J. Cell Biol. 151(5): 951-960.

Fan, F., C.-P. Liu, et al. (1997). "cDNA Cloning and Characterization ofNpap60:A Novel Rat Nuclear Pore-Associated Protein with an Unusual Subcellular Localization during Male Germ Cell Differentiation." Genomics 40(3): 444-453.

Feinstein-Rotkopf, Y. and Arama, E. (2009). "Can't live without them, can live with them: roles of caspases during vital cellular processes " Apoptosis 14(8): 980-995.

Ferrando-May, E., V. Cordes, et al. (2001). "Caspases mediate nucleoporin cleavage, but not early redistribution of nuclear transport factors and modulation of nuclear permeability in apoptosis." Cell death and differentiation **8**: 495-505.

Fornerod, M., Boer J, van Baal S, Jaeglé M, von Lindern M, Murti KG, Davis D, Bonten J, Buijs A, Grosveld G (1995). "Relocation of the carboxyterminal part of CAN from the nuclear envelope to the nucleus as a result of leukemia-specific chromosome rearrangements" Oncogene 10(9): 1739-1748

Foskett, J. K., C. White, et al. (2007). "Inositol Trisphosphate Receptor Ca2+ Release Channels." Physiol. Rev. 87(2): 593-658.

Foyouzi-Youssefi, R., S. Arnaudeau, et al. (2000). "Bcl-2 decreases the free Ca2+ concentration within the ER." Proceedings of the National Academy of Sciences of the United States of America 97(11): 5723-5728.

Gerace, L. and B. Burke (1988). "Functional Organization of the Nuclear Envelope." Annual Review of Cell Biology 4(1): 335-374.

Ghiotto, F., F. Fais, et al. (2010). "BH3-only proteins: The death-puppeteer's wires." Cytometry Part A **77A**(1): 11-21.

Gibson L, H. S., Huang DC, Bernard O, Copeland NG, Jenkins NA, Sutherland GR, Baker E, Adams JM, Cory S (1996). "bcl-w, a novel member of the Bcl-2 family, promotes cell survival." Oncogene 13(4): 665-675

Gil-Parrado, S., A. Fernández-Montalván, et al. (2002). "Ionomycin-activated Calpain Triggers Apoptosis." Journal of Biological Chemistry 277(30): 27217-27226.

Golstein, P. K., G (2007). "Cell death by necrosis: towards a molecular definition" Trends in Biochemical Sciences 32(1)

Gorlich, D., M. J. Seewald, et al. (2003). "Characterization of Ran-driven cargo transport and the RanGTPase system by kinetic measurements and computer simulation." EMBO J 22(5): 1088-1100.

REFERENCES

Greber, U. and L. Gerace (1992). "Nuclear protein import is inhibited by an antibody to a lumenal epitope of a nuclear pore complex glycoprotein." J. Cell Biol. 116(1): 15-30.

Greber, U. and L. Gerace (1995). "Depletion of calcium from the lumen of ER reversibly inhibits passive diffusion and signal-mediated transport into the nucleus." J. Cell Biol. 128(1): 5-14.

Grimm, S. B., Dieter (2007). "The permeability transition pore in cell death." Apoptosis 12(5).

Grütter, M. G. (2000). "Caspases: key players in programmed cell death." Current Opinion in Structural Biology **10**(6): 649-655.

Gustin, K. E. and P. Sarnow (2001). "Effects of poliovirus infection on nucleo-cytoplasmic trafficking and nuclear pore complex composition." EMBO J 20(1/2): 240-249.

Gustin, K. E. and P. Sarnow (2002). "Inhibition of Nuclear Import and Alteration of Nuclear Pore Complex Composition by Rhinovirus." J. Virol. 76(17): 8787-8796.

Hanson, C. J., M. D. Bootman, et al. (2008). "Bcl-2 suppresses Ca2+ release through inositol 1,4,5-trisphosphate receptors and inhibits Ca2+ uptake by mitochondria without affecting ER calcium store content." Cell Calcium 44(3): 324-338.

Higo, T., M. Hattori, et al. (2005). "Subtype-specific and ER lumenal environment-dependent regulation of inositol 1,4,5-trisphosphate receptor type 1 by ERp44." Cell 120: 85.

Hinshaw, J. E., B. O. Carragher, et al. (1992). "Architecture and design of the nuclear pore complex." Cell 69(7): 1133-1141.

Holler, N., R. Zaru, et al. (2000). "Fas triggers an alternative, caspase-8-independent cell death pathway using the kinase RIP as effector molecule." Nat Immunol **1**(6): 489-495.

Huang, Y., Y. C. Park, et al. (2001). "Structural Basis of Caspase Inhibition by XIAP: Differential Roles of the Linker versus the BIR Domain." Cell 104(5): 781-790.

Isgro, T. A. and K. Schulten (2007). "Cse1p-Binding Dynamics Reveal a Binding Pattern for FG-Repeat Nucleoporins on Transport Receptors." Structure 15(8): 977-991.

Itoh, N. and S. Nagata (1993). "A novel protein domain required for apoptosis. Mutational analysis of human Fas antigen." Journal of Biological Chemistry 268(15): 10932-10937.

Jans DA and J. P. (1994). "Negative charge at the casein kinase II site flanking the nuclear localization signal of the SV40 large T-antigen is mechanistically important for enhanced nuclear import." oncogene 9(10): 2961-2968.

Jans, D. A. (2009). "Nuclear transport in development and disease - The importance of importins." Seminars in Cell & Developmental Biology 20(5): 575-575.

Jarnik, M, A. U. (1991). "Toward a more complete 3-D structure of the nuclear pore complex." J Struct Biol. 107(3): 291-308.

REFERENCES

Jayaraman, T. and A. R. Marks (1997). "T cells deficient in inositol 1,4,5-trisphosphate receptor are resistant to apoptosis." Mol. Cell. Biol. 17: 3005.

Jeffers, J. R., E. Parganas, et al. (2003). "Puma is an essential mediator of p53-dependent and -independent apoptotic pathways." Cancer Cell 4(4): 321-328.

Kaffman, A., N. M. Rank, et al. (1998). "Phosphorylation regulates association of the transcription factor Pho4 with its import receptor Pse1/Kap121." Genes & Development 12(17): 2673-2683.

Kaiser, N. a. E., IS (1977). "Calcium dependence of glucocorticoid-induced lymphocytolysis." Proc Natl Acad Sci U S A 74(2): 638-642.

Kasper, L. H., P. K. Brindle, et al. (1999). "CREB Binding Protein Interacts with Nucleoporin-Specific FG Repeats That Activate Transcription and Mediate NUP98-HOXA9 Oncogenicity." Mol. Cell. Biol. 19(1): 764-776.

Kau, T. R., J. C. Way, et al. (2004). "Nuclear transport and cancer: from mechanism to intervention." Nat Rev Cancer 4(2): 106-117.

Kehlenbach, R. H. and L. Gerace (2000). "Phosphorylation of the Nuclear Transport Machinery Down-regulates Nuclear Protein Import in Vitro 10.1074/jbc.M001455200." J. Biol. Chem. 275(23): 17848-17856.

Kerr, J., A. Wyllie, et al. (1972). "Apoptosis-a basic biological phenomenon with wide ranging implications in tissue kinetics." Br J Cancer **26**: 239.

Kim, B. C., H. T. Kim, et al. (2002). "Tumor necrosis factor induces apoptosis in hepatoma cells by increasing Ca2+ release from the ER and suppressing Bcl-2 expression." J. Biol. Chem. 277: 31381.

Kischkel, F. S. H., I Behrmann, M Germer, M Pawlita, P H Krammer, and M E Peter (1995). "Cytotoxicity-dependent APO-1 (Fas/CD95)-associated proteins form a death-inducing signaling complex (DISC) with the receptor." EMBO J 14(22): 5579-5588.

Kretsinger, R. H. (1976). "Calcium-Binding Proteins." Annual Review of Biochemistry 45(1): 239-266.

Kroemer, G., L. Galluzzi, et al. (2009). "Classification of cell death: recommendations of the Nomenclature Committee on Cell Death 2009." Cell Death Differ **16**(1): 3-11.
Kruman, I. I. and M. P. Mattson (1999). "Pivotal Role of Mitochondrial Calcium Uptake in Neural Cell Apoptosis and Necrosis." Journal of Neurochemistry 72(2): 529-540.

Kruman, I., Q. Guo, et al. (1998). "Calcium and reactive oxygen species mediate staurosporine-induced mitochondrial dysfunction and apoptosis in PC12 cells." Journal of Neuroscience Research 51(3): 293-308.

Kubbutat, M. and K. Vousden (1997). "Proteolytic cleavage of human p53 by calpain: a potential regulator of protein stability." Mol. Cell. Biol. 17(1): 460-468.

Kuida, K. Z., T. S.; Na, S.; Kuan, C.-y.; Yang, D.; Karasuyama, and P. F. H.; Rakic, R. A. (1996). "Decreased apoptosis in the brain and premature lethality in CPP32-deficient mice." nature **384**: 368-372.

REFERENCES

Kuida, K., T. F. Haydar, et al. (1998). "Reduced Apoptosis and Cytochrome c-Mediated Caspase Activation in Mice Lacking Caspase 9." Cell **94**(3): 325-337.

Kutay, U., F. R. Bischoff, et al. (1997). "Export of Importin [alpha] from the Nucleus Is Mediated by a Specific Nuclear Transport Factor." Cell 90(6): 1061-1071.

Kuwana, T., L. Bouchier-Hayes, et al. (2005). "BH3 Domains of BH3-Only Proteins Differentially Regulate Bax-Mediated Mitochondrial Membrane Permeabilization Both Directly and Indirectly." Molecular Cell 17(4): 525-535.

Kuwana, T., M. R. Mackey, et al. (2002). "Bid, bax and lipids cooperate to form supramolecular openings in the outer mitochondrial membrane." Cell 111: 331-342.

Lenart, P., G. Rabut, et al. (2003). "Nuclear envelope breakdown in starfish oocytes proceeds by partial NPC disassembly followed by a rapidly spreading fenestration of nuclear membranes." J. Cell Biol. 160(7): 1055-1068.

Letai, A., M. C. Bassik, et al. (2002). "Distinct BH3 domains either sensitize or activate mitochondrial apoptosis, serving as prototype cancer therapeutics." Cancer Cell 2(3): 183-192.

Ley, R., K. Balmanno, et al. (2003). "Activation of the ERK1/2 Signaling Pathway Promotes Phosphorylation and Proteasome-dependent Degradation of the BH3-only Protein, Bim." Journal of Biological Chemistry 278(21): 18811-18816.

Li, C., X. Wang, et al. (2007). "Apoptosis regulation by Bcl-xL modulation of mammalian inositol 1,4,5-trisphosphate receptor channel isoform gating." Proceedings of the National Academy of Sciences 104(30): 12565-12570.

Li, L. Y., X. Luo, et al. (2001). "Endonuclease G is an apoptotic DNase when released from mitochondria." Nature 412: 95-99.

Lidsky, P. V., S. Hato, et al. (2006). "Nucleocytoplasmic Traffic Disorder Induced by Cardioviruses." J. Virol. 80(6): 2705-2717.

Lodish, H. F., N. Kong, et al. (1992). "Calcium is required for folding of newly made subunits of the asialoglycoprotein receptor within the ER." Journal of Biological Chemistry 267(18): 12753-12760.

Loeffler, M. and G. Kroemer (2000). "The Mitochondrion in Cell Death Control: Certainties and Incognita." Experimental Cell Research 256(1): 19-26.

Logue, S. E. and S. J. Martin (2008). "Caspase activation cascades in apoptosis." Biochemical Society Transactions 036(1): 1-9.

Luciano, F., A. Jacquel, et al. (2003). "Phosphorylation of Bim-EL by Erk1//2 on serine 69 promotes its degradation via the proteasome pathway and regulates its proapoptotic function." Oncogene 22(43): 6785-6793.

Ly, J. D. G., D. R.; Lawen, A. (2003). "The mitochondrial membrane potential (Δψm) in apoptosis; an update." Apoptosis 8(2).

Macara, I. G. (2001). "Transport into and out of the Nucleus." Microbiol. Mol. Biol. Rev. 65(4): 570-594.

REFERENCES

MacFarlane, M., M. Ahmad, et al. (1997). "Identification and Molecular Cloning of Two Novel Receptors for the Cytotoxic Ligand TRAIL." Journal of Biological Chemistry **272**(41): 25417-25420.

Mackrill, J. (1999). "Protein-protein interactions in intracellular Ca2+ release channel function." Biochem. J. 337: 345.

Mahajan, R., C. Delphin, et al. (1997). "A Small Ubiquitin-Related Polypeptide Involved in Targeting RanGAP1 to Nuclear Pore Complex Protein RanBP2." Cell 88(1): 97-107.

Majno, G. J., I (1995). "Apoptosis, oncosis, and necrosis. An overview of cell death." Am J Pathol **146** (1): 3-15.

Mansfeld, J., S. Güttinger, et al. (2006). "The Conserved Transmembrane Nucleoporin NDC1 Is Required for Nuclear Pore Complex Assembly in Vertebrate Cells." Molecular Cell 22(1): 93-103.

Martinez-Caballero, S. D., Laurent M. ; Jonas, Elizabeth A. and Kinnally, Kathleen W (2005). "The Role of the Mitochondrial Apoptosis Induced Channel MAC in Cytochrome c Release " Journal of Bioenergetics and Biomembranes, 37(3).

Mason, D. A., N. Shulga, et al. (2005). "Increased nuclear envelope permeability and Pep4p-dependent degradation of nucleoporins during hydrogen peroxide-induced cell death." FEMS Yeast Research 5(12): 1237-1251.

Mathai, J. P., M. Germain, et al. (2005). "BH3-only BIK regulates Bax,Bak-dependent release of Ca2+ from ER stores and mitochondrial apoptosis during stress-induced cell death." J. Biol. Chem. 280: 23829.

Miller, M. W., M. R. Caracciolo, et al. (1999). "Phosphorylation and Glycosylation of Nucleoporins." Archives of Biochemistry and Biophysics 367(1): 51-60.

Minagawa, N., E. A. Kruglov, et al. (2005). "The Anti-apoptotic Protein Mcl-1 Inhibits Mitochondrial Ca2+ Signals." Journal of Biological Chemistry 280(39): 33637-33644.

Mohr, D., S. Frey, et al. (2009). "Characterisation of the passive permeability barrier of nuclear pore complexes." EMBO J 28(17): 2541-2553.

Mooren, O. and et al. (2004). "Nuclear side conformational changes in the nuclear pore complex following calcium release from the nuclear membrane." Physical Biology 1(2): 125.

Moore-Nichols, D., A. Arnott, et al. (2002). "Regulation of Nuclear Pore Complex Conformation by IP3 Receptor Activation." Biophysical Journal 83(3): 1421-1428.

Moroianu, J. (1999). "Nuclear import and export pathways." Journal of Cellular Biochemistry 75(S32): 76-83.

Muzio, M., A. M. Chinnaiyan, et al. (1996). "FLICE, A Novel FADD-Homologous ICE/CED-3-like Protease, Is Recruited to the CD95 (Fas/APO-1) Death-Inducing Signaling Complex." Cell 85(6): 817-827.

Naismith, J. H. and S. R. Sprang (1998). "Modularity in the TNF-receptor family." Trends in Biochemical Sciences 23(2): 74-79.

REFERENCES

Newmeyer, D. D. and S. Ferguson-Miller (2003). "Mitochondria: Releasing Power for Life and Unleashing the Machineries of Death." Cell 112(4): 481-490.

Nicholson, D. W. and N. A. Thornberry (1997). "Caspases: killer proteases." Trends in Biochemical Sciences 22(8): 299-306.

Nikolova, V., C. Leimena, et al. (2004). "Defects in nuclear structure and function promote dilated cardiomyopathy in lamin A/C–deficient mice." The Journal of Clinical Investigation 113(3): 357-369.

O'Connell, A. R., B. W. Lee, et al. (2006). "Caspase-dependant activation of chymotrypsin-like proteases mediates nuclear events during Jurkat T cell apoptosis." Biochemical and Biophysical Research Communications 345(2): 608-616.

O'Connell, A. R., C. Holohan, et al. (2006). "Characterization of a serine protease-mediated cell death program activated in human leukemia cells." Experimental Cell Research 312(1): 27-39.

Oltvai, Z. N., C. L. Milliman, et al. (1993). "Bcl-2 heterodimerizes in vivo with a conserved homolog, Bax, that accelerates programed cell death." Cell 74(4): 609-619.

Paschal, B. and L. Gerace (1995). "Identification of NTF2, a cytosolic factor for nuclear import that interacts with nuclear pore complex protein p62." J. Cell Biol. 129(4): 925-937.

Patre, M., A. Tabbert, et al. (2006). "Caspases Target Only Two Architectural Components within the Core Structure of the Nuclear Pore Complex 10.1074/jbc.M511717200." J. Biol. Chem. 281(2): 1296-1304.

Pavlov, E. V., M. Priault, et al. (2001). "A novel, high conductance channel of mitochondria linked to apoptosis in mammalian cells and Bax expression in yeast." J. Cell Biol. 155(5): 725-732.

Peixoto, P. M., S. Y. Ryu, et al. (2009). "MAC inhibitors suppress mitochondrial apoptosis." Biochemical Journal 423(3): 381-387.
Pemberton, L. F. and B. M. Paschal (2005). "Mechanisms of Receptor-Mediated Nuclear Import and Nuclear Export." Traffic 6(3): 187-198.

Perez-Terzic, C., J. Pyle, et al. (1996). "Conformational States of the Nuclear Pore Complex Induced by Depletion of Nuclear Ca2+ Stores." Science 273(5283): 1875-1877.

Peters, R. (2005). "Translocation Through the Nuclear Pore Complex: Selectivity and Speed by Reduction‐of‐Dimensionality." Traffic 6(5): 421-427.

Pinton, P. and R. Rizzuto (2006). "Bcl-2 and Ca2+ homeostasis in the ER." 13(8): 1409-1418.

Pinton, P., D. Ferrari, et al. (2000). "Reduced Loading of Intracellular Ca2+ Stores and Downregulation of Capacitative Ca2+Influx in Bcl-2-Overexpressing Cells." J. Cell Biol. 148(5): 857-862.

Pinton, P., D. Ferrari, et al. (2001). "The Ca2+ concentration of the ER is a key determinant of ceramide-induced apoptosis: significance for the molecular mechanism of Bcl-2 action." EMBO J. 20: 2690

REFERENCES

Polster, B. M., G. Basañez, et al. (2005). "Calpain I Induces Cleavage and Release of Apoptosis-inducing Factor from Isolated Mitochondria." Journal of Biological Chemistry 280(8): 6447-6454.

Putcha, G. V., S. Le, et al. (2003). "JNK-Mediated BIM Phosphorylation Potentiates BAX-Dependent Apoptosis." Neuron 38(6): 899-914.

Rabut, G., V. Doye, et al. (2004). "Mapping the dynamic organization of the nuclear pore complex inside single living cells." 6(11): 1114-1121.

Rexach, M. and G. Blobel (1995). "Protein import into nuclei: association and dissociation reactions involving transport substrate, transport factors, and nucleoporins." Cell 83(5): 683-692.

Ribbeck, K. and D. Gorlich (2001). "Kinetic analysis of translocation through nuclear pore complexes." EMBO J 20(6): 1320-1330.

Ribbeck, K., G. Lipowsky, et al. (1998). "NTF2 mediates nuclear import of Ran." EMBO J 17(22): 6587-6598.

Rimpler, M. M., U. Rauen, et al. (1999). "Protection against hydrogen peroxide cytotoxicity in Rat-1 fibroblasts provided by the oncoprotein Bcl-2: Maintenance of calcium homeostasis is secondary to the effect of Bcl-2 on cellular glutathione." Biochem. J. 340: 291.

Rivière Y, B. V., Kourilsky P, Israël A. (1991). "Processing of the precursor of NF-kappa B by the HIV-1 protease during acute infection." Nature 350(6319): 625-626.

Roehrig, S., A. Tabbert, et al. (2003). "In vitro measurement of nuclear permeability changes in apoptosis." Analytical Biochemistry 318(2): 244-253.

Rong, Y. and C. W. Distelhorst (2008). "Bcl-2 Protein Family Members: Versatile Regulators of Calcium Signaling in Cell Survival and Apoptosis." Annual Review of Physiology 70(1): 73-91.

Rout, M. P., J. D. Aitchison, et al. (2000). "The Yeast Nuclear Pore Complex: Composition, Architecture, and Transport Mechanism." J. Cell Biol. 148(4): 635-652.

Rout, M. P., J. D. Aitchison, et al. (2003). "Virtual gating and nuclear transport: the hole picture." Trends in Cell Biology 13(12): 622-628.

Rudner, J., A. Lepple-Wienhues, et al. (2001). "Wild-type, mitochondrial and ER-restricted Bcl-2 inhibit DNA damage-induced apoptosis but do not affect death receptor-induced apoptosis." J Cell Sci 114(23): 4161-4172.

Salvesen, G. S. and C. S. Duckett (2002). "IAP proteins: blocking the road to death's door." Nat Rev Mol Cell Biol 3(6): 401-410.

Scaffidi, C., S. Fulda, et al. (1998). "Two CD95 (APO-1/Fas) signaling pathways." EMBO J 17(6): 1675-1687.

REFERENCES

Schulze-Osthoff, K., D. Ferrari, et al. (1998). "Apoptosis signaling by death receptors." European Journal of Biochemistry 254(3): 439-459.

Seo, S. R. a. S., Jeong Taeg (2009). "Calcium overload is essential for the acceleration of staurosporine-induced cell death following neuronal differentiation in PC12 cells." Exp mol med 41(4): 269-276.

Shahin, V., T. Danker, et al. (2001). "Evidence for Ca2+- and ATP-sensitive peripheral channels in nuclear pore complexes 10.1096/fj.00-0838com." FASEB J. 15(11): 1895-1901.

Sharpe, J. C., D. Arnoult, et al. (2004). "Control of mitochondrial permeability by Bcl-2 family members." Biochimica et Biophysica Acta (BBA) - Molecular Cell Research 1644(2-3): 107-113.

Shimizu, S., T. Kanaseki, et al. (2004). "Role of Bcl-2 family proteins in a non-apoptotic programmed cell death dependent on autophagy genes." Nat Cell Biol 6(12): 1221-1228.

Srinivasula, S. M., R. Hegde, et al. (2001). "A conserved XIAP-interaction motif in caspase-9 and Smac/DIABLO regulates caspase activity and apoptosis." Nature 410(6824): 112-116.

Stade, K., C. S. Ford, et al. (1997). "Exportin 1 (Crm1p) Is an Essential Nuclear Export Factor." Cell 90(6): 1041-1050.

Starr, D. A. and M. Han (2003). "ANChors away: an actin based mechanism of nuclear positioning." J Cell Sci 116(2): 211-216.

Stavru, F., G. Nautrup-Pedersen, et al. (2006). "Nuclear pore complex assembly and maintenance in POM121- and gp210-deficient cells 10.1083/jcb.200601002." J. Cell Biol. 173(4): 477-483.

Stehno-Bittel L, L. A. and D. E. Clapham (1995). "Neuron." 14(1): 163.

Stehno-Bittel L, P.-T. C. and D. E. Clapham (1995). "Science." 270(5243): 1835.

Stehno-Bittel L, P.-T. C. L. A. and D. E. Clapham (1996). "Soc. Gen. Physiol. Ser." 51: 195.

Stoffler, D., B. Feja, et al. (2003). "Cryo-electron Tomography Provides Novel Insights into Nuclear Pore Architecture: Implications for Nucleocytoplasmic Transport." Journal of Molecular Biology 328(1): 119-130.

Stoffler, D., K. N. Goldie, et al. (1999). "Calcium-mediated structural changes of native nuclear pore complexes monitored by time-lapse atomic force microscopy." Journal of Molecular Biology 287(4): 741-752.

Strubing, C. and D. E. Clapham (1999). "Active Nuclear Import and Export Is Independent of Lumenal Ca2+ Stores in Intact Mammalian Cells." J. Gen. Physiol. 113(2): 239-248.

Strynadka, N. C. J. and M. N. G. James (1989). "Crystal Structures of the Helix-Loop-Helix Calcium-Binding Proteins." Annual Review of Biochemistry 58(1): 951-999.

REFERENCES

Susin, S. A. (1999). "Molecular characterization of mitochondrial apoptosis-inducing factor." Nature 397: 441-446.

Takahashi, R., Q. Deveraux, et al. (1998). "A Single BIR Domain of XIAP Sufficient for Inhibiting Caspases." Journal of Biological Chemistry 273(14): 7787-7790.

Taylor, C. W., A. A. Genazzani, et al. (1999). "Expression of inositol trisphosphate receptors." Cell Calcium 26: 237.

Terry, L. J. and S. R. Wente (2009). "Flexible Gates: Dynamic Topologies and Functions for FG Nucleoporins in Nucleocytoplasmic Transport." Eukaryotic Cell 8(12): 1814-1827.

Terry, L. J., E. B. Shows, et al. (2007). "Crossing the Nuclear Envelope: Hierarchical Regulation of Nucleocytoplasmic Transport." Science 318(5855): 1412-1416.

Tittel, J. N. and H. Steller (2000). "A comparison of programmed cell death between species." Genome Biology **1**(3): reviews0003.0001 - reviews0003.0006.

Tran, E. J. and S. R. Wente (2006). "Dynamic Nuclear Pore Complexes: Life on the Edge." Cell 125(6): 1041-1053.

Tsujimoto Y, C. J., Jaffe E, Croce CM. (1985). "Involvement of the Bcl-2 gene in human follicular lymphoma." Science 228(4706): 1440-1443.

Unwin, P. N. T. and R. A. Milligan (1982). "A Large Particle Associated with the Perimeter of the Nuclear Pore Complex." J. Cell Biol. 93(1): 63.

Verhagen, A. M. (2002). "HtrA2 promotes cell death through its serine protease activity and its ability to antagonize inhibitor of apoptosis proteins." J Biol Chem 277: 445-454.

Verhagen, A. M., P. G. Ekert, et al. (2000). "Identification of DIABLO, a mammalian protein that promotes apoptosis by binding to and antagonizing IAP proteins." Cell 102: 43-53.

Villunger, A., E. M. Michalak, et al. (2003). "p53- and Drug-Induced Apoptotic Responses Mediated by BH3-Only Proteins Puma and Noxa." Science 302(5647): 1036-1038.

Wang, H. and D. E. Clapham (1999). "Conformational Changes of the in Situ Nuclear Pore Complex." Biophysical Journal 77(1): 241-247.

Wei, L.-H. K.-L. e. a. (2001). "The anti-apoptotic role of interleukin-6 in human cervical cancer is mediated by up-regulation of Mcl-1 through a PI 3-K/Akt pathway." oncogene 20(41).

Wei, M. C. (2001). "Proapoptotic BAX and BAK: a requisite gateway to mitochondrial dysfunction and death." Science 292: 727-730.

Wei, X., V. G. Henke, et al. (2003). "Real-Time Imaging of Nuclear Permeation by EGFP in Single Intact Cells." Biophysical Journal 84(2): 1317-1327.

White, C., C. Li, et al. (2005). "The ER gateway to apoptosis by Bcl-XL modulation of the InsP3R." Nat Cell Biol 7(10): 1021-1028.

REFERENCES

Wileman, T., L. P. Kane, et al. (1991). "Depletion of cellular calcium accelerates protein degradation in the ER." Journal of Biological Chemistry 266(7): 4500-4507.

Willis, S. N., J. I. Fletcher, et al. (2007). "Apoptosis Initiated When BH3 Ligands Engage Multiple Bcl-2 Homologs, Not Bax or Bak." Science 315(5813): 856-859.

Willis, S. N., L. Chen, et al. (2005). "Proapoptotic Bak is sequestered by Mcl-1 and Bcl-xL, but not Bcl-2, until displaced by BH3-only proteins." Genes & Development 19(11): 1294-1305.

Winslow, M. M., J. R. Neilson, et al. (2003). "Calcium signaling in lymphocytes." Curr. Opin. Immunol. 15: 299.

Worman, H. J. and J.-C. Courvalin (2004). "How do mutations in lamins A and C cause disease?" The Journal of Clinical Investigation 113(3): 349-351.

Wu, J., M. J. Matunis, et al. (1995). "Nup358, a Cytoplasmically Exposed Nucleoporin with Peptide Repeats, Ran-GTP Binding Sites, Zinc Fingers, a Cyclophilin A Homologous Domain, and a Leucine-rich Region." Journal of Biological Chemistry 270(23): 14209-14213.

Xu, C., W. Xu, et al. (2008). "BI-1 Regulates ER Ca2+ Homeostasis Downstream of Bcl-2 Family Proteins." Journal of Biological Chemistry 283(17): 11477-11484.
Xu, Q. and J. C. Reed (1998). "Bax Inhibitor-1, a Mammalian Apoptosis Suppressor Identified by Functional Screening in Yeast." Molecular Cell 1(3): 337-346.

Xue, W., L. Zender, et al. (2007). "Senescence and tumour clearance is triggered by p53 restoration in murine liver carcinomas." Nature **445**(7128): 656-660.

Yuste, V. J., R. S. Moubarak, et al. (2005). "Cysteine protease inhibition prevents mitochondrial apoptosis-inducing factor (AIF) release." Cell Death Differ 12(11): 1445-1448.

Zamzami, N. and G. Kroemer (2001). "The mitochondrion in apoptosis: how Pandora's box opens." Nat Rev Mol Cell Biol 2(1): 67-71.

Zhang, X. D., S. K. Gillespie, et al. (2004). "Staurosporine induces apoptosis of melanoma by both caspase-dependent and -independent apoptotic pathways" Molecular Cancer Therapeutics 3(2): 187-197.

Zhang, Y. and Y. Xiong (2001). "Control of p53 Ubiquitination and Nuclear Export by MDM2 and ARF." Cell Growth Differ 12(4): 175-186.

Zhong, F., M. C. Davis, et al. (2006). "Bcl-2 differentially regulates Ca2+ signals according to the strength of T cell receptor activation." J. Cell Biol. 172: 127.

Zong, W.-X., T. Lindsten, et al. (2001). "BH3-only proteins that bind pro-survival Bcl-2 family members fail to induce apoptosis in the absence of Bax and Bak." Genes & Development 15(12): 1481-1486.